



HAL
open science

Copper halide-chalcogenoether and -chalcogenone networks: Chain and cluster motifs, polymer dimensionality and photophysical properties

Adrien Schlachter, Kevin Tanner, Pierre Harvey

► To cite this version:

Adrien Schlachter, Kevin Tanner, Pierre Harvey. Copper halide-chalcogenoether and -chalcogenone networks: Chain and cluster motifs, polymer dimensionality and photophysical properties. *Coordination Chemistry Reviews*, 2021, 448, pp.214176. 10.1016/j.ccr.2021.214176 . hal-04632361

HAL Id: hal-04632361

<https://hal.science/hal-04632361v1>

Submitted on 11 Sep 2024

HAL is a multi-disciplinary open access archive for the deposit and dissemination of scientific research documents, whether they are published or not. The documents may come from teaching and research institutions in France or abroad, or from public or private research centers.

L'archive ouverte pluridisciplinaire **HAL**, est destinée au dépôt et à la diffusion de documents scientifiques de niveau recherche, publiés ou non, émanant des établissements d'enseignement et de recherche français ou étrangers, des laboratoires publics ou privés.

Copper Halide-Chalcogenoether and -Chalcogenone Networks: Chain and Cluster Motifs, Polymer Dimensionality and Photophysical Properties

*Adrien Schlachter, Kevin Tanner and Pierre D. Harvey**

Département de chimie, Université de Sherbrooke, Sherbrooke, PQ, Canada, J1K 2R1.

*Corresponding authors. E-mail address: Pierre.Harvey@USherbrooke.ca (P.D. Harvey),

Keywords : Cluster; Copper; Luminescence; Polymer; Chalcogenoether and Chalcogenone

ABSTRACT: Copper(I) halides react with mono- and polychalcogenoethers and -chalcogenones to form 0-3D coordination materials containing neutral polynuclear $\text{Cu}_x\text{X}_x\text{E}_y$ species (E = S, Se, Te; X = Cl, Br, I; x = 2-8) called secondary building units (SBU). These species exhibit two general types of motifs namely *globular* and *quasi-planar*. Depending on the shape of these polynuclear species and the dimensionality of the network, their properties and applications are profoundly different. In a structural point of view for instance, when X = I, and E = S, the *globular* family includes cubane, open cubane, fused dicubane, fused open dicubane, hexagonal prism, and 1D-polycubane. Concurrently, the *quasi-planar* family includes rhomboid, trinuclear cluster, step staircase, 1D-zig zag ribbon, 1D-acordeon ribbon and 1D-staircase ribbon. Both the cubane and rhomboid motifs are overwhelmingly represented (> 80%). Generally, the *globular* species are generally strongly luminescent. In contrast, the *quasi-planar* family exhibits only modest intensity luminescence or no emission at all. This review provides a thorough statistical analysis of these SBUs, in a structural point of view, along with their photophysical properties.

CONTENTS

1. Introduction.....	2
2. <i>Globular</i> structures of $\text{Cu}_x\text{I}_x\text{S}_y$ species	6
3. <i>Quasi-planar</i> structures of the $\text{Cu}_x\text{I}_x\text{S}_y$ species	14
4. Thione ligands with the $\text{Cu}_x\text{I}_x\text{S}_y$ species.....	20
5. $\text{Cu}_x\text{Br}_x\text{S}_y$ species	21
6. $\text{Cu}_x\text{Cl}_x\text{S}_y$ species	24
7. Cu_xX_xE_y species (X = I, Br, Cl; E = Se, Te).....	27
8. Statistical analysis on the geometry of the SBUs and CP dimensionalities	29
8.1. Occurrence of globular and quasi-planar motifs and dimensionalities	29
8.2. Flexibility of the SBU motifs	37
9. Photophysical Properties of the Cu_xX_xE_y -containing complexes and CPs.....	41
10. Related topics and comments.....	53
10.1. Silver species	54
10.2. The thioether within multitopic ligands.....	55
10.3. $(\text{Cu}_m\text{X}_{m+n})^{n-}$ halogenocuprates.....	56
10.4. Relevant particularities	59
11. Conclusion	62
Declaration of Competing Interest.....	64
Acknowledgements.....	64
References.....	65

1. Introduction

The applications of coordination polymers (CPs) and metal-organic frameworks (MOFs) depend entirely on the structure-property relationship. During the past decades, multiple groups devoted major efforts in designing functional and stimuli-responsive CPs, MOFs or complexes based on mono- and chalcogenoethers, and chalcogenones and copper salts, namely for X = Cl, Br, I, but not exclusively [1–4]. Indeed, thermal catalysis and photocatalytic properties [5–9], sensing of small organic molecules [10], and electrochemical [11], thermoelectric [12], and photovoltaic responses [13] were reported using such species, and when doped, some porous CPs [14,15] and non-porous materials [16] became electrically conductive, just to state a few examples.

Moreover, some compact 3D CP materials comprising parallel $(\text{Cu}_2\text{X}_2\text{S}_4)_n$ sheets ($\text{X} = \text{Cl}, \text{Br}$), were also found to be prone to ultrafast excitation energy migration (ps time scale at 298 K for the triplet state, which typical should normally be μs) through a Dexter mechanism (*i.e.* double electron exchange) [17,18], suggesting that they could also be conducting if appropriately doped, which turned out to be the case [4]. Finally, aggregation induced emission was recently reported for a polymer containing a mixed-donor bidentate ligand ($\text{Ph}_2\text{PCH}_2\text{SPh}$) [19]. During the last decade (2011-2020), a clear increasing interest on these materials became obvious and the number of reported research articles even surpassed the total number of all past investigations prior to this decade (> 2010 ; **Figure 1**).

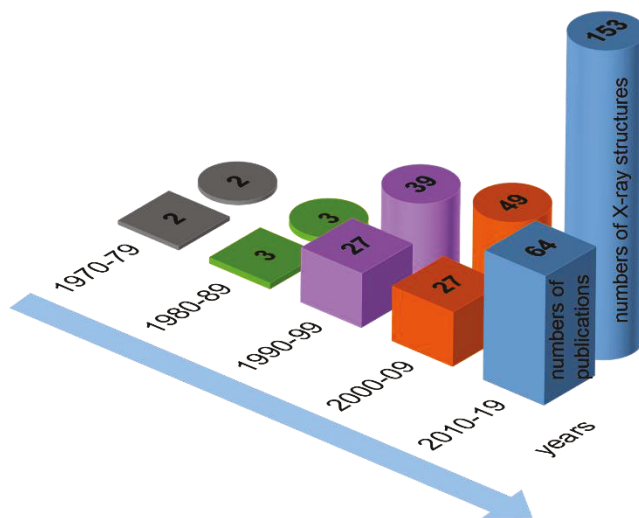


Figure 1. Time evolution of the number of articles and of the number of X-ray structures reporting the chemistry of the complexes and coordination polymers built upon chalcogenoethers and chalcogenones.

Nowadays, the design of functional porous 3D CP materials and MOFs is still a topic of strong interest for sensing purposes. For example, the polydentate organic ligand can be as sophisticated as a polysilsesquioxane, POSS, bearing eight $\text{Si}(\text{CH}_2)_3\text{SAr}$ arms ($\text{Ar} = \text{p-tol}$ or $\text{C}_6\text{H}_3(2\text{-Me})(5\text{-tBu})$) in order to coordinate CuX salts ($\text{X} = \text{Br}, \text{I}$) [20]. For CuI , the p-tol and $\text{C}_6\text{H}_3(2\text{-Me})(5\text{-tBu})$ aromatics lead to two different secondary building units (SBU); a luminescent closed cubane ($\text{Cu}_4\text{I}_4\text{S}_4$) and a non-emissive rhomboid ($\text{Cu}_2\text{I}_2\text{S}_4$), respectively. This seemingly innocent change in the steric trait of the S-pendent group on the octathioether, even remotely placed from the

sulfur, suffices to induce a drastic change in the resulting SBU geometry and ultimately the optical behaviour. This phenomenon is not unique where the simple change of a Ph for p-Tol is enough to change the SBU from a cubane to a fused dicubane ($\text{Cu}_8\text{I}_8\text{S}_6$) [21]. Similarly, rigidifying the C_4 -chain in PhS-chain-SPh, for instance, from $(\text{CH}_2)_4 \rightarrow \text{CH}_2\text{C}\equiv\text{CCH}_2 \rightarrow \textit{trans}\text{-CH}_2\text{CH}=\text{CHCH}_2 \rightarrow \textit{cis}\text{-CH}_2\text{CH}=\text{CHCH}_2 \rightarrow \text{C}\equiv\text{C-C}\equiv\text{C}$ changes the SBU from cubane \rightarrow hexagonal prism ($\text{Cu}_6\text{I}_6\text{S}_6$) or 1D-zig zag ribbon \rightarrow rhomboid \rightarrow cubane \rightarrow step staircase, respectively [12,22–24]. Concurrently, by modifying the chain in (p-Tol)S-chain-S(p-Tol) ligand going from chain = $(\text{CH}_2)_4 \rightarrow \text{CH}_2\text{C}\equiv\text{CCH}_2 \rightarrow \textit{trans}\text{-CH}_2\text{CH}=\text{CHCH}_2 \rightarrow \textit{cis}\text{-CH}_2\text{CH}=\text{CHCH}_2$ leads to 1D-zig zag ribbon, cubane, 1D-zig zag ribbon and rhomboid SBUs, respectively [24–26]. The structures of these SBU motifs are provided in Figures 2 and 3. Examples like these are numerous and are listed herein. Recently, an exhaustive investigation was performed focusing on SBUs and CPs resulting from the coordination of $\text{BzS}(\text{CH}_2)_x\text{SBz}$ ligands ($x = 1\text{-}9$ (except $x = 2,5$); Bz = benzyl, a pendent group considered to be somewhat adaptive with its single S-C and C-C bonds) on CuI [27]. The main conclusion is that when $x \geq 4$, both SBUs, rhomboid and cubane are predictably obtained by reacting the ligands and salt in the appropriate ratio. This concept was previously demonstrated for other flexible chain-containing ligands [28–30]. However, this trend turned out not to be true for $x < 4$ where only the rhomboid SBU was observed ($x = 1$, rhomboid; $x = 3$, rhomboid). This insensitivity of the resulting geometry of the polynuclear species *vis-à-vis* the ligand/metal ratio is in fact found rather common throughout the literature. This distinction, or rather control in forming the cubane *vs* rhomboid, is crucial since the resulting properties and applications rely on this key feature along with the network dimensionality.

The SBUs of these complexes can be divided into two main sub-groups: the *quasi-planar* and the *globular* species. The *quasi-planar* SBUs (Figure 2) are polynuclear with either 0D (*i.e.* discrete motifs), 1D- or 2D, the latter one having a sheet-like structure. They are often non or weakly luminescent, but not systematically. The *globular* SBUs (Figure 3) have 3D-cluster arrangements and may also be 0D, or expanded in 1D. Unlike the first sub-group of SBUs, these *globular* species usually exhibit intense luminescence and rich photophysical properties, although rare exceptions exist (see photophysical properties section below).

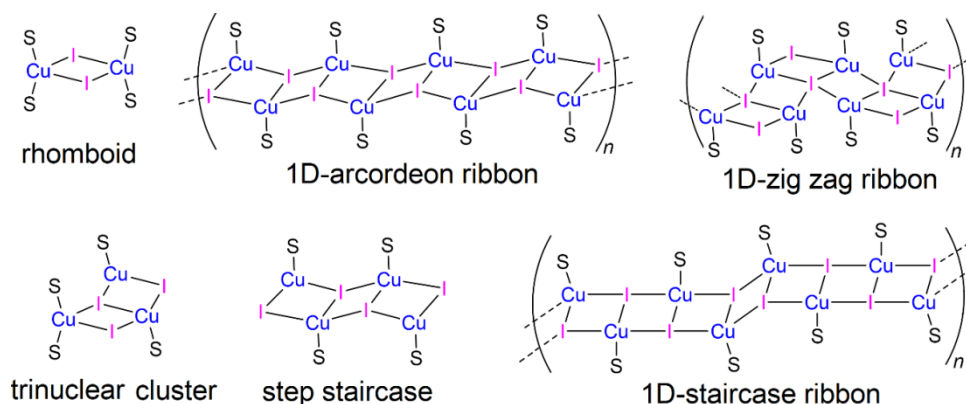


Figure 2. Structures of the rhomboid and various common *quasi-planar* SBUs or 0D complexes encountered for neutral $\text{Cu}_x\text{I}_x\text{S}_y$ motifs (~~often non or weakly luminescent, but not systematically~~).

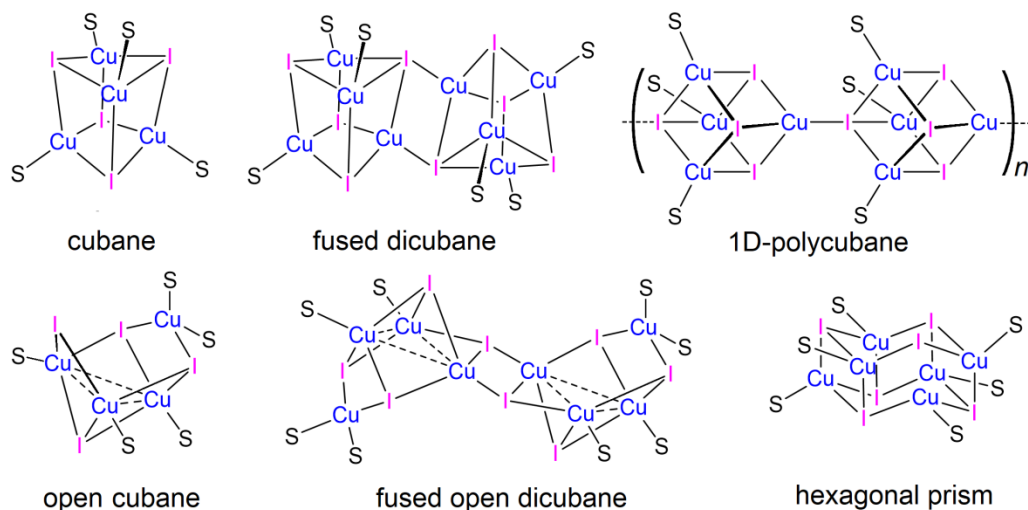


Figure 3. Structures of the cubane and various *globular* SBUs or 0D complexes encountered for neutral $\text{Cu}_x\text{I}_x\text{S}_y$ motifs.

This review article presents and analyses the structural and luminescence properties of the title materials. Specifically, the properties include an exhaustive survey of the SBU structures (*i.e.* for neutral Cu_xX_y species where $\text{X} = \text{Cl}, \text{Br}, \text{I}$) and network dimensionalities along with a statistical analysis permitting to draw conclusions on the resulting traits based on the structure of the assembling ligand. Special topics such metal-containing ligands and their frameworks, CPs built upon pseudohalide salts, silver halide analogues, and halogenocuprates (*i.e.* negatively charged Cu_xX_y SBUs, generally polymeric, mainly where $\text{X} = \text{I}$ and $y = x+1$, but not exclusively) are also included for comparison purposes.

2. Globular structures of $\text{Cu}_x\text{I}_x\text{S}_y$ species

This section focusses on what promotes the formation of *globular* SBUs. The four main types of ligand structures commonly encountered throughout the literature are cyclic and acyclic mono- and dithioethers (**Figure 4**), along with several various polydentates.

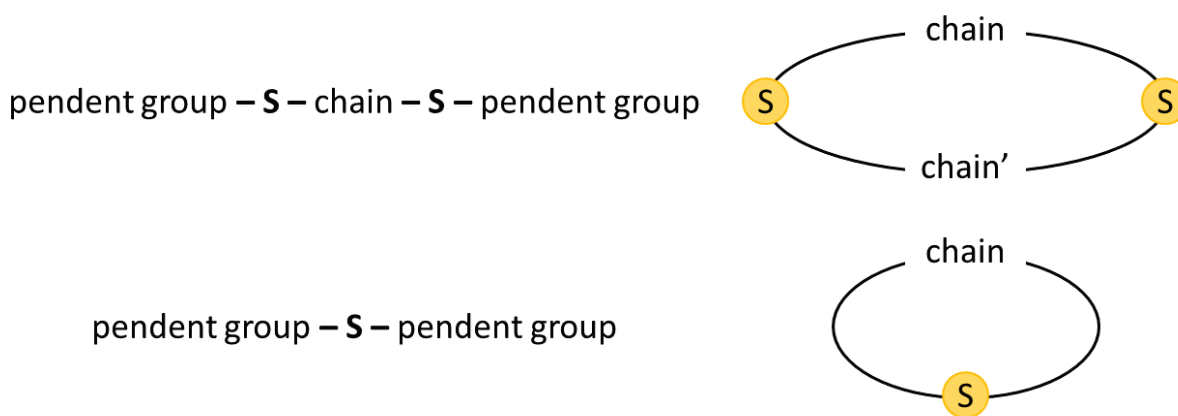
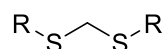


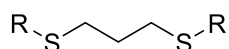
Figure 4. Schematic representations of the general structures of the assembling thioethers.

Over sixty $\text{Cu}_4\text{I}_4\text{S}_4$ closed cubanes as SBUs were characterized by X-ray crystallography. Their structural features are summarized in **Table 1-Table 5** and their ligand structures (along with codes) are provided in **Figure 5, 7-9** [11,18,20–22,24–28,30–74]. For comparison purposes, occasional species containing coordinated monodentate MeCN molecules are included along with seleno-analogues. These species are believed to be reactive intermediates during the formation of the CPs in solution. Throughout the text, the term L/M ratio sensitive is used and means that the formation of *globular* motifs (mostly cubane) or *quasi-planar* ones (mostly rhomboid) can be obtained with the appropriate stoichiometry, respectively 1:1 and 2:1. The first observations are that in the category of the acyclic dithioethers (**Table 1**), only one 0D (*i.e.* discrete) complex has been reported (entry 8, **Table 1**) and that the formation of 3D CPs turns out to be rather rare where only three examples, using a $(\text{CH}_2)_8$ chain **L26**, or a four carbon semi-rigid chain (**L16** and **L18**), have been isolated. Furthermore, only 1D CPs crystallizes when the chain is a single methylene (*i.e.* RSCH_2SR). When MeCN's are linked to the Cu_4I_4 cluster, the dimensionality is lower (*i.e.* 0D) demonstrating that MeCN is strictly a monodentate ligand. Moreover, CPs containing rhomboids are known for the $(\text{PhSCH}_2)_2$ (**L66**) ligand (below), but no $\text{Cu}_4\text{I}_4\text{S}_4$ cubanes

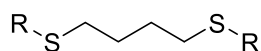
have been isolated for this dithioether. For the shorter chain-containing dithioethers, with three or four carbon atoms, regardless of whether the chain is flexible or semi-rigid, and the nature of the R group, the CP dimensionality is mostly 2D. The only exception is observed for **L18**, which gives a 3D CP.



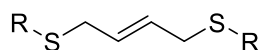
- L1** : R = Ph
L2 : R = p-Tol
L3 : R = m-Tol
L4 : R = o-Tol
L5 : R = 4-MeOC₆H₄
L6 : R = 4-BrC₆H₄
L7 : R = 5-tBu-2-MeC₆H₃
L8 : R = 2,4-Me₂C₆H₃



- L9** : R = Ph



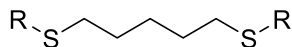
- L10** : R = Et
L11 : R = n-Bu
L12 : R = t-Bu
L13 : R = Ph
L14 : R = Cy
L15 : R = Bz



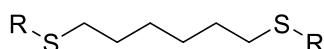
- L16** : R = Ph



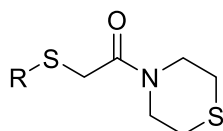
- L17** : R = p-Tol
L18 : R = Ph



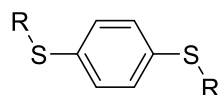
- L19** : R = Ph
L20 : R = p-Tol



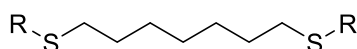
- L21** : R = Ph
L22 : R = Bz



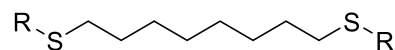
- L23** : R = Cy



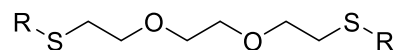
- L24** : R = Et



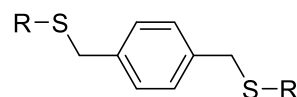
- L25** : R = Bz



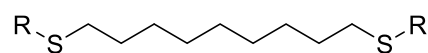
- L26** : R = 4-MeOC₆H₄
L27 : R = Ph
L28 : R = Bz
L29 : R = tBuC₆H₄
L30 : R = p-Tol



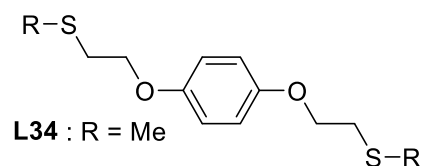
- L31** : R = Bz



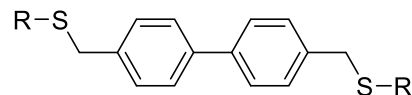
- L32** : R = Cy



- L33** : R = Bz



- L34** : R = Me



- L35** : R = Et

Figure 5. Structures and codes of acyclic dithioether ligands forming *globular* Cu_xI_xS_y used in this review.

Table 1. Structural features of the *globular* Cu_xI_xS_y-containing materials: dithioethers/CuI; cubanes at the top, other *globular* species at the bottom.

#	cluster	xD-Formula	Cu-Cu distances [Average] (Å)	L/M ratio sensitive?	ref	#CCDC
1	Cubane	1D-[Cu ₄ I ₄ (L1) ₂] _n ^a	2.661, 2.661, 2.677, 2.639, 2.801, 2.801 [2.707]	—	[30,54]	974326*
	Cubane	1D-[Cu ₄ I ₄ (L1) ₂] _n ^a	2.698, 2.700, 2.815, 2.666, 2.795, 2.671 [2.724]	—	[30,54]	974327
2	Cubane	1D-[Cu ₄ I ₄ (L2) ₂] _n	2.682, 2.653, 2.829, 2.682, 2.829, 2.756 [2.739]	—	[30]	974333
3	Cubane	1D-[Cu ₄ I ₄ (L3) ₂] _n	2.640, 2.700, 2.717, 2.703, 2.789, 2.859 [2.735]	—	[30]	974335
4	Cubane	?D-[Cu ₄ I ₄ (L4) ₂] _n ^b		—	[30]	-
5	Cubane	1D-[Cu ₄ I ₄ (L5) ₂] _n	2.802, 2.663, 2.718, 2.625, 2.802, 2.718 [2.721]	—	[30]	974334
6	Cubane	1D-[Cu ₄ I ₄ (L6) ₂] _n	2.643, 2.684, 2.834, 2.740, 2.684, 2.834 [2.736]	—	[30]	974329*
7	Cubane	1D-[Cu ₄ I ₄ (L7) ₂] _n	2.868, 2.781, 2.582, 2.582, 2.781, 2.868 [2.744]	—	[30]	974336
8	Cubane	0D-[Cu ₄ I ₄ (L8) ₂ (MeCN) ₂] ₂	2.679, 2.697, 2.687, 2.689, 2.737, 2.650 [2.690]	—	[11,30]	782636
9	Cubane	2D-[Cu ₄ I ₄ (L9) ₂] _n	2.705, 2.704, 2.768, 2.704, 2.756, 2.727 [2.727]	yes	[28]	906348
10	Cubane	2D-[Cu ₄ I ₄ (L10) ₂] _n	2.724, 2.756, 2.726, 2.644, 2.699, 2.771 [2.712]	—	[18,50]	1488036
11	Cubane	2D-[Cu ₄ I ₄ (L11) ₂] _n	2.761, 2.723, 2.711, 2.680, 2.708, 2.777 [2.740]	—	[44]	801246
12	Cubane	2D-[Cu ₄ I ₄ (L12) ₂] _n	2.847, 2.829, 2.829, 3.028, 2.966, 2.966 [2.911]	—	[44]	801247
13	Cubane	2D-[Cu ₄ I ₄ (L13) ₂] _n ^c	2.651, 2.698, 2.715, 2.692, 2.670, 2.743 [2.695]	—	[22]	692868
14	Cubane	?D-[Cu ₄ I ₄ (L14) ₂] _n ^b		yes	[31]	-
15	Cubane	2D-[Cu ₄ I ₄ (L131) ₂] _n ^d	2.772, 2.820, 2.794, 2.687, 2.794, 2.772 [2.773]	yes	[24]	1418767*
16	Cubane	2D-[Cu ₄ I ₄ (L17) ₂] _n	2.714, 2.688, 2.765, 2.645, 2.685, 2.788 [2.714]	—	[25]	1993267
17	Cubane	1D-[Cu ₄ I ₄ (L19) ₂] _n	2.664, 2.677, 2.750, 2.750, 2.757, 2.677 [2.712]	yes	[28]	906350
18	Cubane	?D-[Cu ₄ I ₄ (L20) ₂] _n ^b		yes	[28]	-
19	Cubane	1D-[Cu ₄ I ₄ (L21) ₂] _n		yes	[26]	-
20	Cubane	2D-[Cu ₄ I ₄ (L22) ₂] _n	2.754, 2.740, 2.722, 2.750, 2.703, 2.720 [2.732]	yes	[27]	1960070
21	Cubane	2D-[Cu ₄ I ₄ (L23) ₂] _n ^e	2.833, 2.789, 2.755, 2.740, 2.625, 2.631 [2.729]	yes	[53,57]	660763*
22	Cubane	1D-[Cu ₄ I ₄ (L23) ₂] _n ^e	2.734, 2.718, 2.781, 2.775, 2.709, 2.650 [2.728]	yes	[53]	660765
23	Cubane	2D-[Cu ₄ I ₄ (L24) ₂] _n	2.783, 2.861, 2.879, 2.810, 2.831, 2.721 [2.814]	yes	[45]	785686
24	Cubane	2D-[Cu ₄ I ₄ (L25) ₂] _n	2.700, 2.679, 2.690, 2.702, 2.691, 2.678 [2.690]	yes	[27]	1960074
25	Cubane	3D-[Cu ₄ I ₄ (L26) ₂] _n	2.720, 2.835, 2.720, 2.835, 2.720, 2.835 [2.777]	yes	[3]	-
26	Cubane	1D-[Cu ₄ I ₄ (L27) ₂] _n ^f	2.735, 2.793, 2.661, 2.678, 2.715, 2.724 [2.718]	—	[21]	1038661
27	Cubane	2D-[Cu ₄ I ₄ (L28) ₂] _n	2.729, 2.729, 2.729, 2.710, 2.729, 2.710 [2.723]	yes	[27]	1960078
28	Cubane	2D-[Cu ₄ I ₄ (L31) ₂] _n ^g	2.778, 2.801, 2.801, 2.801, 2.801, 2.778 [2.793]	—	[60,69]	250264
29	Cubane	1D-[Cu ₄ I ₄ (L29) ₂] _n ^f	2.772, 2.714, 2.776, 2.685, 2.688 [2.723]	—	[34]	-
30	Cubane	1D-[Cu ₄ I ₄ (L32) ₂] _n ^g	2.772, 2.857, 2.825, 2.805, 2.830, 2.790 [2.813]	—	[52]	649210
31	Cubane	2D-[Cu ₄ I ₄ (L33) ₂] _n	2.717, 2.780, 2.802, 2.695, 2.719, 2.764 [2.746]	yes	[27]	1960082*
32	Cubane	1D-[Cu ₄ I ₄ (L34) ₂] _n ^h	2.784, 2.720, 2.708, 2.824, 2.634, 2.740 [2.735]	—	[49]	739727
33	Cubane	2D-[Cu ₄ I ₄ (L35) _{1.5}] _n ⁱ	2.725, 2.755, 2.724, 2.725, 2.755, 2.724 [2.735]	yes	[45]	785688
34	1D-polycubane	3D-[Cu ₄ I ₄ (L15) _{1.5}] _n	2.701, 2.701, 2.701, 2.878, 2.878, 2.878 [2.790]	yes	[27,50]	1960067
35	Hexagonal prism	3D-[Cu ₆ I ₆ (L18) ₃] _n		—	[22]	692869
36	Fused dicubane	2D-[Cu ₈ I ₈ (L30) ₃] _n		—	[21,34]	1038660

^a phase transition with temperature, two space groups (*C2/c* and *P2₁/c*) ; ^b based on chem. anal.+ luminescence ; ^c interpenetrated network ; ^d SBU sensitive to *cis-* vs *trans-* ; ^e rare case of asymmetric ligand ; ^f SBU sensitive to substituent ; ^g 8-atom chain ; ^h forms γ -nanocrystals with heat ; ⁱ 14-atom chain ; * multiple temperature available.

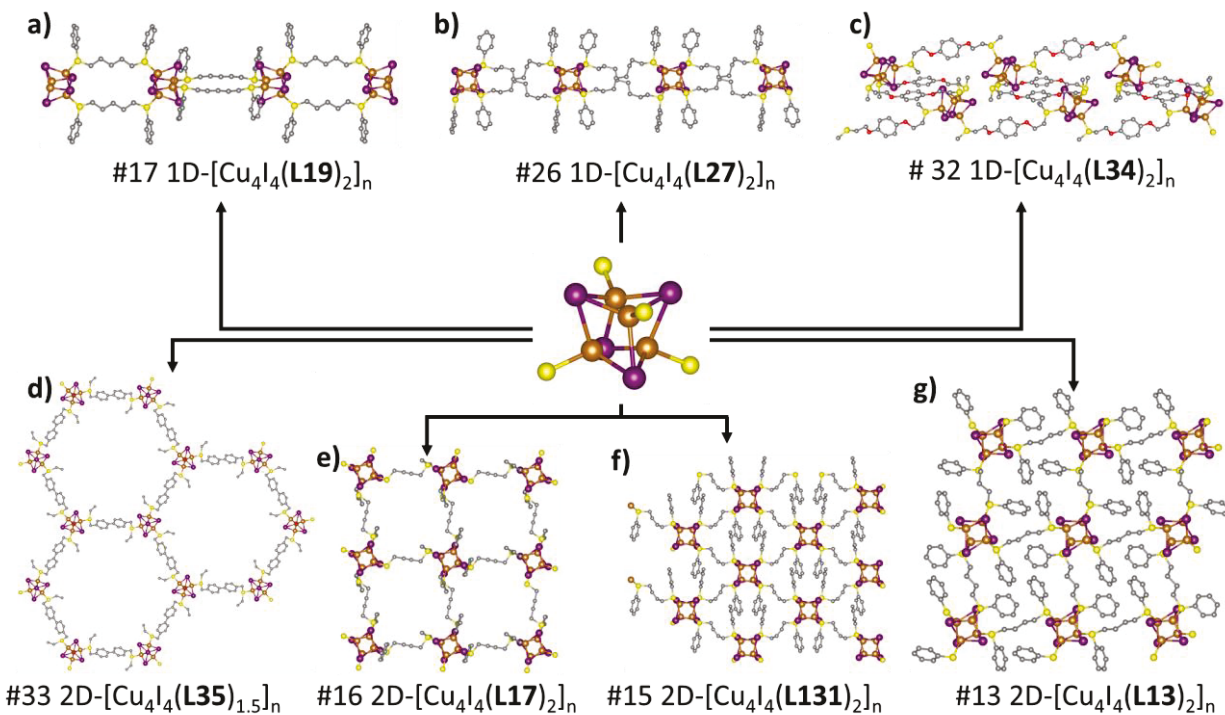


Figure 6. Schemes illustrating how the cubane motifs $\text{Cu}_4\text{I}_4\text{S}_4$ can be linked with acyclic dithioether ligands to form various coordination polymers listed in **Table 1**. Color code: O, red ; S, yellow; Cu, orange ; I, purple ; C, grey. The hydrogen atoms were omitted for clarity as well as the C_6H_5 groups for e). The images were reproduced using the cif files from the Cambridge Crystallographic Data Centre; CCDC number: a) 906350, b) 1038661, c) 739727, d) 785688, e) 1418767, f) 1418767 and g) 692868.

The next observation is that the nature of the short chain length plays a determining role in the resulting dimensionality of the $\text{Cu}_4\text{I}_4\text{S}_4$ cubane-containing CPs. For longer chains (5-atoms or more, ~~including one diseleno ligand containing CP (entry 20, Table 1, L22 = $\text{BzS}(\text{CH}_2)_6\text{SBz}$ [27])~~), the dimensionality (eight 1D, seven 2D, three 3D) is randomly distributed with no specific trend, except for the clear predominance of 1D and 2D CPs over 0D and 3D, and for the fact that both $(\text{CH}_2)_7$ -containing ligands form 3D CPs only. Moreover, when R is benzyl, the nature of the SBU (cubane vs rhomboid) is sensitive to the initial ligand/metal ratio. This observation about dimensionality being randomly distributed is also noted for the cyclic dithioether ligands (*i.e.* four 1D, excluding one MeCN-containing species, five 2D, one 3D; **Table 2**). In these cases, the cycles are composed of two S---S segments containing 5-atoms or more each. In proportion, the resemblance between these two sub-families (acyclic (**Table 1**) and cyclic (**Table 2**) dithioethers

with chain segments of 5-atoms or more) is notable. Excluding the MeCN-containing species and CPs which have not been formally characterized by crystallography, the occurrence of larger *globular* clusters (*i.e.* $\text{Cu}_{2n}\text{I}_{2n}\text{S}_y$; $n = 3, 4$) vs $\text{Cu}_4\text{I}_4\text{S}_4$ cubane is $\sim 10\%$ (3 vs 32 (acyclic), 1 vs 10 (cyclic)). Interestingly, the larger *globular* polynuclear species lead mostly to the formation of 3D CP, with one exception being a 2D (entry 13, **Table 2**), most likely reflecting on the cluster size and the multi-positional trait of their coordination sites.

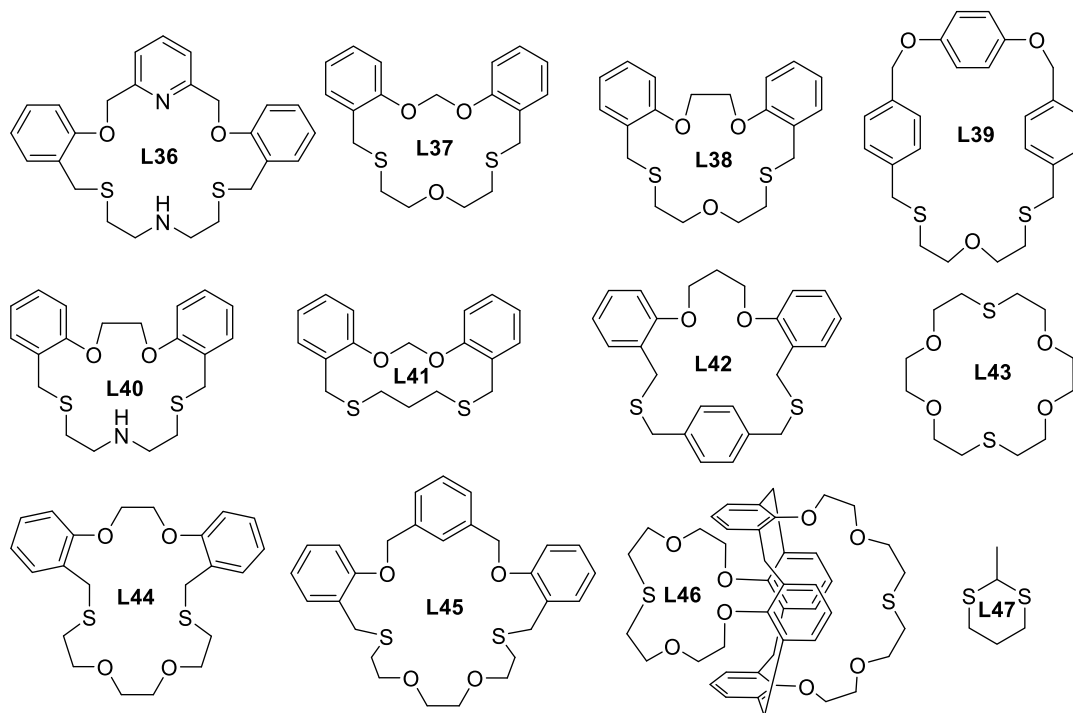


Figure 7. Structures and codes of the cyclic dithioether ligands used in this review.

Table 2. Structural features of the *globular* $\text{Cu}_x\text{I}_x\text{S}_y$ -containing materials: cyclic dithioethers/ CuI ; cubanes at the top, the *globular* species at the bottom.

#	cluster	xD-Formula	Cu-Cu distances [Average] (Å)	L/M ratio sensitive?	ref	#CCDC
1	Cubane	1D- $[\text{Cu}_4\text{I}_4(\text{L36})_2]_n$	2.632, 2.702, 2.699, 2.646, 2.668, 2.662 [2.668]	yes	[33]	1813889
2	Cubane	2D- $[\text{Cu}_4\text{I}_4(\text{L37})_2]_n$	2.842, 2.721, 2.823, 2.674, 2.851, 2.753 [2.777]	—	[39]	1050009
3	Cubane	1D- $[\text{Cu}_4\text{I}_4(\text{L38})_2]_n^a$	2.769, 2.770, 2.695, 2.799, 2.773, 2.698 [2.751]	—	[39]	1050010
4	Cubane	1D- $[\text{Cu}_4\text{I}_4(\text{L39})_2]_n$	2.731, 2.742, 2.711, 2.731, 2.711, 2.820 [2.741]	—	[68]	1252292
5	Cubane	2D- $[\text{Cu}_4\text{I}_4(\text{L40})_2]_n$	2.771, 2.733, 2.793, 2.793, 2.651, 2.771 [2.752]	—	[67]	-
6	Cubane	?D- $[\text{Cu}_4\text{I}_4(\text{L41})_2 \cdot 2.5\text{H}_2\text{O}]_n^b$	2.727, 2.719, 2.744, 2.691, 2.707, 2.780 [2.728]	—	[40]	-
7	Cubane	2D- $[\text{Cu}_4\text{I}_4(\text{L42})_2]_n \cdot \text{CH}_2\text{Cl}_2^c$	2.770, 2.654, 2.755, 2.675, 2.663, 2.747 [2.710]	—	[42]	863930 863931
8	Cubane	2D- $[\text{Cu}_4\text{I}_4(\text{L43})_2]_n^d$	2.642, 2.727, 2.762, 2.667, 2.849, 2.656 [2.717]	—	[43]	822021
9	Cubane	1D- $[\text{Cu}_4\text{I}_4(\text{L44})_2]_n^e$	2.704, 2.597, 2.797, 2.704, 2.797, 2.765 [2.727]	—	[46]	787695

10	Cubane	1D-[Cu ₄ I ₄ (L45) ₂] _n	2.670, 2.767, 2.703, 2.641, 2.647, 2.689 [2.686]	—	[47]	809854
11	Cubane	1D-[Cu ₄ I ₄ (L46)(MeCN) ₂] _n	2.665, 2.769, 2.789, 2.720, 2.769, 2.789 [2.750]	—	[55]	677839
12	Cubane	3D-[Cu ₄ I ₄ (L43) ₂] _n	2.717, 2.723, 2.787, 2.723, 2.724, 2.717 [2.732]	—	[59]	280751
13	Cubane	2D-[Cu ₄ I ₄ (L43)(NaSCN)] _n ^f	2.700, 2.751, 2.581, 2.723, 2.708, 2.783 [2.708]	—	[61]	157619
14	1D-Cu ₅ I ₆	2D- [Cu ₅ I ₆ (L43)(NaMeCN)] _n ^g		—	[76]	135284
15	Fused open dicubane	3D-[Cu ₈ I ₈ (L47) ₄] _n		yes	[74]	1827915

^a tubular structure ; ^b emissive ; ^c binary mixture of isomorphs ; ^d SBU = sensitive with time ; ^e sensitive to addition of KI ; ^f Na(SCN)₂ inside the thiacycrown ; ^g Na(MeCN)₂ inside the thiacycrown sensitive to addition of NaI or KI.

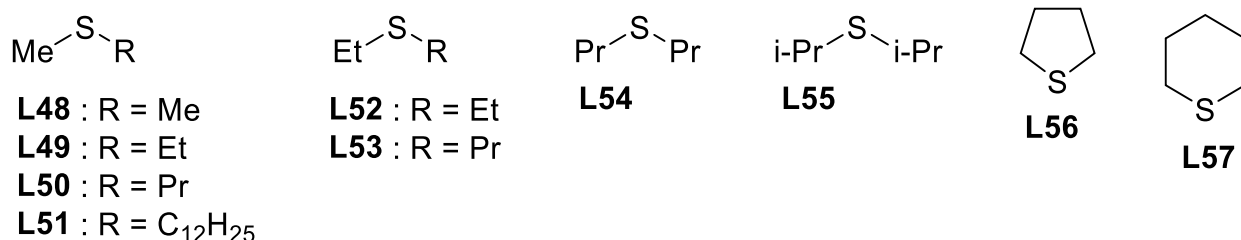


Figure 8. Structures and codes of acyclic and cyclic monothioether ligands used in this review.

Table 3. Structural features of the cubane-containing materials: acyclic and cyclic monothioethers/CuI; cubane at the top, other *globular* species at the bottom.

#	cluster	xD-Formula	Cu-Cu distances [Average] (Å)	L/M ratio sensitive?	ref	#CCDC
1	Cubane	1D-[Cu ₄ I ₄ (L52) ₃] _n ^a	2.813, 2.787, 2.776, 2.717, 2.890, 2.782 [2.794]	—	[48,64]	789005*
2	Cubane	1D-[Cu ₄ I ₄ (L50) ₃] _n	2.697, 2.713, 2.840, 2.753, 2.735, 2.700 [2.740]	—	[36]	1047404*
3	Cubane	0D-[Cu ₄ I ₄ (L53) ₄]	2.725, 2.726, 2.682, 2.725, 2.682, 2.829 [2.728]	—	[36]	1047397
4	Cubane	0D-[Cu ₄ I ₄ (L55) ₄]	2.675, 2.855, 2.858, 2.675, 2.855, 2.858 [2.796]	—	[36]	1047408*
5	Cubane	0D-[Cu ₄ I ₄ (L51) ₄] ^b	2.858, 2.855, 2.675, 2.675, 2.855, 2.858 [2.796]	—	[62]	200099
6	Open cubane	2D-[Cu ₄ I ₄ (L48) ₃] _n		yes	[36]	1047394
7	Step cubane	1D-[Cu ₄ I ₄ (L49) ₃] _n ^c		—	[36]	1047413*
8	Open flower basket	2D-[Cu ₄ I ₄ (L48) ₃] _n ^d		yes	[58]	628588
9	Fused dicubane	0D-[Cu ₈ I ₈ (L55) ₆] ^e		yes	[36]	1047398

^a also refs.[65,66] ; ^b mixed with crystals of a Cu₃I₄-species ; ^c heptane, in MeCN SBU ; ^d in MeSMe ; ^e SBU sensitive to solvent used ; * multiple temperature available.

Table 4. Structural features of the cubane-containing materials: cyclic monothioethers/CuI.

#	cluster	xD-Formula	Cu-Cu distances [Average] (Å)	L/M ratio sensitive?	ref	#CCDC
1	Cubane	3D-[Cu ₄ I ₄ (L56) ₂] _n	2.672, 2.736, 2.648, 2.758, 2.754, 2.636 [2.701]	yes	[37]	977480
2	Cubane	2D- {[Cu ₄ I ₄ (L56)](L56) ₂ (Cu ₂ I ₂)-(L56) ₂ [Cu ₄ I ₄ (NCMe)]} _n ^a	2.754, 2.700, 2.691, 2.700, 2.700, 2.658 [2.701]	yes	[37]	977481

3	Cubane	0D-[Cu ₄ I ₄ (L56) ₄] ^b	2.735, 2.717, 2.837, 2.761, 2.806, 2.719 [2.763] 2.742, 2.739, 2.837, 2.806, 2.670, 2.769 [2.761]	yes	[37]	977482 *
4	Cu ₈ I ₈	0D-[Cu ₄ I ₄ (L57) ₄]		yes	[38]	-

^a presence of NCMe ; ^b 2 isomorphs + phase transition ; * multiple temperature available.

For the acyclic monothioether R-S-R' ligands (**Table 3**), as the size of the substituents increases, the dimensionality of the cubane-containing materials decreases from 2D → 1D → 0D, including the globular fused dicubane (entry 9). This trend clearly stems from the steric hindrance effect of the substituents. It is noteworthy, that the absence of 3D materials in this category is likely due the relative size of the ligand compared to that of the clusters. Interestingly in this category, the occurrence of larger *globular* clusters (*i.e.* Cu_{2n}I_{2n}S_y; n = 3, 4) vs Cu₄I₄S₄ cubane is also ~10% (1 vs 8). Despite the very small sampling, this trend is also noted for the cyclic monothioether ligand-containing species (**Table 4**); **L56** (3D to 0D) [37] → **L57** (0D) [38]. Importantly, the structural outcome of the materials is very dependent on how the synthesis is performed (*i.e.* ligand/metal ratio, temperature, nature of the solvent), and how the samples are treated afterward (*i.e.* heating and grinding, thus leading to thermo- and mechanochromism) and change of structure as, for example, ligand **L56** is very volatile. Moreover, no globular Cu_xI_xS_y-containing materials have been isolated so far with this type of ligand. This may be explained by a simple steric effect induced by the large size of the cluster and its multiple coordination sites, versus the shape of the cyclic ligand.

Polythioethers containing from 3 S- to 8 S-donor atoms are also able to incorporate cubanes within their CPs (**Table 5**). This category stands out as the occurrence of 3D materials dominates (three 3D, one 2D and one 1D) and may reflect the multi-directional geometry of these ligands.

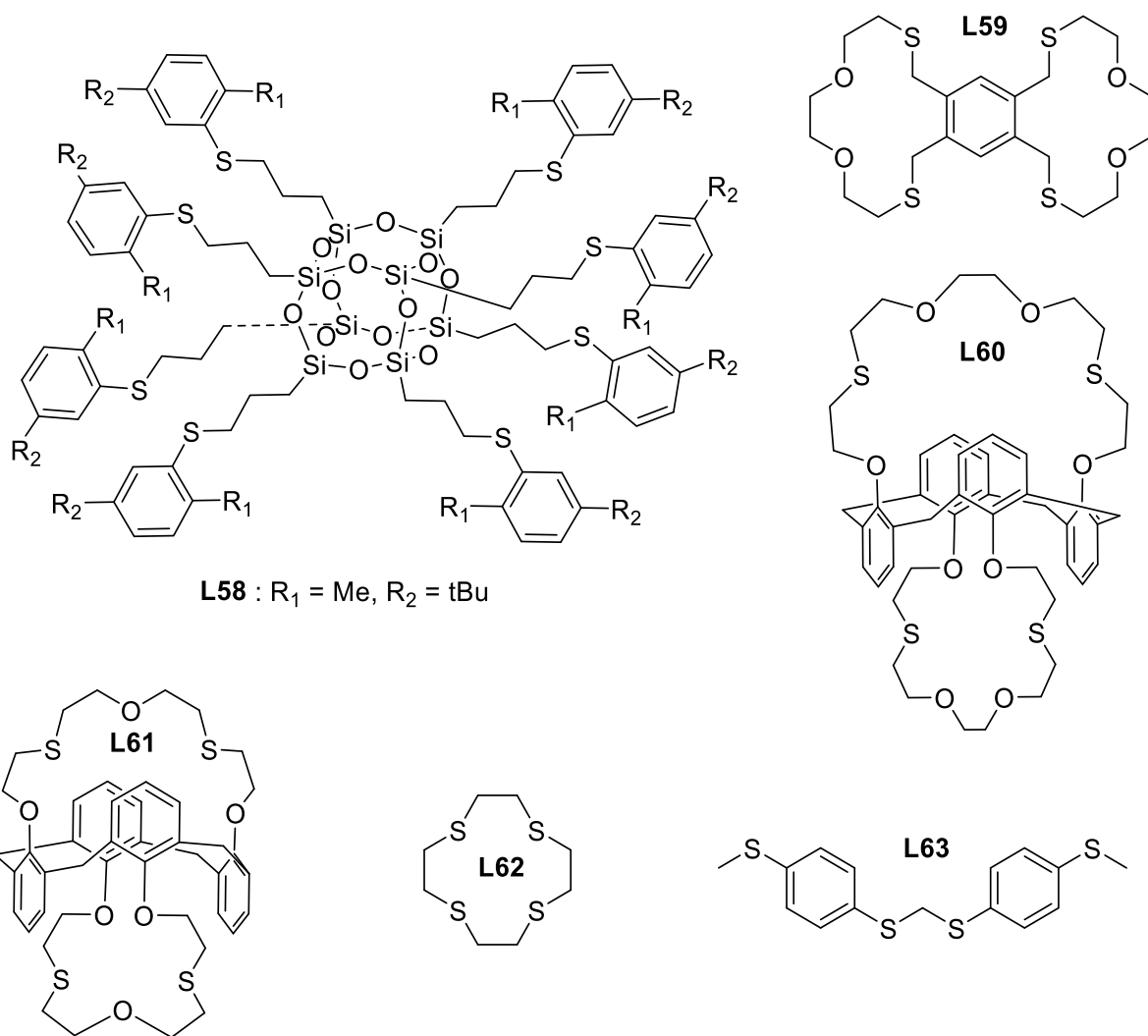


Figure 9. Structures of polythioethers ligands.

Table 5. Structural features of the cubane-containing materials: polythioethers/CuI.

#	cluster	xD-Formula	Cu-Cu distances [Average] (Å)	ref	#CCDC
1	Cubane	$3\text{D}[\text{Cu}_4\text{I}_4(\mathbf{L58})_{0.5}]_n^a$	2.791, 2.700, 2.700, 2.700, 2.700, 2.791 [2.730]	[20]	1573709
2	Cubane	$1\text{D}[\text{Cu}_4\text{I}_4(\mathbf{L59})]_n \cdot 2\text{CH}_3\text{CN}^b$	2.624, 2.949, 2.624, 2.839, 2.901, 2.911 [2.808]	[35]	1419091
3	Cubane + Rhomboid	$3\text{D}[(\text{Cu}_2\text{I}_2)\mathbf{L60}(\text{Cu}_4\text{I}_4)]_n \cdot (\text{CH}_2\text{Cl}_2)(\text{CH}_3\text{CN})^c$	2.810, 2.739, 2.671, 2.675, 2.739, 2.810 [2.741]	[51]	695117
4	Cubane	$3\text{D}[\text{Cu}_4\text{I}_4(\mathbf{L61})]_n^d$	2.658, 2.744, 2.805, 2.748, 2.607, 2.995 [2.760]	[56]	661963
5	Cubane	$2\text{D}[\text{Cu}_4\text{I}_4(\mathbf{L62})]_n$	2.640, 2.713, 2.713, 2.713, 2.713, 2.640 [2.689]	[63]	159365
6	Cubane	$?D[\text{Cu}_4\text{I}_4(\mathbf{L63})]_n^e$		[32]	-

^a SBU = substituent sensitive ; ^b flat bicyclic ligand ; ^c SBU = temp. sensitive ; ^d mixt. of two CPs ; ^e based on chem. anal. + lumin.

Tables 1-5 also provide the Cu^{•••}Cu distances along with their average. Notably, the average Cu^{•••}Cu separations always fall slightly under the sum of the van der Waals radius (*i.e.* < 2.8 Å).

The few exceptions include entry 12 in Table 1 (2.911 Å) and three that are close to this sum (Table 1; entries 23 (2.814) and 30 (2.813 Å); Table 5; entry 2 (2.808 Å)). In brief, the closed cubane SBUs exhibit weak Cu \cdots Cu interactions. The shortest average Cu \cdots Cu distance is 2.668 Å (Table 2, entry 1), which approaches the sum of the covalent radius (2.64 Å), suggesting strong Cu \cdots Cu interactions. The shortest Cu-Cu distance is 2.632 Å (also Table 2, entry 1). The relatively modest structural flexibility of the cubane motif compared to the rhomboid is further analyzed in Section 8.2. In overall, these recurrent structural features bear a consequence on the photophysical properties, namely regarding the nature of the lowest energy excited state to be described below. In addition, the presence of multiple Cu-I and weak Cu \cdots Cu interactions has for effect to render the cluster structure more rigid. This significant feature is beneficial to reduce the efficiency of the non-radiative deactivation pathways, thus rendering this *globular* cluster more emissive. The photophysical properties are described below.

3. *Quasi-planar* structure of the Cu_xI_xS_y species

The Cu₂I₂S₄ rhomboid geometry is also common as SBUs and motifs for discrete complexes [11,15,16,20,24,27–29,31,35–37,43,45,47,51–54,57,63,66,67,71,74,77–97]. The main reason stems from its small size and its significant packing adaptability. The structural features of the corresponding CPs are provided in **Table 7-Table 8** (the ligand structures are placed in **Figures 10, 12-13**). It is noteworthy that several seleno-analogues exist, and their CPs are presented below. Again, sensitive to the L/M ratio means that the formation of *globular* motifs (mostly cubane) or *quasi-planar* ones (most often rhomboid) can be directed with the appropriate L/M stoichiometry. Overall, the number of reported examples of rhomboid-containing materials is comparable to that of the Cu₄I₄S₄ cubanes. The acyclic dithioether ligands have a strong propensity to stabilize this (rhomboid) geometry (**Table 7**). Despite the small sampling, for ligands of the general structure RE-CH₂-ER, only 1D CPs are formed (E = S [27], Se [70], Te [70]), which mirrors the trend for the cubane-containing materials (**Table 1**). Again, the seleno- and telluroether species will be presented below. This early mention is to stress that the series behave the same way. In addition, the Cu \cdots Cu distances turned out to be highly variable (2.582 (Table 9, entry 4) < Cu \cdots Cu < 3.367 Å (Table 7, entry 4)), contrasting with the cubane motif. This feature is further analyzed in Section 8.2.

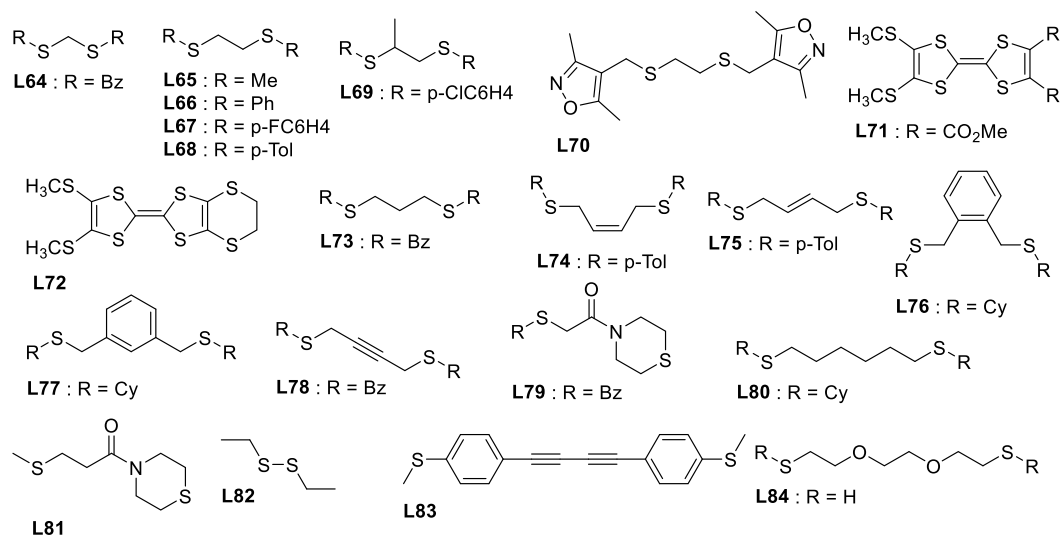


Figure 10. Structures and codes of acyclic dithioether ligands forming *quasi-planar* neutral Cu_xI_xS_y used in this review.

Table 6. Structural features of the *quasi-planar*-containing materials: acyclic dithioethers/CuI; rhomboids at the top, other *quasi-planar* species at the bottom.

#	cluster	xD-Formula	Cu-Cu distance (Å)	L/M ratio sensitive?	ref	#CCDC
1	Rhomboid	1D-[Cu ₂ I ₂ (L64) ₂] _n	2.774	no	[27]	1960061
2	Rhomboid	0D-[Cu ₂ I ₂ (L65) ₂] ^a	2.687	—	[95]	-
3	Rhomboid	2D-[Cu ₂ I ₂ (L66) ₂] _n	2.806	—	[54]	623107
4	Rhomboid	1D-[Cu ₂ I ₂ (L67) ₂] _n	2.781	—	[7]	1835102
5	Rhomboid	2D-[Cu ₂ I ₂ (L69) ₂] _n	2.898	—	[6]	1873371
6	Rhomboid	?D-[Cu ₂ I ₂ (L70)] ^b	—	—	[8]	-
7	Rhomboid	0D-[Cu ₂ I ₂ (L71) ₂]	2.647	—	[93]	256153
8	Rhomboid	0D-[Cu ₂ I ₂ (L72) ₂]	2.732	—	[16,94]	1219211
9	Rhomboid	2D-[Cu ₂ I ₂ (L9) ₂] _n	2.734	—		
10	Rhomboid	2D-[Cu ₂ I ₂ (L9) ₂] _n	2.826	yes	[28]	906347
11	Rhomboid	1D-[Cu ₂ I ₂ (L73) ₂] _n	3.092	no	[27]	1960064
12	Rhomboid	2D-[Cu ₂ I ₂ (L15) ₂] _n	2.796	yes	[27]	1960068
13	Rhomboid	2D-[Cu ₂ I ₂ (L16) ₂] _n ^c	2.856	yes	[24]	1418762*
14	Rhomboid	2D-[Cu ₂ I ₂ (L16) ₂] _n	2.675	—		
15	Rhomboid	2D-[Cu ₂ I ₂ (L74) ₂] _n ^c	2.952	yes	[24]	1418780
16	Rhomboid	0D-[Cu ₂ I ₂ (L76) ₂]	2.956	—	[52]	649208
17	Rhomboid	0D-[Cu ₂ I ₂ (L78) ₂]	2.928	—	[29]	1040060
18	Rhomboid	1D-[Cu ₂ I ₂ (L19) ₂] _n	3.009	yes	[28]	906351
19	Rhomboid	2D-[Cu ₂ I ₂ (L20) ₂] _n	2.855	yes	[28]	906353
20	Rhomboid	2D-[Cu ₂ I ₂ (L77) ₂] _n	2.757	—	[52]	649209
21	Rhomboid	1D-[Cu ₂ I ₂ (L23) ₂] _n ^d	2.980	yes	[53]	660759
22	Rhomboid	2D-[Cu ₂ I ₂ (L79) ₂] _n ^d	2.856	yes	[57]	616429
23	Rhomboid	2D-[Cu ₂ I ₂ (L22) ₂] _n	2.828	yes	[27]	1960071
24	Rhomboid	1D-[Cu ₂ I ₂ (L14) ₂] _n	3.241	yes	[31]	952723
25	Rhomboid	2D-[Cu ₂ I ₂ (L81) ₂] _n	2.904	—	[98]	615567
26	Rhomboid	2D-[Cu ₂ I ₂ (L24) ₂] _n	2.833	yes	[45]	785685
27	Rhomboid	2D-[Cu ₂ I ₂ (L25) ₂] _n	2.742	yes	[27]	1960075
28	Rhomboid	1D-[Cu ₂ I ₂ (L28) ₂] _n	2.848	yes	[27]	1960079

27	Rhomboid	1D-[Cu ₂ I ₂ (L33) ₂] _n	2.777	yes	[27]	1960084
28	Rhomboid	2D-[Cu ₂ I ₂ (L130) ₂] _n	2.796	yes	[26]	-
29	Rhomboid	2D-[Cu ₂ I ₂ (L35) ₂] _n · (MeCN)(H ₂ O) ^c	2.836	yes	[45]	785687
30	1D-twisted ribbon	1D-[Cu ₂ I ₂ (L82) ₂] _n		—	[99]	1110569
31	1D-accordion ribbon	3D-[Cu ₄ I ₄ (L18) ₂] _n		yes	[12]	1855099
32	Step staircase	2D-[Cu ₄ I ₄ (L83) ₃] _n		—	[23]	-
33	1D-accordion ribbon	2D-[Cu ₂ I ₂ (L75) ₂] _n		—	[24]	1418779
34	1D-accordion ribbon	2D-[Cu ₂ I ₂ (L84) ₂] _n		—	[96]	230595
35	1D-staircase ribbon	1D-[Cu ₂ I ₂ (L68) ₂] _n		—	[26]	-
36	1D-staircase ribbon	2D-[Cu ₂ I ₂ (L129) ₂] _n		—	[26]	-

^a no X-ray data ; ^b butterfly ; ^c SBU sensitive to *cis-* vs *trans-* ; ^d rare case of asymmetric ligand ; ^e 14-atom chain ; * multiple temperature available.

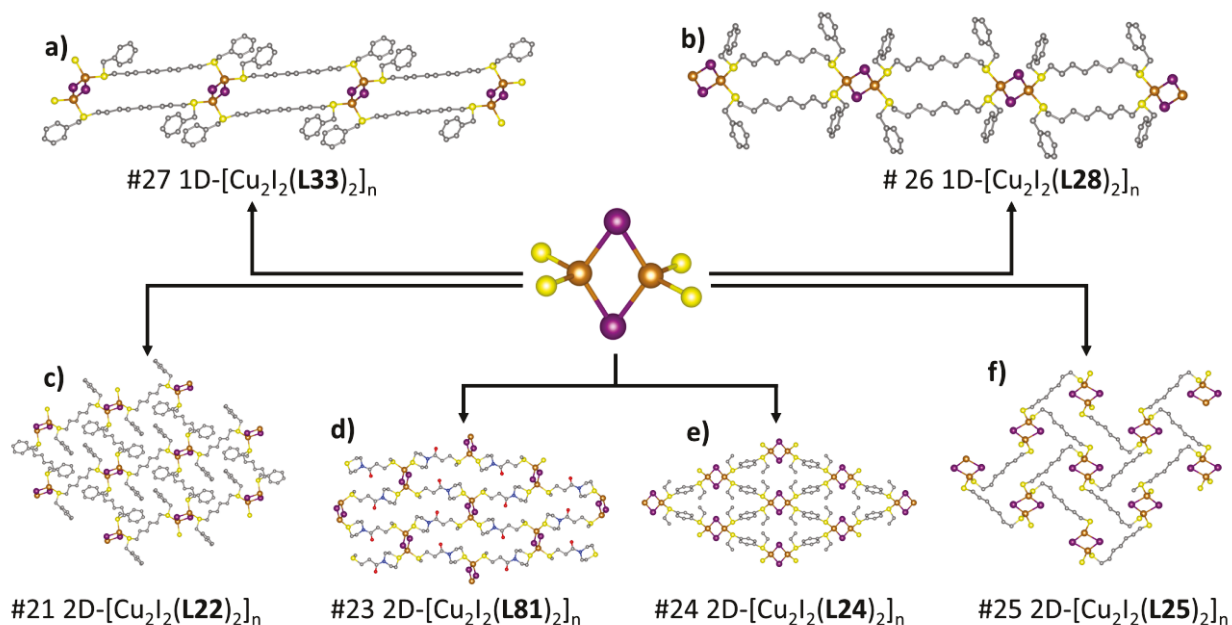


Figure 11. Scheme illustrating how the rhomboid motifs Cu₂I₂S₄ can be linked with acyclic dithioether ligands to form various coordination polymers listed in **Table 6**. Color code: O, red ; S, yellow; Cu, orange ; I, purple ; C, grey, Hydrogen atoms were omitted for clarity. The images were reproduced using the cif files from the Cambridge Crystallographic Data Centre; CCDC number: a) 1960084, b) 1960079, c) 1960071, d) 615567, e) 785685 and f) 1960075.

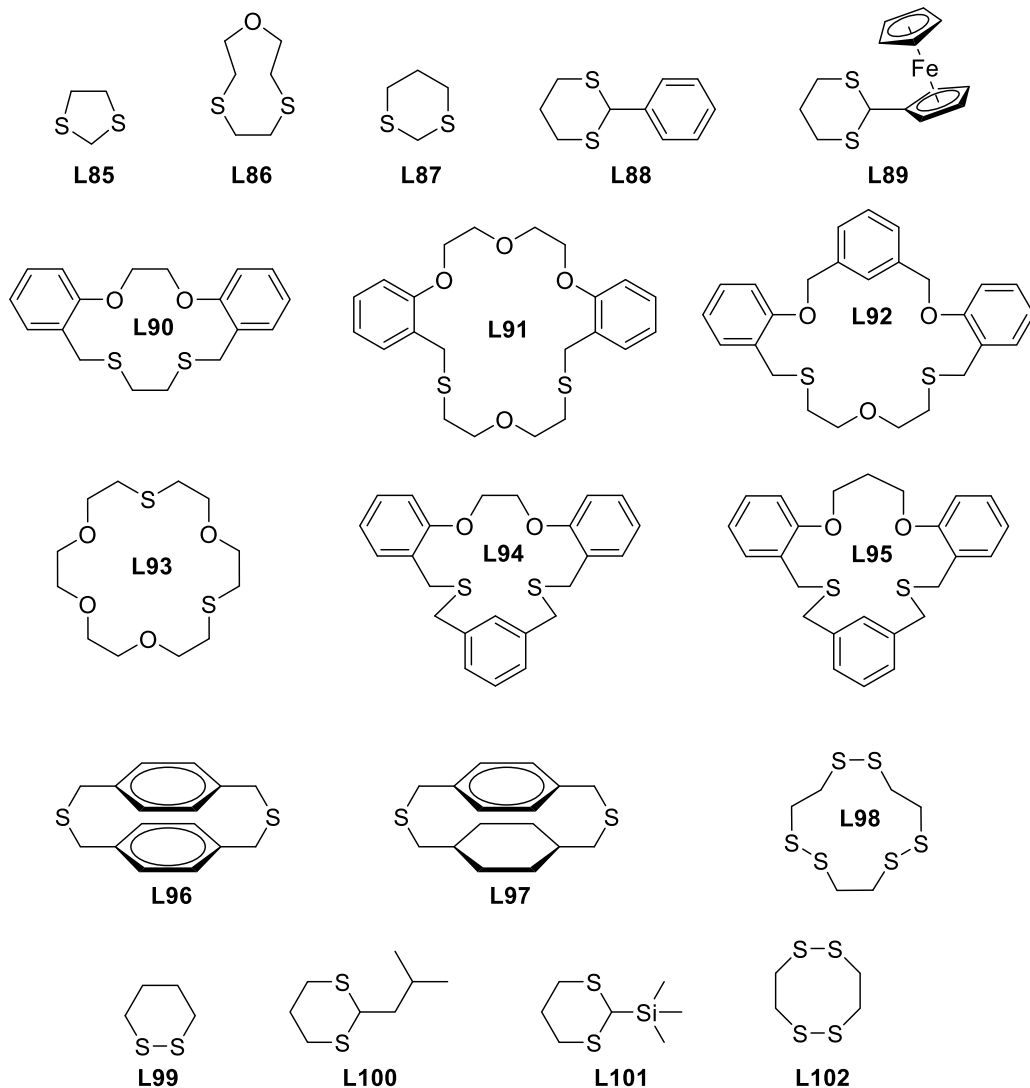


Figure 12. Structures and codes of other cyclic dithioether ligands.

Table 7. Structural features of the quasi-planar-containing materials: cyclic dithioethers/CuI; rhomboids at the top, other *quasi-planar* species at the bottom.

#	cluster	xD-Formula	Cu-Cu distance (Å)	L/M ratio sensitive?	ref	#CCDC
1	Rhomboid	2D-[Cu ₂ I ₂ (L85) ₂] _n	2.908	—	[97]	1533541*
2	Rhomboid	0D-[Cu ₂ I ₂ (L86) ₂] _n	2.860	—	[96]	230598
3	Rhomboid	1D-[Cu ₂ I ₂ (L87) ₂] _n	2.890	no	[77]	1888353
4	Rhomboid	1D-[Cu ₂ I ₂ (L47) ₂] _n ^a	3.367	yes	[74]	1827913
5	Rhomboid	2D-[Cu ₂ I ₂ (L47) ₂] _n ^a	2.766	yes	[74]	1827914
6	Rhomboid	1D-[Cu ₂ I ₂ (MeCN) ₂ (L88)] _n	2.696	yes	[77]	1888654
7	Rhomboid	0D-[Cu ₂ I ₂ (L89) ₂ (MeCN) ₂]	2.690	yes	[77]	1888524
8	Rhomboid	1D-[Cu ₂ I ₂ (L90) ₂] _n · MeCN ^b	3.208	—	[82]	790794
9	Rhomboid	0D-[Cu ₂ I ₂ (L90) ₂]	2.762, 2.688	—	[82]	790793
10	Rhomboid	0D-[Cu ₂ I ₂ (L38)] ^c	2.683	—	[67,68]	725340
11	Rhomboid	0D-[Cu ₂ I ₂ (L91) ₂]	2.846	—	[79]	965570

12	Rhomboïd	0D-[Cu ₂ I ₂ (L92) ₂] · CH ₂ Cl ₂	2.701, 2.802	—	[47]	809852
13	Rhomboïd	1D-[Cu ₂ I ₂ (L93) ₂] _n	3.068	—	[86]	207825
14	Rhomboïd	1D-[Cu ₂ I ₂ (L43) ₂] _n ^d	2.973	—	[43]	822022
15	Rhomboïd	1D-[Cu ₂ I ₂ (L94) ₂] _n · CH ₂ Cl ₂	3.072	—	[83]	679192
16	Rhomboïd	2D-[Cu ₂ I ₂ (L95) ₂] _n	3.169	—	[83]	679193
17	Rhomboïd	2D-[Cu ₂ I ₂ (L96) ₂] _n · THF	3.179	—	[15]	1316861
18	Rhomboïd	2D-[Cu ₂ I ₂ (L97) ₂] _n · 2 H ₂ O	2.877	—	[85]	273267
19	Rhomboïd	1D-[Cu ₂ I ₂ (L98) ₂] _n ^e	2.795	—	[88]	1119623
20	Rhomboïd	1D-[Cu ₂ I ₂ (L99) ₂] _n	2.684	—	[80]	776927
21	Rhomboïd	2D-[Cu ₂ I ₂ (L43) ₂] _n ^f	2.756	no	[76]	135283
22	Linked rhomboïd	1D-[Cu ₂ I ₂ (L89)] _n		yes	[77]	1888515
23	Step staircase	2D-[Cu ₄ I ₄ (L34)(MeCN) ₂] _n ^g		yes	[49]	739725
24	Step staircase	2D-[Cu ₈ I ₈ (L34) ₃ (MeCN) ₂] _n ^g		yes	[49]	739726
25	Trinuclear cluster	2D-[Cu ₃ I ₃ (L100) ₂] _n		—	[77]	1888479
26	Trinuclear cluster	2D-[Cu ₃ I ₃ (L88) ₂] _n		—	[77]	1888490
27	1D-zig zag ribbon	1D-[Cu ₂ I ₂ (L101)] _n		—	[77]	1888483
28	1D-zig zag ribbon	1D-[Cu ₂ I ₂ (L89)] _n		—	[77,97]	1533543
29	Cu ₄ I ₅	2D-[{Cu ₄ I ₅ (L43) ₂ }K] _n ^h		—	[76]	135285
30	1D-acordeon ribbon	1D-[Cu ₂ I ₂ (L102)] _n		—	[88]	1119621

^a synthesis is solvent dependent ; ^b mixture with 0D ; ^c mixture with 1D ; ^d slow, + [Co(H₂O)₆]ClO₄ ; ^e behaves like a bidentate ; ^f sensitive to addition of NaI or KI ; ^g solvent depend. ; ^h K⁺ shared between 2 thiacycrown sens. to addition of NaI or KI ; * multiple temperature available.

Table 8. Structural features of the rhomboids-containing materials: monothioethers/CuI, cyclic and acyclic, rhomboids at the top, other *quasi-planar* species at the bottom.

#	cluster	xD-Formula	Cu-Cu distance (Å)	L/M ratio sensitive?	ref	#CCDC
1	Rhomboïd	0D-[Cu ₂ I ₂ (L56) ₄] ^a	2.675	—	[37,66,91]	-
2	Rhomboïd	2D-[{Cu ₂ I ₂ } ₃ (L56) ₆] _n · MeCN ^a	2.972	—	[37]	977484
3	Rhomboïd and cubane	2D-[[Cu ₄ I ₄ (L56) ₂](L56) ₂ (Cu ₂ I ₂)(L56) ₂ [Cu ₄ I ₄ (L56)(MeCN)] _n ^a	2.754	—	[37]	977481
4	Rhomboïd	1D-[Cu ₂ I ₂ (L48) ₃] _n ^b	2.684	—	[36,66]	-
5	1D-staircase ribbon	1D-[Cu ₄ I ₄ (L49) ₂ (MeCN) ₂] _n		—	[36]	1047395

^a sensitive to exp. conditions; ^b in n-heptane.

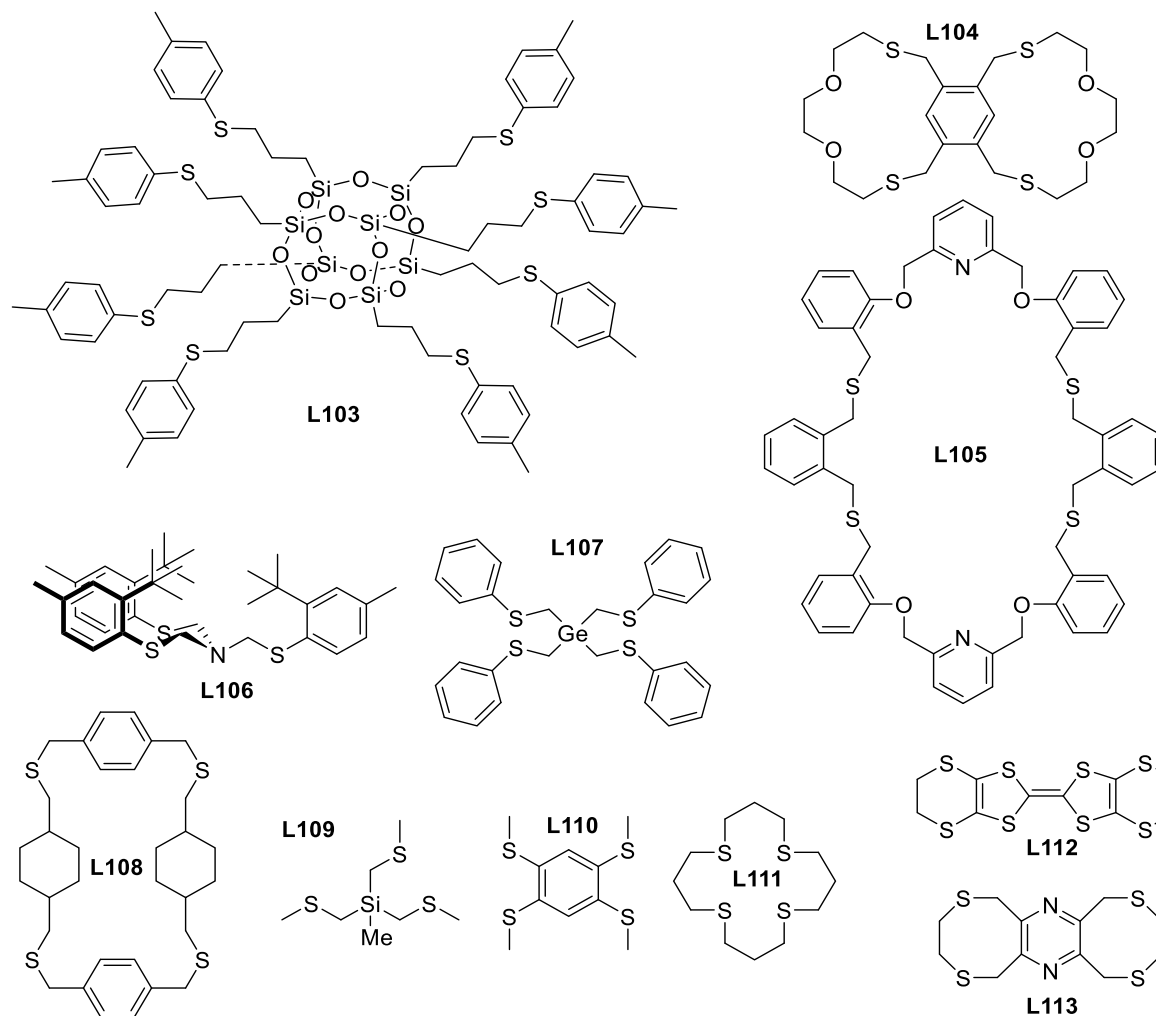


Figure 13. Structures of polythioethers ligands.

Table 9. Structural features of the rhomboid-containing materials: polythioethers/CuI.

#	cluster	xD-Formula	Cu-Cu distance (Å)	L/M ratio sensitive?	ref	#CCDC
1	Rhomboid	3D-[Cu ₂ I ₂ (L103) _{0.5}] _n ^a	2.739	—	[20]	1573708
2	Rhomboid	1D-[Cu ₂ I ₂ (L104)] _n ^b	2.876	—	[35]	1419092
3	Rhomboid	0D-[(Cu ₂ I ₂) ₂ (L105) ₂ ·(2CH ₃ CN)(2 toluene)] ^c	2.902 2.965	—	[78]	1417220
4	Rhomboid	0D-[Cu ₂ I ₂ (L106) ₂] ^d	2.582	—	[11]	782635
5	Rhomboid	2D-[Cu ₂ I ₂ (L107)] _n	2.943	—	[81]	698029
6	Rhomboid	3D-[Cu ₂ I ₂ (L108)] _n ·THF	2.883	—	[84]	635118
7	Rhomboid	3D-[Cu ₂ I ₂ (L61)] _n ^a	2.689	—	[56]	661962
8	Rhomboid	0D-[Cu ₂ I ₂ (L109) ₂]	2.863	—	[87]	221614
9	Rhomboid	1D-[Cu ₂ I ₂ (L110) ₂] _n	2.816	—	[89,90]	-
10	Rhomboid	3D-[Cu ₂ I ₂ (L111) ₂] _n	2.808	yes	[63]	159366
11	Rhomboid	0D-[Cu ₂ I ₂ (L112) ₂]	2.732 2.734	—	[16]	1219211
12	Rhomboid	2D-[Cu ₂ I ₂ (L113)] _n	2.776	—	[100]	1994655
13	Trinuclear cluster	3D-[Cu ₃ I ₃ (L60)(MeCN)] _n ·(CH ₂ Cl ₂)(2H ₂ O) ^e	—	—	[51]	695115
14	Trinuclear cluster	3D-[Cu ₃ I ₃ (L60)] _n ·(0.5H ₂ O) ^e	—	—	[51]	695116

^a SBU sensitive to substituents ; ^b cyclic ; ^c 2 x cyclic-L ; ^d steric and dandling arm ; ^e T depend.

4. Thione ligands with the $\text{Cu}_x\text{I}_x\text{S}_y$ species

This category of S-containing ligands exhibits a similar coordination scheme as that of the thioethers but strikingly favors the formation of rhomboid and step staircase SBUs. The less cumbersome C=S moiety provides other SBU and discrete cluster motifs (**Figure 14**). Examples are presented in

Table 10 [9,99,101–110]. The ligand structures are placed in **Figure 15**. This type of ligand shares obvious structural resemblance and coordination traits with the acyclic monoethers (monodentate and bridging) and so the resulting CuI-containing materials bear the same or similar SBU motifs (**Table 8** vs

Table 10). These geometries are all *globular* shaped, except for the 1D-polyrhomboid. Another notable feature is that the electron richer C=S center renders this ligand stronger than thioethers. Consequently, for ditopic ligands containing one or two amine centers, the thione unit binds the metal preferably first. In overall, the accommodating rhomboid motif is also a frequently encountered geometry in this category (seven examples vs three other quasi-planar motifs: *i.e.* step staircase and 1D-polyrhomboid). Only three *globular* motifs are reported so far and notably no cubane-shaped species have been reported for the thione/ $\text{Cu}_x\text{I}_x\text{S}_y$ -containing materials. Concurrently, one cubane complex of formula $\text{Cu}_4\text{X}_4(\text{L116})_4$ is known [109], which is rare for X = Cl, Br, suggesting that the absence of Cu_4I_4 -cubane complexes in this list is most likely due to the small sampling available.

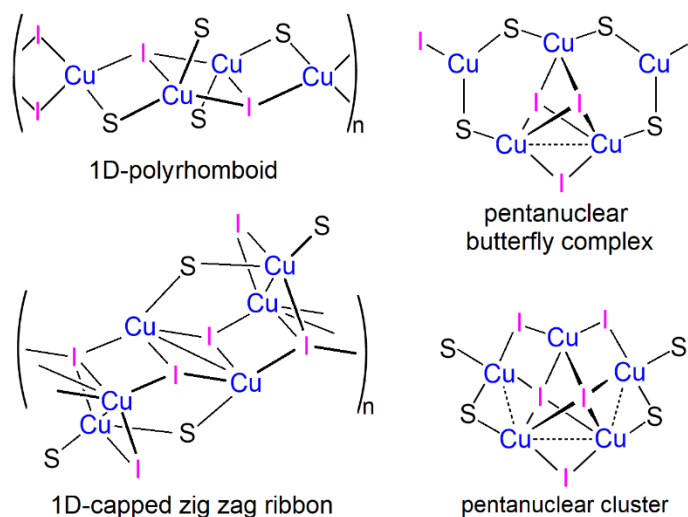


Figure 14. Structures of the various SBUs or discrete complexes encountered for neutral $\text{Cu}_x\text{I}_x\text{S}_y$ motifs when thione-containing ligands are used as assembling entity.

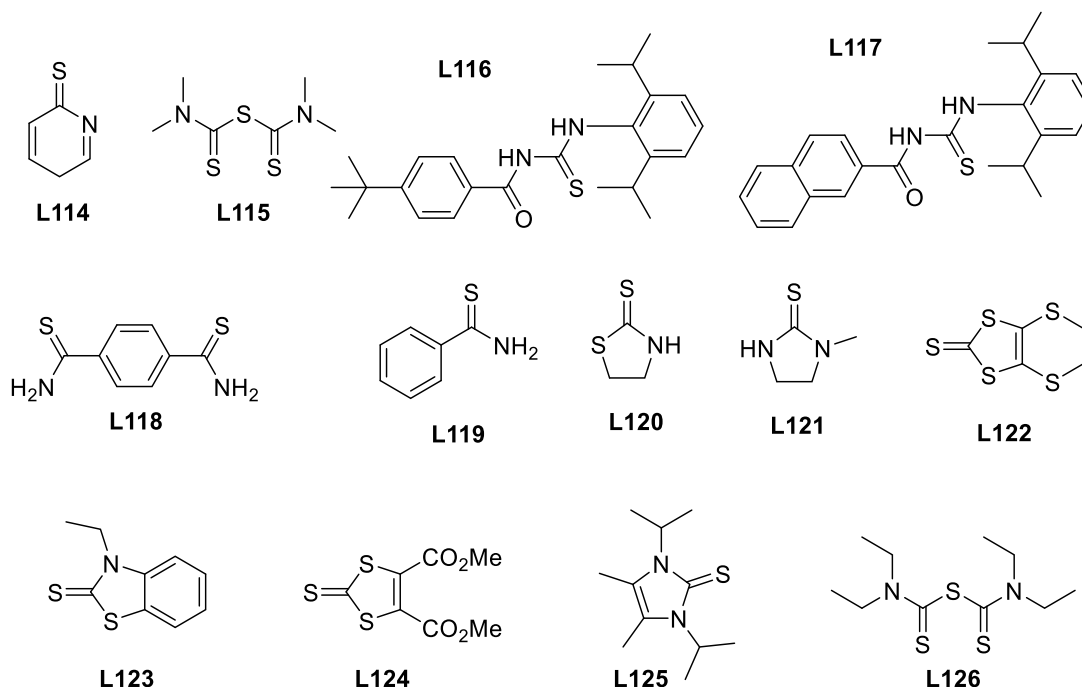


Figure 15. Structures of thione-containing ligands.

Table 10. Structural features of the thione-containing/ Cu_xI_x materials. The *quasi-planar* motifs are placed at the top, and the *globular* ones at the bottom.

#	cluster	xD-Formula	ref	#CCDC
1	Rhomboïd	0D- $[\text{Cu}_2\text{I}_2(\text{L114})_4]^a$	[103]	1181710
2	Rhomboïd	0D- $[\text{Cu}_2\text{I}_2(\text{L115})_2]$	[104]	1249836
3	Rhomboïd	0D- $[\text{Cu}_2\text{I}_2(\text{L116})_2]$	[109]	1450707
4	Rhomboïd	0D- $[\text{Cu}_2\text{I}_2(\text{L117})_2]$	[109]	1450708
5	Rhomboïd	2D- $[\text{Cu}_2\text{I}_2(\text{L118})_2]_n \cdot \text{DMF}^b$	[101]	1835557
6	Rhomboïd	0D- $[\text{Cu}_2\text{I}_2(\text{L119})_4] \cdot \text{MeCN}^c$	[101]	1835548*
7	Rhomboïd	1D- $[\text{Cu}_2\text{I}_2(\text{L119})_2]_n^c$	[101]	1835540
8	Rhomboïd	0D- $[\text{Cu}_4\text{I}_4(\text{L120})_4]$	[102]	880493
9	1D-polyrhomboid	1D- $[\text{Cu}_4\text{I}_4(\text{L121})_4]_n^d$	[102]	880492
10	Step staircase	3D- $[\text{Cu}_4\text{I}_4(\text{L122})_4]_n^e$	[108]	1217211
11	Step staircase	3D- $[\text{Cu}_4\text{I}_4(\text{L123})_5]_n^e$	[9,110]	1827572
12	1D-acordeon ribbon	1D- $[\text{Cu}_2\text{I}_2(\text{L124})_2]_n$	[93]	256154
13	Pentannuclear butterfly complex	0D- $[\text{Cu}_5\text{I}_5(\text{L125})_4] \cdot \text{THF}$	[105]	1041989
14	Pentannuclear cluster	0D- $[\text{Cu}_5\text{I}_5(\text{L126})_2] \cdot (\text{MeCN})(\text{EtOH})^a$	[106,107]	1278976
15	1D-capped zig zag ribbon	1D- $[\text{Cu}_3\text{I}_3(\text{L119})]_n^c$	[101]	1835550*

^a two thione functions, chelate ; ^b two thione functions ; ^c L/M ratio and condition-dependent ; ^d condition-dependent;

^e bidentate ; * multiple temperature available.

5. $\text{Cu}_x\text{Br}_x\text{S}_y$ species

$\text{Cu}_x\text{Br}_x\text{S}_y$ -containing materials have also been significantly explored where about sixty X-ray structures have been reported (Table 11-Table 16). It is noteworthy that the resulting SBUs are overwhelmingly $\text{Cu}_2\text{Br}_2\text{S}_4$ rhomboid, but interestingly several new motifs for SBUs have been identified (*i.e.* not already observed for the iodide; Figure 16). The ligand structures are placed in Figure 17.

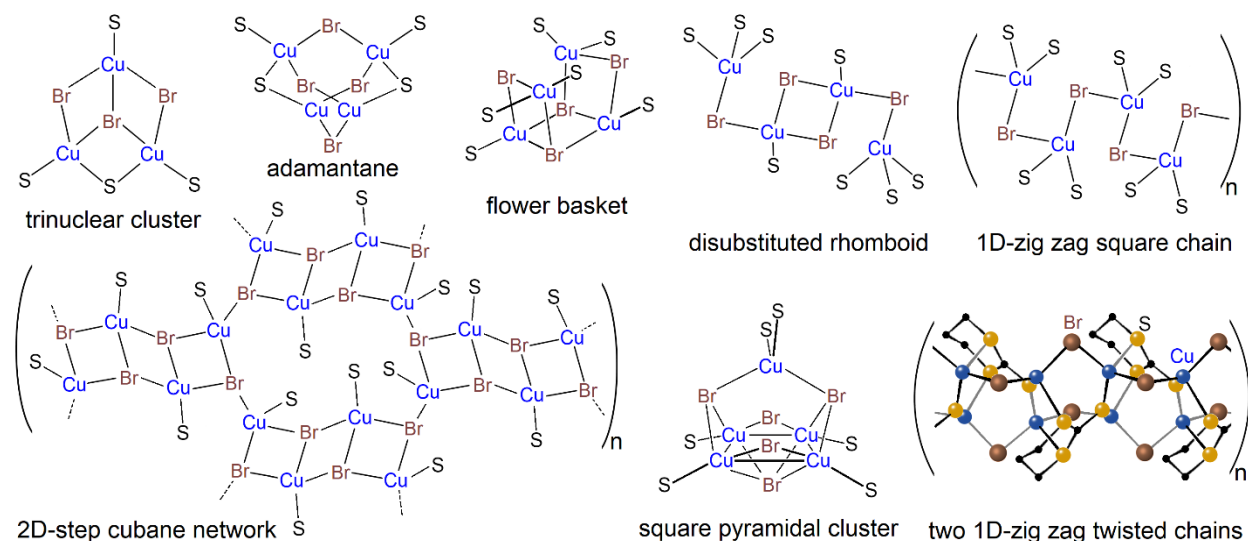


Figure 16. Structures of the various SBUs or discrete complexes encountered for neutral $\text{Cu}_x\text{Br}_x\text{S}_y$ motifs when mono- and dithioether- and thione-containing ligands are used as assembling entity. The motifs that are already represented (cubane, rhomboid, 1D-zig zag ribbon) for the $\text{Cu}_x\text{I}_x\text{S}_y$ species and the simple Cu-Br-Cu-Br chain are not included in this figure.

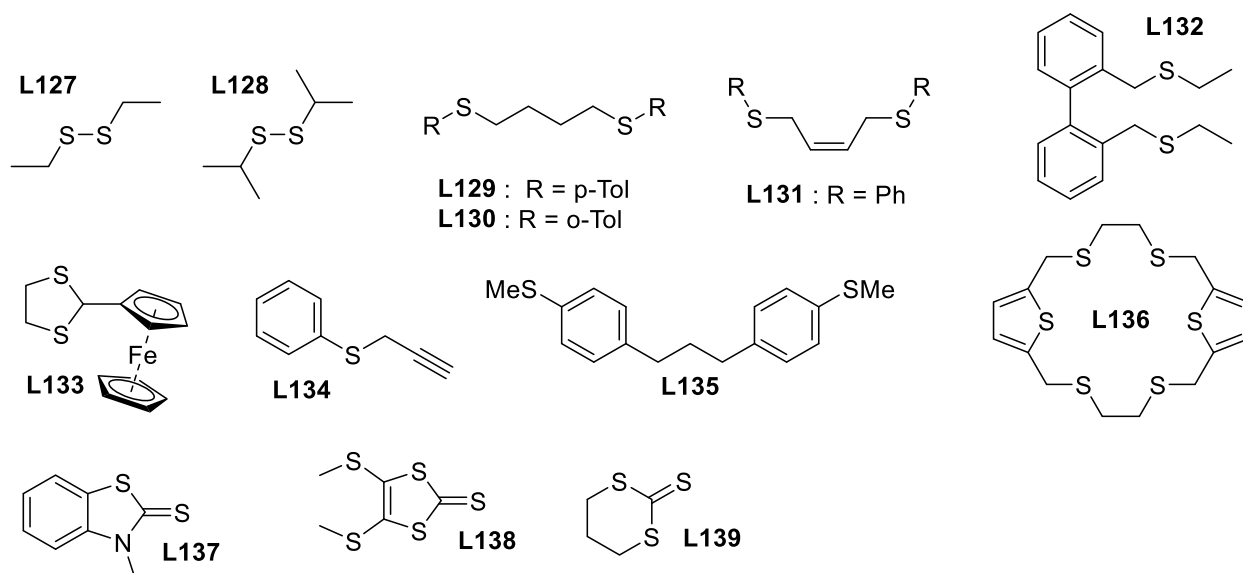


Figure 17. Structures of cyclic, acyclic thio diether and thiones ligands.

Table 11. Structural features of the $Cu_xBr_xS_y$ -containing materials: acyclic dithioethers/CuBr.

#	cluster	xD-Formula	Cu-Cu distance (Å)	L/M ratio sensitive?	ref	#CCDC
1	2D-step cubane network	2D-[$Cu_4Br_4(L127)_2$] _n		—	[111,112]	288131
2	1D-distorted ribbon	1D-[$Cu_5Br_5(L128)$] _n		—	[111]	288129
3	-Cu-Br- chain	1D-[$Cu_2Br_2(L127)_2$] _n		—	[111]	288132
4	Rhomboid	1D-[$Cu_2Br_2(L5)_2$] _n	2.8097	—	[30,32]	974339
5	Rhomboid	1D-[$Cu_2Br_2(L64)_2$] _n	2.8829	—	[27]	1960062
6	Rhomboid	1D-[$Cu_2Br_2(L1)_2$] _n	2.9192	—	[30]	974337
7	Rhomboid	0D-[$Cu_2Br_2(L2)_4$]	2.8099	yes	[30]	974338
8	Rhomboid	1D-[$Cu_2Br_2(L3)_2$] _n	2.8503	—	[30]	974340
9	Rhomboid	0D-[$Cu_2Br_2(L4)_2(MeCN)_2$]	3.0667	yes	[30]	974341
10	Rhomboid	0D-[$Cu_2Br_2(L70)$] _a	-	—	[8]	-
11	Rhomboid	1D-[$Cu_2Br_2(L9)$] _n ^b	2.7761	—	[28]	906349
12	-Cu-Br- chain	1D-[$CuBr(L73)$] _n	2.7941	—	[27]	1960065
13	Rhomboid	3D-[$Cu_2Br_2(L10)$] _n	4.1169	—	[18]	1488068
14	Rhomboid	2D-[$Cu_2Br_2(L129)$] _n	3.459	—	[26]	-
15	Rhomboid	1D-[$Cu_2Br_2(L15)_2$] _n ^c	2.8678	—	[27]	1960069
16	Rhomboid	2D-[$Cu_2Br_2(L15)_2$] _n ^c	3.0159	—	[27]	1960069
17	Rhomboid	2D-[$Cu_2Br_2(L16)_2$] _n	2.9951	—	[24]	1418771
18	Rhomboid	0D-[$Cu_2Br_2(L131)_2$]	2.7422	—	[24]	1418776
19	Rhomboid	?D-[$Cu_2Br_2(L75)_2$] _n	2.9008	—	[24]	-
20	Rhomboid	2D-[$Cu_2Br_2(L74)_2$] _n	2.7396	—	[24]	1418781
21	Rhomboid	0D-[$Cu_2Br_2(L78)_2$]	-	—	[29]	1040061
22	Rhomboid	1D-[$Cu_2Br_2(L17)_2$] _n	2.9943	—	[29]	1042236
23	Rhomboid	1D-[$Cu_2Br_2(L19)$] _n	2.9662	—	[28]	906352
24	Rhomboid	1D-[$Cu_2Br_2(L20)$] _n	2.9306	—	[28]	906354
25	Rhomboid	2D-[$Cu_2Br_2(L22)_2$] _n	2.919	—	[27]	1960072
26	Rhomboid	2D-[$Cu_2Br_2(L25)_2$] _n	3.035	—	[27]	1960076
27	Rhomboid	1D-[$Cu_2Br_2(L28)_2$] _n	2.9597	—	[27]	1960080

28	Rhomboid	1D-[Cu ₂ Br ₂ (L33) ₂] _n	2.9178	—	[27]	1960085
29	Rhomboid	1D-[Cu ₂ Br ₂ (L132) ₂]	2.918	—	[113,114]	1309328

^a butterfly, deduced from molecular modelling ; ^b structure containing a half molecule of the free ligand ; ^c Rare case of coexistence of topological isomers within the same crystal structure.

Table 12. Structural features of the Cu_xBr_xS_y-containing materials: cyclic dithioethers/CuBr.

#	cluster	xD-Formula	Cu-Cu distance (Å)	L/M ratio sensitive?	ref	#CCDC
1	1D-zig zag square chain	1D-[CuBr(L85) _n]		—	[97]	1533544
2	Rhomboid	1D-[Cu ₂ Br ₂ (L87) ₂] _n	2.9143	—	[77]	1888455
3	Rhomboid	1D-[Cu ₂ Br ₂ (L47) ₂] _n	3.176	—	[77]	1888460
4	Rhomboid	2D-[Cu ₂ Br ₂ (L100) ₂] _n	2.9057	—	[77]	1888480
5	1D-zig zag ribbon	1D-[Cu ₂ Br ₂ (L101) _n]		—	[77]	1888487
6	Trinuclear cluster	2D-[Cu ₃ Br ₃ (L88) ₂] _n		—	[77]	1888497
7	Staircase	0D-[Cu ₄ Br ₄ (L133) ₂ (MeCN) ₂]	2.8601	—	[97]	1533539
			3.089			
8	Rhomboid	0D-[Cu ₂ Br ₂ (L90) ₂]	2.919	—	[82]	742122
9	Rhomboid	0D-[Cu ₂ Br ₂ (L86) ₂]	2.852	—	[115]	1222362
10	Rhomboid	2D-[Cu ₂ Br ₂ (L41) ₂] _n	3.187	—	[40]	950548
11	Rhomboid	1D-[Cu ₂ Br ₂ (L42) ₂] _n · (2CH ₂ Cl ₂)	2.927	—	[42]	863929
12	-Cu-Br- chain	3D-[CuBr(L96) _n ·MeCN]		—	[14]	232773
13	Rhomboid	1D-[Cu ₂ Br ₂ (L96)(MeCN) ₂] _n	3.128	—	[15]	1316860

Table 13. Structural features of Cu_xBr_xS_y-containing materials: acyclic monothioethers/CuBr.

#	cluster	xD-Formula	Cu-Cu distance (Å)	L/M ratio sensitive?	ref	#CCDC
1	Rhomboid	2D-[Cu ₂ Br ₂ (L48) ₂] _n	2.9512	—	[65,66]	1197543
2	Flower basket + rhomboid	2D[(Cu ₃ Br ₃)(L49) ₃] _n	3.053	—	[36,48]	1047413*
3	Step staircase + rhomboid	1D-[(Cu ₃ Br ₃)(L50) ₃] _n	2.899	yes	[36]	1047399
4	Square pyramidal cluster	2D-[(Cu ₅ Br ₅)(L50) ₃] _n	-	yes	[41]	947670
5	Square pyramidal cluster	2D-[(Cu ₅ Br ₅)(L54) ₃] _n	-	—	[116]	1852284
6	Rhomboid	0D-[Cu ₂ Br ₂ (L134) ₄]	3.006	—	[117]	818803

* multiple temperature available.

Table 14. Structural features of the Cu_xBr_xS_y-containing materials: cyclic monothioethers/CuBr.

#	cluster	xD-Formula	Cu-Cu distance (Å)	L/M ratio sensitive?	ref	#CCDC
1	Rhomboid	2D-[Cu ₂ Br ₂ (L56) ₂] _n	2.778	—	[66]	1190132

Table 15. Structural features of the Cu_xBr_xS_y-containing materials: polythioethers/CuBr.

#	cluster	xD-Formula	Cu-Cu distance (Å)	L/M ratio sensitive?	ref	#CCDC
1	Rhomboid	3D-[Cu ₂ Br ₂ (L103) _{0.5}] _n	2.7825	—	[20]	1573681
2	Rhomboid	1D-[Cu ₂ Br ₂ (L63) ₂] _n	2.679	—	[32]	1479591
			2.613			
3	Rhomboid	1D-[Cu ₂ Br ₂ (L110) _n]	3.107	—	[90]	1294193
4	Rhomboid chain	3D-[Cu ₄ Br ₄ (L62) ₂] _n	3.025	yes	[63]	159364
5	Rhomboid	2D-[Cu ₂ Br ₂ (L136) _n]	2.924	—	[118]	1249902
6	Rhomboid + CuBr	1D-[Cu ₃ Br ₃ (L109) ₂] _n	3.182	—	[119]	140413

Table 16. Structural features of the thione-containing/ Cu_xBr_x materials.

#	cluster	xD-Formula	Cu-Cu distance (Å)	L/M ratio sensitive?	ref	#CCDC
1	Rhomboid	0D- $[\text{Cu}_2\text{Br}_2(\text{L137})_4]$	-		[120]	-
2	Rhomboid	0D- $[\text{Cu}_2\text{Br}_2(\text{L138})_4]$	2.893		[121]	846479
3	Rhomboid	0D- $[\text{Cu}_2\text{Br}_2(\text{L139})_4]$	3.205		[122]	1293533
4	Two 1D-zig zag twisted chains	1D- $[\text{Cu}_2\text{Br}_2(\text{L139})_4]_n \cdot \text{THF}$			[122]	1293532
5	Adamantane-like	0D- $[\text{Cu}_4\text{Br}_4(\text{L116})_4]_b$			[109]	1450706
6	-Cu-Br- chain	1D- $[\text{Cu}_2\text{Br}_2(\text{L119})_2]_n^c$		yes	[101]	1835552*

* multiple temperature available.

6. $\text{Cu}_x\text{Cl}_x\text{S}_y$ species

The X-ray structures of many $\text{Cu}_x\text{Cl}_x\text{S}_y$ -containing materials have also been reported, but to a much lesser extent (nearly 40 X-ray structures; **Table 17-Table 22**). The dominant SBUs are again the $\text{Cu}_2\text{Cl}_2\text{S}_4$ rhomboid, but also, some new motifs have been observed (*i.e.* not already observed for the iodide and bromide; **Figure 18**). The ligand structures are shown in **Figure 19**.

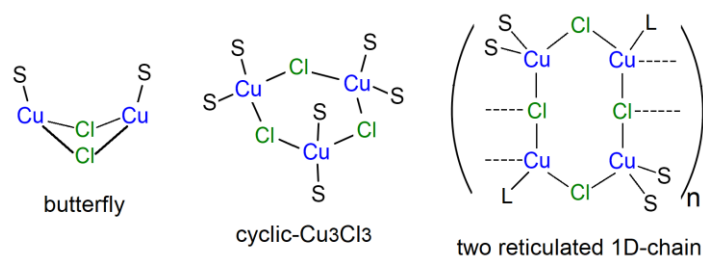


Figure 18. Structures of the various SBUs or discrete complexes encountered for neutral $\text{Cu}_x\text{Cl}_x\text{S}_y$ motifs when mono- and dithioether- and thione-containing ligands are used as assembling entity. The motifs that are already represented (rhomboid, step staircase, adamantane, 1D-zig zag ribbon) for the $\text{Cu}_x\text{I}_x\text{S}_y$ species and the simple Cu-Cl-Cu-Cl chain are not included in this figure.

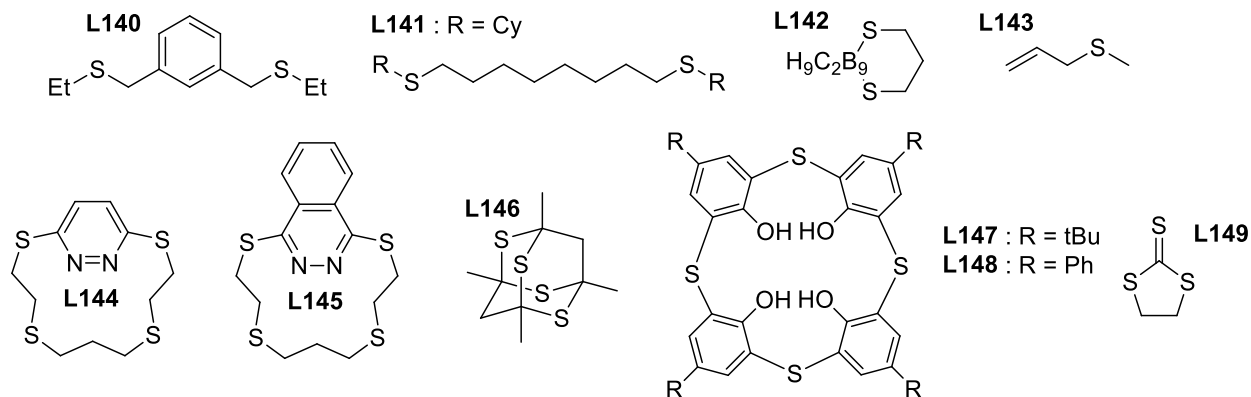


Figure 19. Structures of cyclic, acyclic thio, dihydroether and thiones ligands.

Table 17. Structural features of the $\text{Cu}_x\text{Cl}_x\text{S}_y$ -containing materials: acyclic dithioethers/ CuCl .

#	cluster	xD-Formula	Cu-Cu distance (Å)	L/M ratio sensitive?	ref	#CCDC
1	1D-zig zag ribbon	1D- $[\text{Cu}_2\text{Cl}_2(\mathbf{L128})_2]_n$		—	[111]	288130
2	-Cu-Cl- chain	2D- $[\text{CuCl}(\mathbf{L64})]_n$	4.2016	—	[27]	1960063
3	Rhomboid	0D- $[\text{Cu}_2\text{Cl}_2(\mathbf{L70})]_n^a$		—	[8]	-
4	-Cu-Cl- chain	1D- $[\text{CuCl}(\mathbf{L73})]_n$	3.9595	—	[27]	1960066
5	Rhomboid	3D- $[\text{Cu}_2\text{Cl}_2(\mathbf{L10})]_n^b$	3.290	—	[17]	1886287*
6	Rhomboid	0D- $[\text{Cu}_2\text{Cl}_2(\mathbf{L15})]_n$	2.9083	—	[27]	1960087
7	Rhomboid	2D- $[\text{Cu}_2\text{Cl}_2(\mathbf{L12})_2]_n$	3.123	—	[2]	-
8	Linked Rhomboid	2D- $[\text{Cu}_4\text{Cl}_4(\mathbf{L78})]_n^c$		—	[29]	1042237
9	Rhomboid	2D- $[\text{Cu}_2\text{Cl}_2(\mathbf{L140})_2]_n$	3.0983	—	[123]	1267372
10	Rhomboid	2D- $[\text{Cu}_2\text{Cl}_2(\mathbf{L22})_2]_n$	2.9570	—	[27]	1960073
11	Rhomboid	2D- $[\text{Cu}_2\text{Cl}_2(\mathbf{L96})_2]_n \cdot \text{MeCN}$	2.978	—	[14]	232774
12	Rhomboid	2D- $[\text{Cu}_2\text{Cl}_2(\mathbf{L25})_2]_n$	2.695	—	[27]	1960077
13	Rhomboid	1D- $[\text{Cu}_2\text{Cl}_2(\mathbf{L28})_2]_n$	2.9297	—	[27]	1960081
14	Rhomboid	2D- $[\text{Cu}_2\text{Cl}_2(\mathbf{L141})]_n$	3.0253	—	[2]	-
15	Rhomboid	1D- $[\text{Cu}_2\text{Cl}_2(\mathbf{L33})_2]_n$	2.8883	—	[27]	1960086

^a butterfly, deduced from molecular modelling ; ^b parallel 2D-layers ; ^c two reticulated 1D-chain ; * multiple temperature available.

Table 18. Structural features of the $\text{Cu}_x\text{Cl}_x\text{S}_y$ -containing materials: cyclic dithioethers/ CuCl .

#	cluster	xD-Formula	Cu-Cu distance (Å)	L/M ratio sensitive?	ref	#CCDC
1	Rhomboid	2D- $[\text{Cu}_2\text{Cl}_2(\mathbf{L87})]_n$	2.809	—	[77]	1888456
2	Rhomboid	1D- $[\text{Cu}_2\text{Cl}_2(\mathbf{L47})_2]_n$	3.0517	—	[77]	1888477
3	Rhomboid	2D- $[\text{Cu}_2\text{Cl}_2(\mathbf{L100})_2]_n$	2.8715	—	[77]	1888481
4	1D-zig zag ribbon	1D- $[\text{Cu}_2\text{Cl}_2(\mathbf{L101})]_n$	2.883	—	[77]	1888489
5	-Cu-Cl- chain	1D- $[\text{CuCl}(\mathbf{L85})]_n^b$	-	—	[97]	1533540
6	Rhomboid (proposed)	0D- $[\text{Cu}_2\text{Cl}_2(\mathbf{L142})_2][\text{NMe}_4]_2$	-	—	[124]	-
7	Rhomboid	2D- $[\text{Cu}_2\text{Cl}_2(\mathbf{L41})]_n$	3.178	—	[40]	950547

Table 19. Structural features of $\text{Cu}_x\text{Cl}_x\text{S}_y$ -containing materials: acyclic monothioethers/ CuCl .

#	cluster	xD-Formula	Cu-Cu distance (Å)	L/M ratio sensitive?	ref	#CCDC
1	Rhomboid	2D-[Cu ₂ Cl ₂ (L48) ₂] _n	2.983	—	[65,66]	1190129
2	Cu(II) ₂ Cu(I)Cl ₅	2D-[Cu(I)Cu(II) ₂ Cl ₅ (L54) ₂] _n ^a	3.410 3.265	—	[116]	1851726
3	Rhomboid	2D-[Cu ₂ Cl ₂ (L134) ₂] _n ^b	3.238	—	[117]	818801
4	-Cu-Cl- chain	2D-[Cu ₂ Cl ₂ (L143) ₂] _n	-	—	[117]	818802

^a Cu(I)/Cu(II) mixed valence, ^b ditopic.

Table 20. Structural features of the Cu_xCl_xS_y-containing materials: cyclic monothioethers/CuCl.

#	cluster	xD-Formula	Cu-Cu distance (Å)	L/M ratio sensitive?	ref	#CCDC
1	Rhomboid	1D-[(Cu ₂ Cl ₂) ₂ (L56) ₃] _n ^a	2.836	—	[66,125]	1190131
2	Rhomboid	2D-[(Cu ₂ Cl ₂) ₂ (L56) ₂] _n ^b	2.996	—	[125]	1246844
3	Rhomboid	2D-[(Cu ₂ Cl ₂) ₂ (L56) ₂] _n ^c	2.906	—	[125]	1246845
4	-Cu-Cl- chain	2D-[(Cu ₂ Cl ₂) ₃ (L56) ₂] _n ^d	-	—	[125]	1246846

^a in MeOH, ^b in THF, ^c in CH₂Cl₂, ^d in DME.

Table 21. Structural features of the Cu_xCl_xS_y-containing materials: polythioethers/CuCl.

#	cluster	xD-Formula	Cu-Cu distance (Å)	L/M ratio sensitive?	ref	#CCDC
1	Rhomboid	1D-[Cu ₂ Cl ₂ (L144) ₂] _n ^a	2.816	—	[112]	1298994
2	Cyclic-Cu ₃ Cl ₃	1D-[Cu ₃ Cl ₃ (L145) ₂] _n ^a	-	—	[126]	1172104
3	Step staircase	1D-[Cu ₄ Cl ₄ (L146) ₂] _n	3.005, 2.954, 3.366, 3.471	—	[127]	-
4	Rhomboid	2D-[Cu ₂ Cl ₂ (L147)] _n ·MeOH	2.655	yes	[128]	735303
5	Cu(II) ₄ Cl ₃	0D-[Cu(II) ₄ Cl ₃ (L147)(HCO ₂)(MeOH) ₂ (H ₂ O)] _n (CHCl ₃)(MeOH) _{2.7}	-	yes	[128]	735305
6	Rhomboid	2D-[Cu ₂ Cl ₂ (L148)] _n ·(MeOH)(CHCl ₃) _{0.5}	2.867	yes	[128]	735304
7	Cu(II) ₄ Cl ₄	0D-[Cu(II) ₄ Cl ₄ (L148)(MeOH) ₄] _n	-	yes	[128]	735306

^a bidentate.

Table 22. Structural features of the thione-containing/Cu_xCl_x materials.

#	cluster	xD-Formula	Cu-Cu distance (Å)	L/M ratio sensitive?	ref	#CCDC
1	Two 1D-zig zag twisted chains	1D-[Cu ₂ Cl ₂ (L149)] _n	3.030	—	[129]	1289810
2	Rhomboid	0D-[Cu ₂ Cl ₂ (L137) ₄]	3.059	—	[120]	906821
3	Adamantane-like	0D-[Cu ₄ Cl ₄ (L116) ₄] _n	-	—	[109]	1450705

7. Cu_xX_xE_y species (X = I, Br, Cl; E = Se, Te)

Multiple seleno- and telluroether, and selone ligands were used to prepare various CPs (Table 23; 23 X-ray structures) [70–73,92,130–134]. The ligand structures are placed in Figure 20. Clear trends are depicted. First, excluding the two MeCN-containing materials, the only two cluster motifs reported are Cu₂X₂E₄ rhomboid and Cu₄X₄E₄ cubane. This observation is fully

consistent with the fact that these motifs are also dominant for the $\text{Cu}_x\text{I}_x\text{S}_y$ species. Second, the number of cubane and rhomboid motifs for $\text{Cu}_x\text{I}_x\text{Se}_y$ species are the same. This observation also applies to the $\text{Cu}_x\text{I}_x\text{S}_y$ species above. Third, for the Cu_xX_xE_y species ($X = \text{Br}, \text{Cl}; E = \text{Se}, \text{Te}$), all SBU motifs are rhomboid, which is also in line with the dominance of this motif when X is Cl or Br . Fourth, similarly to the thione ligands and despite the very small sampling, the rhomboid was the only motif reported for the selone ligand ($X = \text{I}$) with no occurrence of cubane. The only striking difference with the $\text{Cu}_x\text{X}_x\text{S}_y$ species is the large propensity of the Cu_xX_xE_y ($E = \text{Se}, \text{Te}$) to form discrete complexes (just about the same as the occurrence for 1D CP). Their structural properties are presented below.

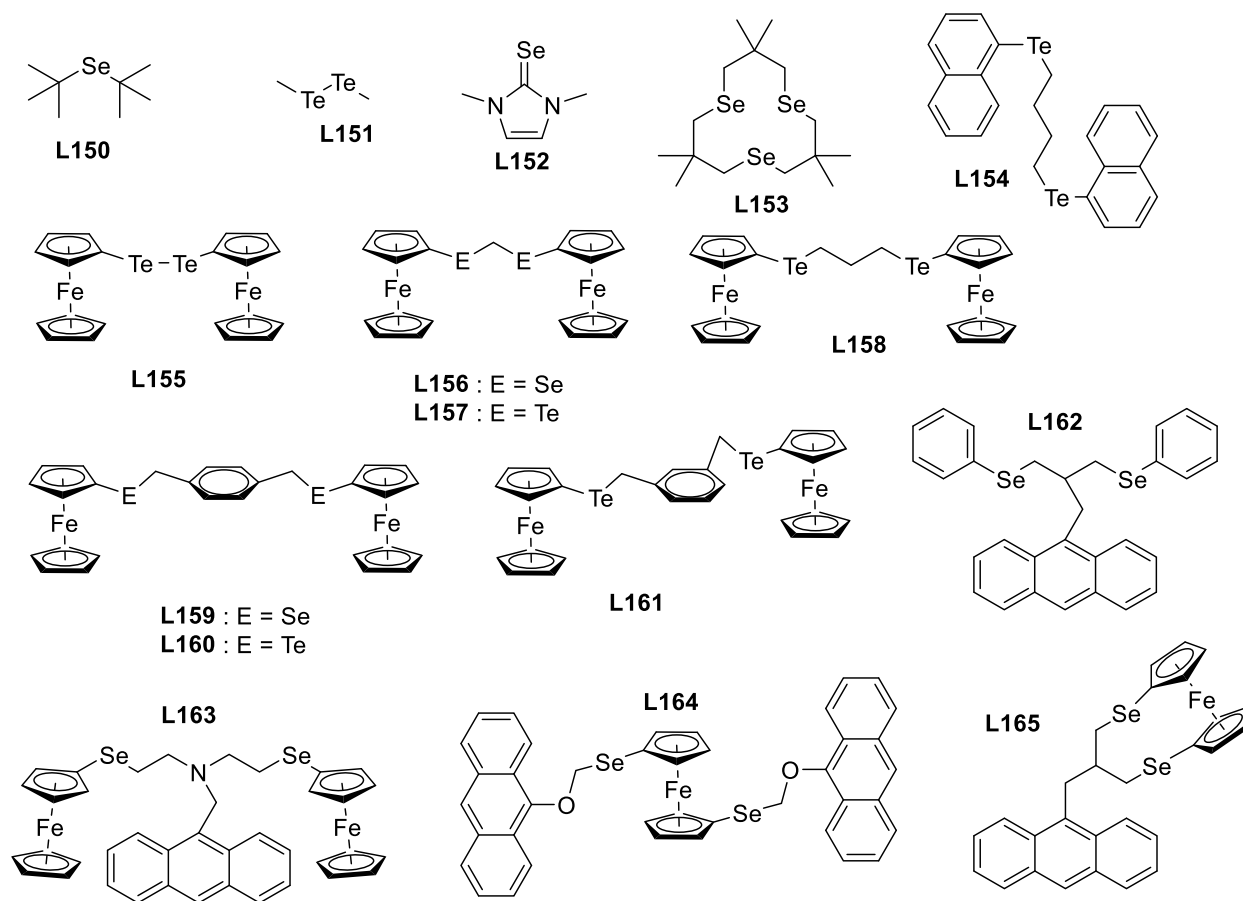


Figure 20. Structures of seleno- and telluroether, and selone ligands.

Table 23. List of Cu_xX_xE_y -containing complexes and CPs where $X = \text{I}, \text{Br}, \text{Cl}$ and $E = \text{Se}, \text{Te}$.

#	cluster	xD-Formula	Cu-Cu distance [average] (Å)	ref	#CCDC
---	---------	------------	------------------------------	-----	-------

1	Cubane	0D-[Cu ₄ I ₄ (L150) ₄]	2.997, 3.287, 3.001, 3.282, 3.205, 3.228 [3.167]	[73]	1835505
2	Rhomboïd	1D-[Cu ₂ I ₂ (L162) ₂] _n	2.681	[92]	-
3	Cubane	1D-[Cu ₄ I ₄ (L156) ₂] _n ^a	2.673, 2.844, 2.745, 2.673, 2.773, 2.745 [2.742]	[70]	1418330
4	Rhomboïd	1D-[Cu ₂ I ₂ (L156) ₂] _n ^b	2.807	[70]	1418329
5	1D-polyrhomboid	2D-[Cu ₄ I ₄ (L159) ₂ (MeCN) ₂] _n	2.728, 2.803	[70]	1418331
6	Rhomboïd	0D-[Cu ₂ I ₂ (L164) ₂]	2.782	[71]	1023397
7	Rhomboïd	0D-[Cu ₂ Br ₂ (L164) ₂]	2.793	[71]	1023398
8	Rhomboïd	0D-[Cu ₂ I ₂ (L165) ₂] · (CH ₂ Cl ₂) _{1.25}	2.612	[71]	1034753
9	Cubane	1D-[Cu ₄ I ₄ (L163) ₂] _n · CH ₂ Cl ₂	2.752, 2.893, 2.810, 2.887, 2.788, 2.768 [2.816]	[71]	992606
10	Cubane	3D-[Cu ₄ I ₄ (L153) ₂] _n · MeCN	2.780, 2.826, 2.989, 3.040, 3.202, 3.085 [2.987]	[72]	1221768
11	Rhomboïd	2D-[Cu ₂ Cl ₂ (L151) ₂] _n	3.381	[134]	1308789
12	Step staircase	0D-[Cu ₄ I ₄ (L155) ₂ (MeCN) ₂]	2.813, 3.392	[70,131]	1418326
13	Rhomboïd	1D-[Cu ₂ I ₂ (L157) ₂] _n	2.804	[70,131]	1418327
14	Rhomboïd	1D-[Cu ₂ Br ₂ (L157) ₂] _n	2.848	[70,131]	1418328
15	Rhomboïd	0D-[Cu ₂ Br ₂ (L154) ₂] ^c	2.919, 3.107	[133]	1487838
16	Rhomboïd	2D-[Cu ₂ I ₂ (L160) ₂] _n	2.908	[131,132]	1823307
17	Rhomboïd	2D-[Cu ₂ Br ₂ (L160) ₂] _n	2.906	[131,132]	1823306
18	Rhomboïd	1D-[Cu ₂ I ₂ (L161) ₂] _n	3.472	[131,132]	1823308
19	Rhomboïd	0D-[Cu ₂ I ₂ (L158) ₂] ^d	2.757	[131,132]	1823305
20	Rhomboïd	0D-[Cu ₂ Br ₂ (L158) ₂] ^e	2.696	[131,132]	1823304
21	Rhomboïd + 2CuI	0D-[Cu ₂ I ₂ (L152) ₄ (μ-CuI) ₂] ^f	2.607	[130]	804911
22	Rhomboïd + 2CuBr	0D-[Cu ₂ Br ₂ (L152) ₄ (μ-CuBr) ₂] ^g	2.631	[130]	804917

^a mixed with entry 4 ; ^b mixed with entry 3 ; ^c two polymorph ; ^d chelating ligand ; ^e bridging ligand ; ^f two Se-(CuI)-Se ; ^g two Se-(CuBr)-Se.

8. Statistical analysis on the geometry of the SBUs and CP dimensionalities

8.1. Occurrence of globular and quasi-planar motifs and dimensionalities

The occurrences of *globular* vs *quasi-planar* motifs and the various CP dimensionalities of Cu₄I₄S₄-cubane vs Cu₂I₂S₄-rhomboid-containing CPs are compared in **Table 24** – **Table 27**, **Figures 21** and **22**. From **Table 24** and **Table 25**, the closed Cu₄I₄S₄-cubane (83%) and Cu₂I₂S₄-rhomboid (78% when considering only the thioethers) motifs are significantly more stabilized than any other motifs. Referring to Tables 1-4, when the effect of the L/M ratio is specifically tested with the appropriate ratio (*i.e.* 1:1), the formation of the cubane motif *versus* another motif, appears to be good prediction (20 cubanes vs 1 fused open cubane) regardless of the mono-thioether and polythioether ligands used. Similarly, the formation of the Cu₂I₂S₄-rhombic unit, again with the appropriate L/M (2:1) ratio (when tested), is systematic using dithio- or polyether assembling ligands (61 examples found against zero for any other shape). For the thione ligands, the Cu₂I₂S₄-rhombic motif is often obtained (~50%) but the size of the data bank (

Table 10, 15 entries) does not allow us to firmly pin down the key features that promote this motif.

Table 24. Comparison of the occurrence of the various *globular* $\text{Cu}_x\text{I}_x\text{S}_y$ motifs (based on X-ray data).^a

	cubane	open cubane	fused dicubane	fused open dicubane	hexagonal prism	1D-polycubane	other
Table 1	29	-	1	-	1	1	-
Table 2	11	-	-	1	-	-	1
Table 3	5	1	2	-	-	-	2
Table 4	2	-	-	-	-	-	1
Table 5	5	-	-	-	-	-	-
Total	52 (83%)	1	3	1	1	1	4

^a**Table 1** = acyclic dithioethers/CuI. **Table 2** = cyclic dithioethers/CuI. **Table 3** = acyclic mono-thioethers/ CuI. **Table 4** = cyclic monothioethers/CuI. **Table 5** = polythioethers/CuI. Structures including a coordinated MeCN or were not determined by X-ray crystallography are not included.

Table 25. Comparison of the occurrence of the various *quasi-planar* $\text{Cu}_x\text{I}_x\text{S}_y$ motifs (based on X-ray data). Thioether-containing materials are at the top, and thione-containing species are at the bottom.^a

	rhomboid	step staircase	1D-acordeon	others
Table 6	27	1	3	5
Table 7	19	-	1	6
Table 8	3	-	-	-
Table 9	12	-	-	2
Total 1	61 (78%)	1	4	13
	rhomboid	step staircase	1D-acordeon	others
Table 10	8	2	1	4
Total 2	69 (74%)	3	5	17

^a**Table 6** = acyclic dithioethers/CuI. **Table 7** = cyclic dithioethers/CuI. **Table 8** = acyclic and cyclic monothioethers/CuI.

Table 9 = polythioethers/CuI.

Table 10 = thione/CuI. Total 1 is the sum of **Table 6** to

Table 9, and Total 2 is the sum of Total 1 and

Table 10. Note that all motifs containing coordinated MeCN ligands or were not characterized by X-ray crystallography are not included, except entry 13 of

Table 9 for which obvious steric hindrance secures the integrity of the trinuclear cluster.

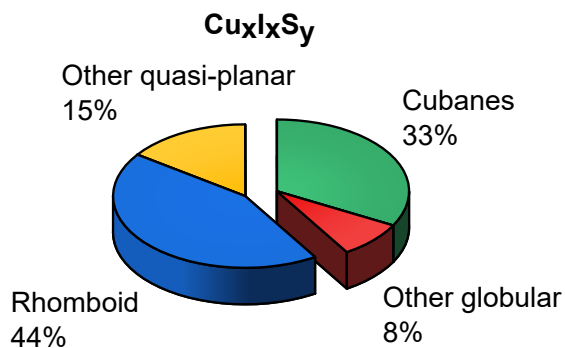


Figure 21. Pie diagram comparing the occurrence of the various *globular* Cu_xI_xS_y and *quasi-planar* Cu_xI_xS_y motifs (based on X-ray data).

The occurrence of the fused open dicubane and fused open cubane motifs instead of their closed versions stems from ring tensions between the Cu_xI_x-units and the mono- or dithioethers. This behavior is an experimental evidence that the Cu_xI_x clusters (here x = 4, 8) try to accommodate the CP formation by sacrificing a Cu-I bond for the sake a crystal packing of the CP. Parallely, this conclusion also suggests that the occurrence of the motifs other than cubane and rhomboid listed in **Table 11** and **Table 12** may also result from accommodations of the CuI aggregates. This suggestion is strongly supported by the fact that non-rhomboid *quasi-planar* species are found for CPs for the constraining monothioethers, which are more prone to steric problems combined with the proximity of the two binding sites on the same Cu atom in the rhomboid geometry. This change in SBU structure provides the necessary distance for the reduction of the steric issues and thus the stabilisation of the Cu_xI_xS_y motif.

Table 26. Comparison of the occurrence of the various CP dimensionalities of the Cu₄I₄S₄-cubane-containing CPs (based on X-ray data).^a

	cubane	0D	1D	2D	3D
Table 1	1	13	15	1	
Table 2	-	6	5	1	
Table 3	3	2	-	-	
Table 4	1	-	-	1	
Table 5	-	1	1	2	
Total	5	22	21	5	

^a **Table 1** = acyclic dithioethers/CuI. **Table 2** = cyclic dithioethers/CuI. **Table 3** = acyclic thioethers/CuI. **Table 4** = cyclic thioethers/CuI. **Table 5** = polythioethers/CuI. Structures that were not determined by X-ray crystallography are not included.

Table 27. Comparison of the occurrence of the various CP dimensionalities of the $\text{Cu}_2\text{I}_2\text{S}_4$ -rhombooid-containing CPs (based on X-ray data).^a

rhombooid	0D	1D	2D	3D
Table 6	4	10	13	-
Table 7	5	9	7	-
Table 8	1	1	1	-
Table 9	4	2	2	4
Table 10^b	6	1	1	-
Total	20	23	24	4

^a**Table 6** = acyclic dithioethers/CuI. **Table 7** = cyclic dithioethers/CuI. **Table 8** = acyclic and cyclic thioethers/CuI.

Table 9 = polythioethers/CuI.

Table 10 (thione/CuI), the sampling is too. ^bIn these cases, the thione ligands are bidentates acting as a bridge, and not structurally fit for a chelate geometry. Structures that were not determined by X-ray crystallography are not included.



Figure 22. Pie diagrams comparing the occurrence of the various CP dimensionalities (based on X-ray data). Left, the $\text{Cu}_2\text{I}_2\text{S}_4$ -rhombooid-containing CPs. Right, $\text{Cu}_4\text{I}_4\text{S}_4$ -cubane-containing CPs.

The resulting CP dimensionalities are largely 1D and 2D in similar proportion for CPs containing $\text{Cu}_4\text{I}_4\text{S}_4$ -cubane SBUs. This is particularly evident with the dithioether ligands, illustrating the adaptability of the ligand to exclude chelating situations for flexible ligands. Concurrently, the rhombooid SBUs is more often encountered in 1D-CPs, although 0D and 2D species are also observed.

A similar series of analyses have been performed for the $\text{Cu}_x\text{Br}_x\text{S}_y$ - and $\text{Cu}_x\text{Cl}_x\text{S}_y$ -containing materials (**Table 11-Table 22**; **Figures 23-27**), and similar conclusions can be drawn for the *quasi-planar* materials. The propensity to generate rhomboid SBUs exhibits negligible variations whether the ligand is a thioether or a thione and that the ratio of occurrences of $\text{Cu}_2\text{X}_2\text{S}_4$ -rhomboid *vs* other *quasi-planar* SBUs is the same for $\text{X} = \text{Br}$ and I , and a little smaller for $\text{X} = \text{Cl}$. A graphical representation of these relative trends is provided in **Figure 26**. Moreover, very few *globular*-shaped SBUs in these two series ($\text{X} = \text{Cl}, \text{Br}$) have been isolated ($\sim 6\%$; $\text{X} = \text{Br}$, 5 *globular vs* 58 *quasi-planar*, $\text{X} = \text{Cl}$, 1 *globular vs* 41 *quasi-planar*). Even more striking is the absence of cubane-shaped motifs despite the fact that the $\text{Cu}_4\text{Br}_4\text{L}_4$ ($\text{L} = \text{N-}$ and P-donor ligand) [135–142] and $\text{Cu}_4\text{Cl}_4\text{L}_4$ ($\text{L} = \text{N-}$ and P-donor ligand) [143–147] cubane complexes are quite common (note that the provided references are not exhaustive since these ligands are not the subject of this review). The structures of these six globular SBUs ($\text{X} = \text{Cl}, \text{Br}$) are adamantane ($\text{Cu}_4\text{X}_4\text{S}_4$), flower basket ($\text{Cu}_4\text{Br}_4\text{S}_6$) and square pyramidal cluster ($\text{Cu}_5\text{Br}_5\text{S}_3$).

Table 28. Comparison of the occurrence (X-ray structures) of the various $\text{Cu}_x\text{Br}_x\text{S}_y$ motifs.^a

	rhomboid	other motifs
Table 11: acyclic dithioethers/ $\text{Cu}_x\text{Br}_x\text{S}_y$ CPs	22	4
Table 12: cyclic dithioethers/ $\text{Cu}_x\text{Br}_x\text{S}_y$ CPs	7	4
Table 13: acyclic monothioethers/ $\text{Cu}_x\text{Br}_x\text{S}_y$ CPs	2	2
Table 14: cyclic monothioethers/ $\text{Cu}_x\text{Br}_x\text{S}_y$ CPs	1	0
Table 15: polythioethers/ $\text{Cu}_x\text{Br}_x\text{S}_y$ CPs	4	2
Total 1	36 (76%)	12
Table 16: thione-containing/ $\text{Cu}_x\text{Br}_x\text{S}_y$ CPs	3	3
Total 2	39 (72%)	15

^aThe other motifs include 2D-step cubane network, 1D-distorted ribbon, -Cu-Br- chain, 1D-zig zag, square chain, 1D-zig zag ribbon, staircase, trinuclear cluster, square pyramidal cluster, two 1D-zig zag twisted chains, flower basket, and adamantane-like. Total 2 = Total 1 + Table 16. Structures including a coordinated MeCN or were not determined by X-ray crystallography are not included.

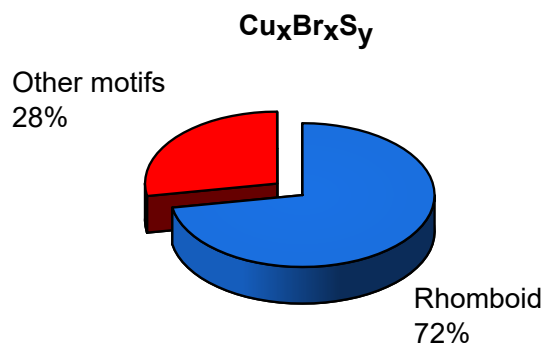


Figure 23. Comparison of the occurrence of the various Cu_xBr_xS_y motifs (based on X-ray data).

Table 29. Comparison of the occurrence of the various CP dimensionalities of the rhomboid Cu₂Br₂S₄-containing CPs (based on X-ray data).

rhomboid	0D	1D	2D	3D
Table 11: acyclic dithioethers/Cu _x Br _x S _y CPs	4	12	6	1
Table 12: cyclic dithioethers/Cu _x Br _x S _y CPs	2	4	2	-
Table 13: acyclic monothioethers/Cu _x Br _x S _y CPs	1	-	1	-
Table 14: cyclic monothioethers/Cu _x Br _x S _y CPs	-	-	1	-
Table 15: polythioethers/Cu _x Br _x S _y CPs	-	2	1	1
Table 16: thione-containing/Cu _x Br _x S _y CPs	2	-	-	-
Total	9	8	11	2

Structures that were not determined by X-ray crystallography are not included.

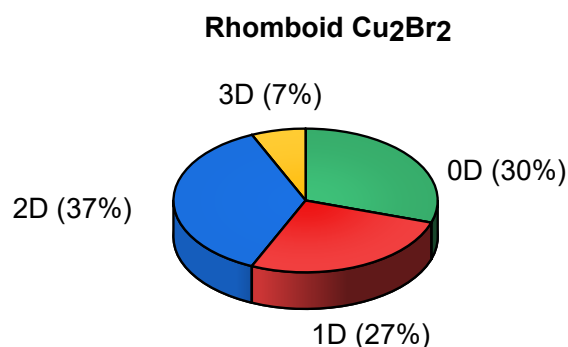


Figure 24. Pie diagram comparing the occurrence of the various Cu_xBr_xS_y dimensionalities (based on X-ray data).

Table 30. Comparison of the occurrence (X-ray structures) of the various Cu_xCl_xS_y motifs.^a

	rhomboid	other motifs
Table 17: acyclic dithioethers/Cu _x Cl _x S _y CPs	11	3

Table 18: cyclic dithioethers/ $\text{Cu}_x\text{Cl}_x\text{S}_y$ CPs	4	2
Table 19: acyclic monothioethers/ $\text{Cu}_x\text{Cl}_x\text{S}_y$ CPs	2	2
Table 20: cyclic monothioethers/ $\text{Cu}_x\text{Cl}_x\text{S}_y$ CPs	3	1
Table 21: polythioethers/ $\text{Cu}_x\text{Cl}_x\text{S}_y$ CPs	3	2
Total 1	23 (70%)	10
Table 22: thione-containing/ $\text{Cu}_x\text{Cl}_x\text{S}_y$ CPs	1	2
Total 2	24 (67%)	12

^a The other motifs include 1D-zig zag ribbon, Cu-Cl-Cu-Cl chain, cyclic- Cu_3Cl_3 , step staircase, two 1D-zig, adamantane-like and zig twisted chains. Structures including a coordinated MeCN or were not determined by X-ray crystallography are not included.

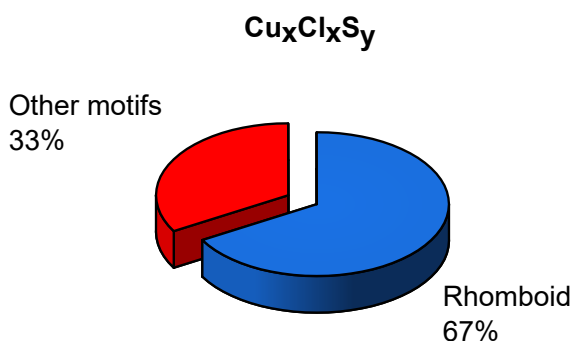


Figure 25. Comparison of the occurrence of the various $\text{Cu}_x\text{Cl}_x\text{S}_y$ motifs (based on X-ray data).

Table 31. Comparison of the occurrence of the various CP dimensionalities of the rhomboid $\text{Cu}_2\text{Cl}_2\text{S}_4$ -containing CPs (based on X-ray data).

rhomboid	0D	1D	2D	3D
Table 17: acyclic dithioethers/ $\text{Cu}_x\text{Cl}_x\text{S}_y$ CPs	1	2	6	1
Table 18: cyclic dithioethers/ $\text{Cu}_x\text{Cl}_x\text{S}_y$ CPs	-	1	3	-
Table 19: acyclic monothioethers/ $\text{Cu}_x\text{Cl}_x\text{S}_y$ CPs	-	-	2	-
Table 20: cyclic monothioethers/ $\text{Cu}_x\text{Cl}_x\text{S}_y$ CPs	-	1	2	-
Table 21: polythioethers/ $\text{Cu}_x\text{Cl}_x\text{S}_y$ CPs	-	1	2	-
Table 22: thione-containing/ $\text{Cu}_x\text{Cl}_x\text{S}_y$ CPs	1	-	-	-
Total	2	5	15	1

Structures that were not determined by X-ray crystallography are not included.

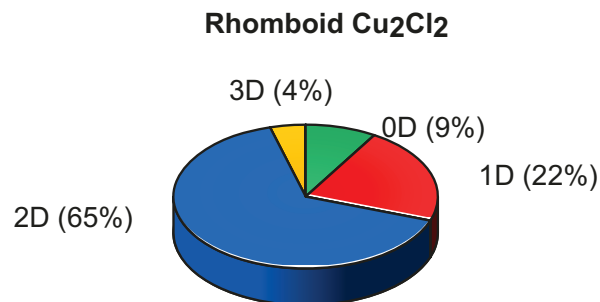


Figure 26. Comparison of the occurrence of the various $\text{Cu}_x\text{Cl}_x\text{S}_y$ dimensionalities (based on X-ray data).

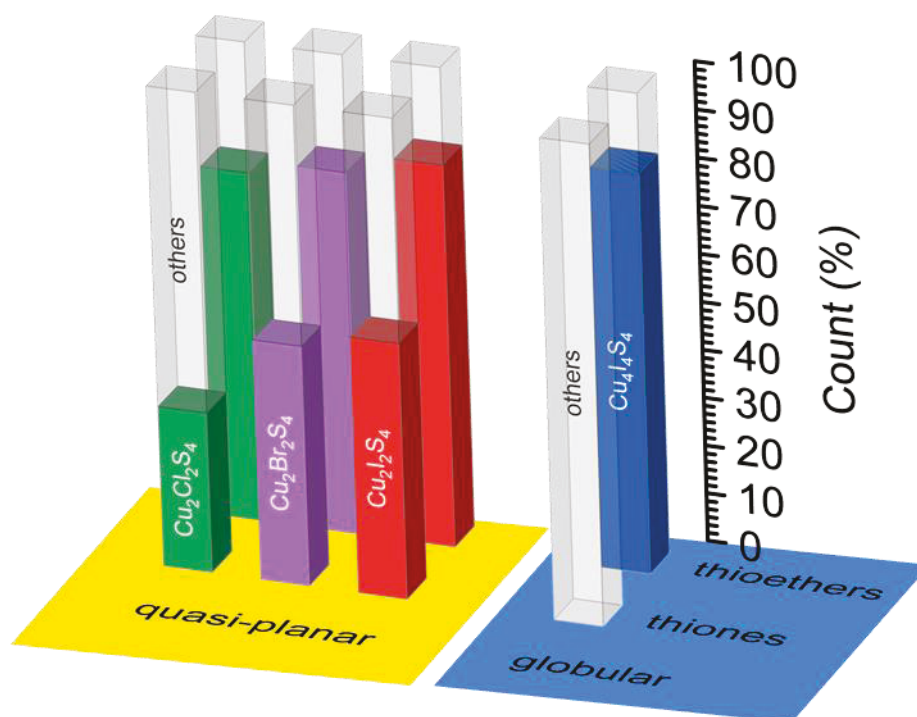


Figure 27. Relative percentage of the occurrence of $\text{Cu}_2\text{X}_2\text{S}_4$ -rhomboid motifs ($\text{X} = \text{Cl}, \text{Br}, \text{I}$) for the *quasi-planar* SBUs (yellow carpet) and of the occurrence of $\text{Cu}_4\text{I}_4\text{S}_4$ -closed cubane (blue carpet) when the S-donor ligand is a thioether (back row) and thione (front row). The transparent portions of the graph (two of them are labelled **others**) represent SBUs other than $\text{Cu}_2\text{X}_2\text{S}_4$ -rhomboids of $\text{Cu}_4\text{I}_4\text{S}_4$ -closed cubane. The sums of the colored and transparent portions = 100%. Note that there are very few or no globular SBUs ($\text{X} = \text{Cl}, \text{Br}$) for both thioethers and thiones.

The chalcogenoether ligands where E is Se or Te form exclusively rhomboid and closed cubane SBUs (**Table 23**; 22 entries, excluding the two cases with coordinated CH₃CN). This observation represents a major difference with the thioether- and thione-containing ligands (**Figure 27**). The relative occurrence of Cu₂I₂Se₄-rhomboid vs Cu₄I₄Se₄-closed cubane is ~50-50%, a ratio that resembles that of Cu₂I₂S₄-rhomboid vs Cu₄I₄S₄-closed cubane (**Table 24** and **Table 25**, top; 51 vs 61). Two materials containing the selenone-containing ligands have been characterized so far (**Table 23**, entries 21 and 22), and in both cases, the rhomboid is observed.

One very interesting observation is the propensity of the Cu₂X₂S₄ rhomboid motifs to favor a given CP structure dimension. Based on geometry alone, the probability of favoring a type of structure dimensionality should be identical for all three salts, but experimentally, this is not the case (**Figure 28**). Indeed, two trends are unambiguous. First, for all four categories of materials, the formation of 1D- and 2D-CPs are the most probable outcomes. Second, there is a clear evolution of the propensity of favoring 1D- and 2D-CPs (66, 75, 84 %) over 0D- and 3D-materials (34, 25, 16 %) when going from iodide, to bromide, to chloride, respectively. Again, this trend is not geometrically related as the motifs are identical but are clearly halide dependent. The comparison of the trends observed for the closed cubane Cu₄I₄S₄ motif and rhomboid Cu₂I₂S₄ motif (i.e. identical halide) support this conclusion as they are approximately the same (with the exception of the discrete molecules). The sampling appears to be large enough to trust these trends but no explanation is possible for the moment.

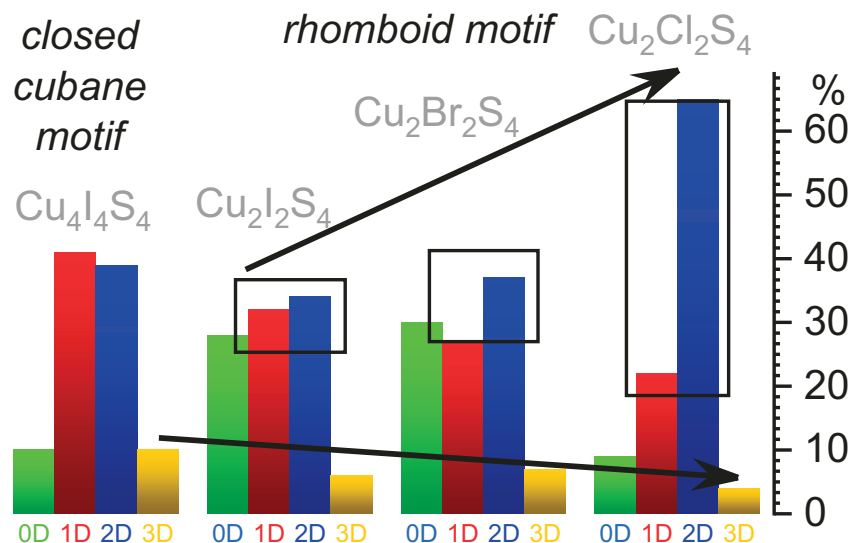


Figure 28. Graph reporting the percentage of occurrence of 0D-, 1D-, 2D- and 3D- materials for the closed cubane $\text{Cu}_4\text{I}_4\text{S}_4$ motifs and the rhomboid $\text{Cu}_2\text{X}_2\text{S}_4$ motifs ($\text{X} = \text{Cl}, \text{Br}, \text{I}$).

8.2. Flexibility of the SBU motifs

One of the main conclusions of the statistical analysis is that the closed cubane geometry is the most encountered geometry among the *globular* species (83% of occurrence; **Table 24**) indicating clearly that this is the most stable structure. Deviation from this structure could often be rationalized by obvious steric hindrance, ring tension, or both, meaning that the CuI salt can readily adapt the SBU upon stress within the bulk. The recent evidence for this is the work by Bai et al where using the same ligand **L18** ($\text{PhSCH}_2\text{C}\equiv\text{CCH}_2\text{SPh}$), two different SBUs were obtained: hexagonal prism and ribbon [12]. These observations suggest that the SBUs must be flexible as well. It was recognized earlier that two extreme geometries for $\text{Cu}_4\text{I}_4(\text{pyridine})_4$ exist [148], which are *stella quadrangular* and *closed cubane* (**Figure 29**). These two forms differ intrinsically in the resulting $\text{Cu}\cdots\text{Cu}$ separations (shorter for *stella quadrangular* and longer for *closed cubane*) and consequently noticeable from the averaged X-ray $\text{Cu}\cdots\text{Cu}$ distances. The closed $\text{Cu}_4\text{I}_4\text{S}_4$ cubanes included in this review also exhibit variable averaged X-ray $\text{Cu}\cdots\text{Cu}$ distances. Moreover, several investigations reporting the $\text{Cu}\cdots\text{Cu}$ distances *versus* temperature for various globular species demonstrated a significant change with the temperature (**Figure 30**)

[24,25,30,36,74]. Moreover, the graph reporting the number of occurrence (population) vs Cu···Cu distance exhibits a large span going from 2.566 to 2.891 Å ($\Delta = 0.325$ Å) with a spread at half maximum 2.68-2.82 Å and average of 2.737 Å (**Figure 31**). This somewhat large distribution illustrates the flexibility of the closed cubane structure, most likely in order to adapt to some solid state packing stresses. It is noteworthy that there is no relationship between the dimensionality of the CPs and the mean Cu···Cu distances (**Figure 31**, left). Therefore, the fact that the two 2D-CPs shown in **Figure 30** exhibit longer mean Cu···Cu distances than those of the 1D-CP is only coincidental.

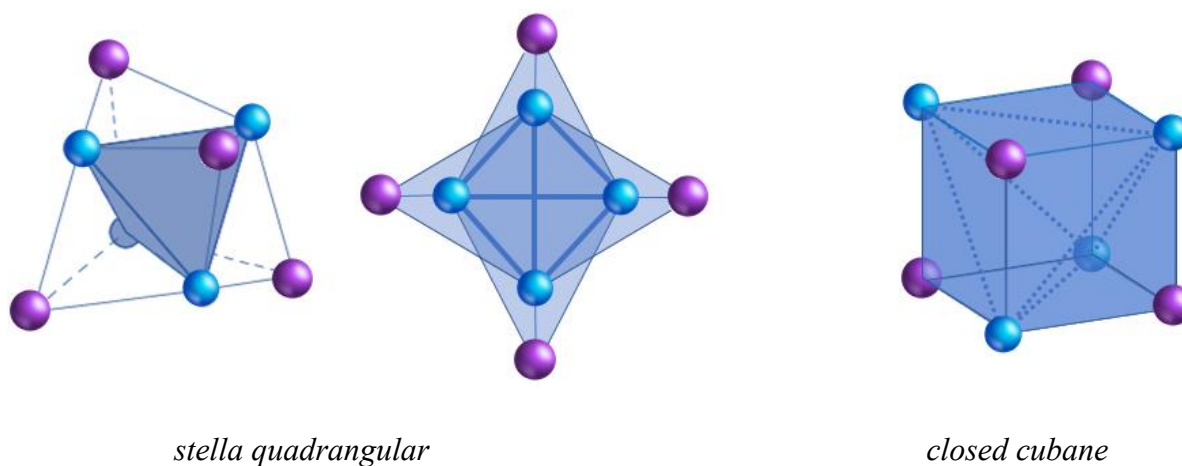


Figure 29. Representations of the two extreme cases of SBU geometry for the $\text{Cu}_4\text{I}_4\text{L}_4$ SBU.

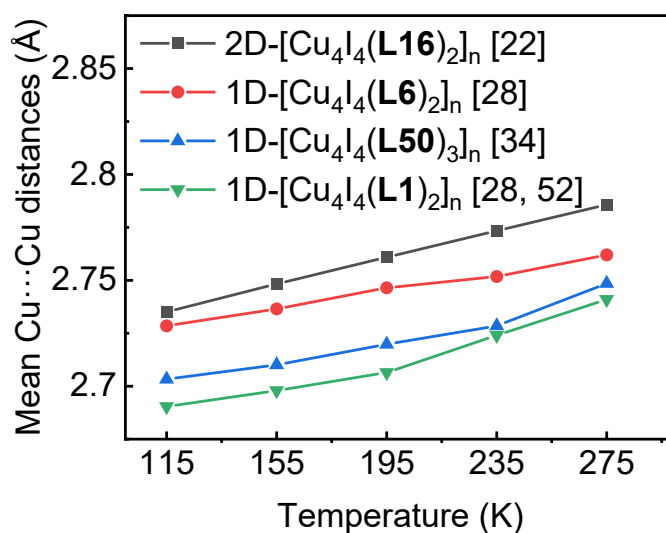


Figure 30. Mean Cu \cdots Cu distances vs temperature for five closed Cu₄I₄S₄ cubane-containing CPs.

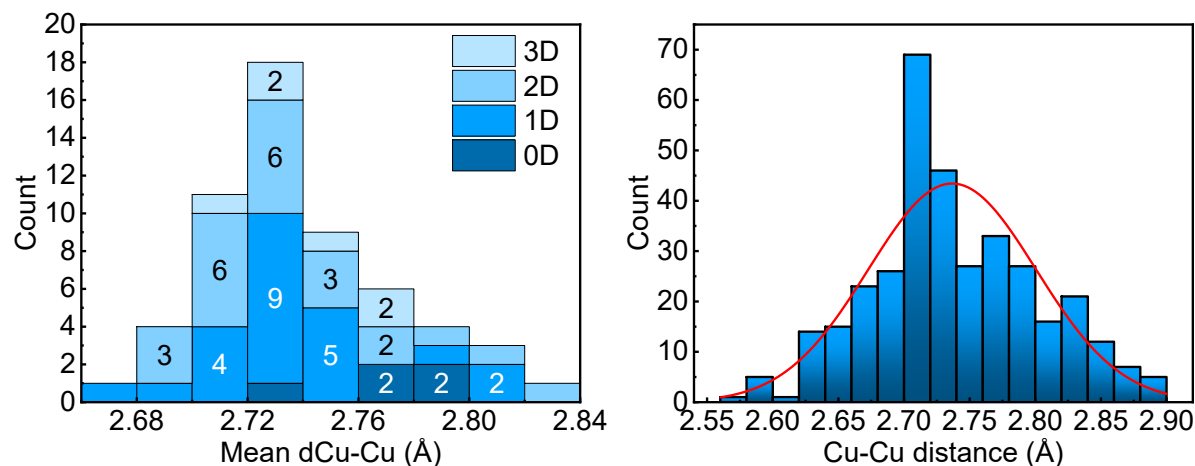


Figure 31. Left: Distribution of the number of occurrences (Count) of mean Cu \cdots Cu distance vs distance for the closed cubanes indicating the dimensionality of the CPs. Right: Number of occurrences (Count) of a given Cu \cdots Cu distance vs distance for the closed Cu₄I₄S₄ cubane-containing CPs. Note that most data are for room temperature but on some occasions the reported data are for a lower temperature. From **Figure 30**, this difference impacts by ~ 0.03 Å the extrapolated Cu \cdots Cu distance at room temperature. The sum of the van der Waals radii = 2.80 Å.

Similarly, the flexibility of the rhomboid Cu₂I₂S₄ motif is evidenced from the long mean distance of 2.848 Å (compared to 2.739 Å for the closed Cu₄I₄S₄ cubanes), and the larger span of 2.582 to 3.367 Å ($\Delta = 0.785$ Å; **Figure 32**, left). These differences are due to the larger number of Cu-I bonds and the presence of multiple cuprophylic interactions [149,150] in the closed cubane compared to the rhomboid. Moreover, there is no trend correlating the resulting CP dimensionality and the Cu \cdots Cu distance for the rhomboid Cu₂I₂S₄ SBUs as well (**Figure 32**). The comparison of these Cu₂I₂S₄ characteristics with those of the Cu₂X₂S₄ motifs (X = Cl, Br) also indicates a large span in Cu \cdots Cu distances. The minimum and maximum Cu \cdots Cu separations are respectively 2.655 and 3.290 Å for X = Cl ($\Delta = 0.635$ Å; **Figure 32**, left), and 2.613 and 3.459 Å for X = Br ($\Delta = 0.846$ Å; **Figure 32**, middle). The monitoring of the average Cu \cdots Cu distances for X = Cl, Br and I, and their comparisons with that of the closed cubane stresses an evolution of the skeleton flexibility: closed Cu₄I₄S₄ cubane < Cu₂X₂S₄ rhomboids (*i.e.* from less to more flexible skeleton) and Cu₂I₂S₄ < Cu₂Br₂S₄ < Cu₂Cl₂S₄ simply illustrating the

failure of the hybridization theory (and the VSEPR, valence shell electron repulsion pair repulsions) as one goes down in the periodic table.

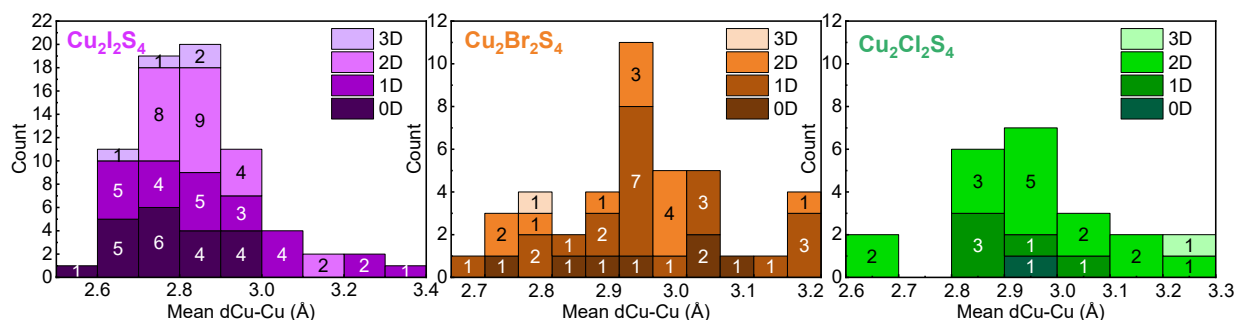


Figure 32. Distribution of the number of occurrences (Count) of the Cu...Cu distance vs distance for the rhomboid Cu₂X₂S₄ motifs (X = Cl, Br, I) indicating the dimensionality of the CPs.

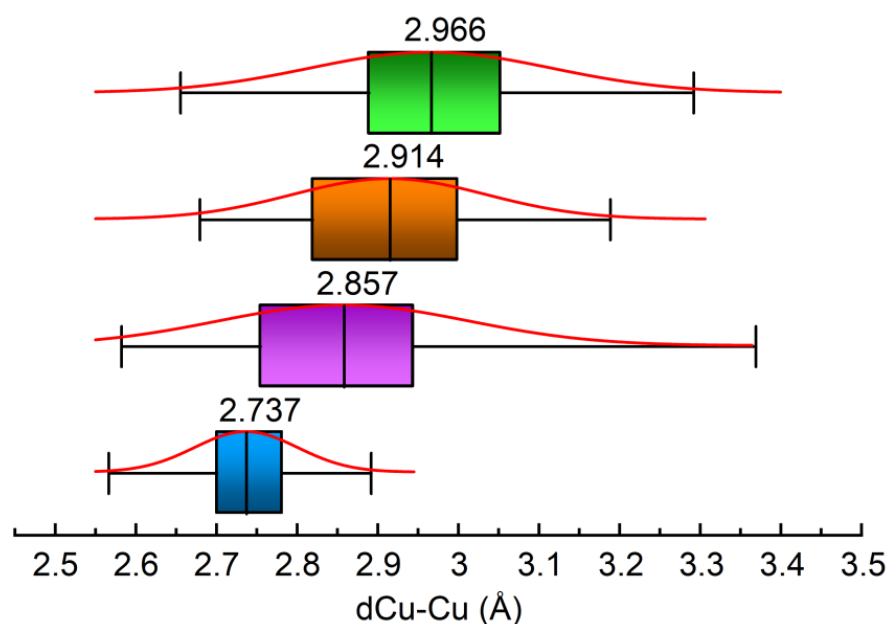


Figure 33. Comparison of the distribution of the number of occurrences (illustrated as a red Gaussian issued from the data from **Figure 31** and **32**) of the Cu...Cu distance vs distance for the closed Cu₄I₄S₄ cubane (blue) and the Cu₂X₂S₄ rhomboids (X = Cl (green), Br (brown), I (purple)). The rectangles represent the distribution span containing the values in the range of 25-75% of the data, and the central bars are the average values. The minima and maxima are the bars in the extremities of the black lines.

9. Photophysical Properties of the $\text{Cu}_x\text{X}_x\text{E}_y$ -containing complexes and CPs

The most reported property for these species is luminescence and this section addresses their photophysical behavior. Again, the two categories of chromophores are the *quasi-planar* and *globular* species. This structural separation also bears a significant difference in their photophysical behavior. Indeed, the *globular* clusters are generally strongly luminescent (**Table 32**) whereas the *quasi-planar* species are moderately emissive or non-emissive (**Table 33**, including some rare examples of chloride derivatives). This separation is also based on the nature of the lowest excited states. The *globular* chromophores invariably exhibit lower energy cluster-centered (CC^*) triplet excited states whereas the *quasi-planar* species exhibit metal/halide-to-ligand charge transfer (M/XLCT). These assignments are based on density functional theory (DFT) calculations and the references are provided inside **Table 32** and **Table 33**. These conclusions are also consistent with the well-documented literature and the pioneer work by Peter Ford based on *ab initio* calculations at the RHF SCF level on a model cluster $\text{Cu}_4\text{I}_4(\text{NH}_3)_4$ [151]. A small difference with the $\text{Cu}_x\text{X}_x\text{E}_y$ -containing chromophores herein, is that the $\text{Cu}_4\text{I}_4\text{L}_4$ -cubanes in solution occasionally exhibit two emission bands labelled *high energy* and *lower energy* bands [152,153]. While the *low energy* band is assigned to CC^* , the *high energy* one is assigned to M/XLCT or sometime to halide-to-ligand charge transfer (XLCT). **Figure 34** (a) exhibits the potential energy surfaces explaining the occurrence of the *high energy* and *lower energy* bands and their temperature-dependent relative population. The two examples are $\text{Cu}_4\text{I}_4(\text{pyridine})_4$ and $\text{Cu}_4\text{I}_4(2\text{-(diphenylmethyl)pyridine})_4$. One example of such case is provided in **Figure 35** where the two emission bands are clearly observed upon changing the temperature. The position of these *high energy* and *lower energy* bands is also function of the average Cu-I distance. **Figure 34** (b) exhibits the variation of the S_0 , T_1 and T_2 state energies as a function of the Cu-I distances of the $[\text{Cu}_4\text{I}_4\text{py}_4]$ complexes and the resulting positions of the triplet emissions where the T_1 and T_2 energy minima are.

For the globular $\text{Cu}_x\text{I}_x\text{S}_y$ species, this high energy band has been scarcely observed. In all cases, their luminescence bands have been assigned to triplet emissions with no evidence of emitting singlet states, which is consistent with the expected heavy atom effect accelerating the rate for the non-radiative intersystem crossing process. The commonly reported photophysical parameters are the emission maxima (λ_{em}), the full width at half-maximum (FWHM), emission

quantum yields (Φ_e), and emission lifetimes (τ_e). For the *globular* chromophores (**Table 32**), the λ_{em} values of the CC* bands range from 500 to 670 nm, with a tail extending to the near-IR region on occasion. Only a few Φ_e data have been reported so far and range from 0.10 to 0.61 (the uncertainties are generally $\pm 10\%$), which is considered high and characteristic of these types of chromophores [154]. Typically, τ_e ranges from ~ 0.2 to $\sim 25 \mu s$ (*i.e.* the spread is one order of magnitude).

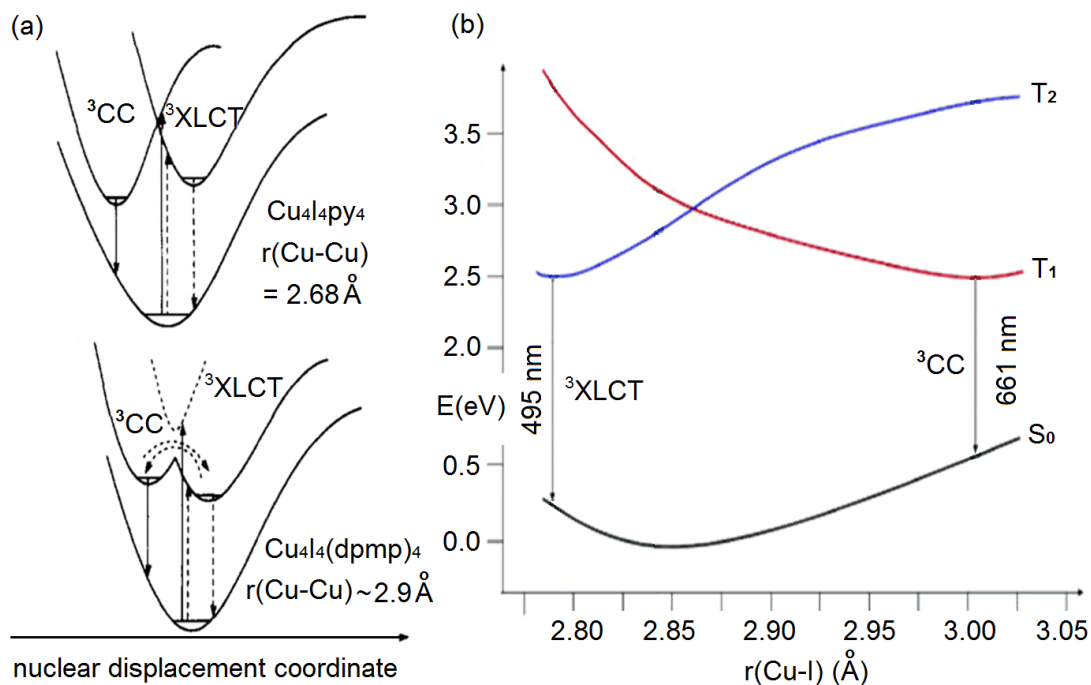


Figure 34. a) Potential energy surfaces illustrating ³CC (Cluster Centered) and ³XLCT (Halide-to-Ligand Charge Transfer) excited states depending on the Cu-Cu distances inside Cu₄I₄ cubane cluster (dpmp = 2-(diphenylmethyl)pyridine). Adapted with permission from *Inorg. Chem.* 1993, 32, 6, 869–874. Copyright 2021 American Chemical Society. b) Excitation energy vs Cu-I distance inside [Cu₄I₄py₄] cubane cluster for the optimized S₀, T₁ and T₂ structures. Number in parentheses are the energy converted to nm for easier reading. Adapted with permission from *Inorg. Chem.* 2006, 45, 26, 10576-10584. Copyright 2021 American Chemical Society.

Two very interesting and striking features are the occasional and the somewhat counter-intuitive blue-shifts of the emission bands and some shortening of the emission lifetimes upon cooling. It is noteworthy that these two odd behaviors are unrelated. The former behavior is not specifically associated with the chalcogeno-ligands as other N-donor ligands promote this same behavior

[153,155]. Normally the Cu•••Cu separations in the $\text{Cu}_{2n}\text{I}_{2n}$ ($n = 1-4$) skeletons shrink upon cooling [24,30,36,74], which leads to a red-shift of the CC* emission band as the HOMO-LUMO gap decreases. It also causes a depopulation of the upper vibronic levels (following a Boltzmann distribution) on each vibronic state, thus removing higher energy vibronic transitions and their corresponding components (sometime called *hot bands*) from the spectral envelope. This common phenomenon also results in an apparent red-shift of the emission band upon cooling, as well as a decrease in FWHM [156]. Indeed, examples of FWHM decreases upon cooling for $\text{Cu}_x\text{I}_x\text{S}_y$ species are provided in **Table 32**. However, in the solid state, in addition to the Cu•••Cu distance shortening and depopulation of the upper vibronic levels, a lattice contraction also occurs upon cooling. This common trait has a tremendous consequence of the excited state distortion of the chromophore in the excited state. The nature of these distortions has been addressed for the cubane $\text{Cu}_4\text{I}_4(\text{pyridine})_4$ using DFT calculations [148]. As the medium becomes more rigid upon cooling the skeleton distortion becomes more difficult to achieve and the emission band blue shifts [153]. This effect is called rigido-chromism. An example for such behavior is provided in **Figure 35** [27]. As for the second feature where the emission lifetimes decrease at lower temperature, no explanation was proposed for this counter-intuitive phenomenon. One can only speculate that as the lattice contraction occurs, closer intermolecular contacts become more frequent and non-radiative processes through collisions and frictional motions become more effective. This process would be structure specific. Furthermore, attempts to correlate the τ_e values or any photophysical parameters with the cluster geometry and structural metrics, namely the Cu•••Cu separations, ligand structure, dimensionality of the CP, and lattice density, even for small groups of structurally related species, appear futile (**Table 32**) [27], for ubiquitous lattice packing reasons.

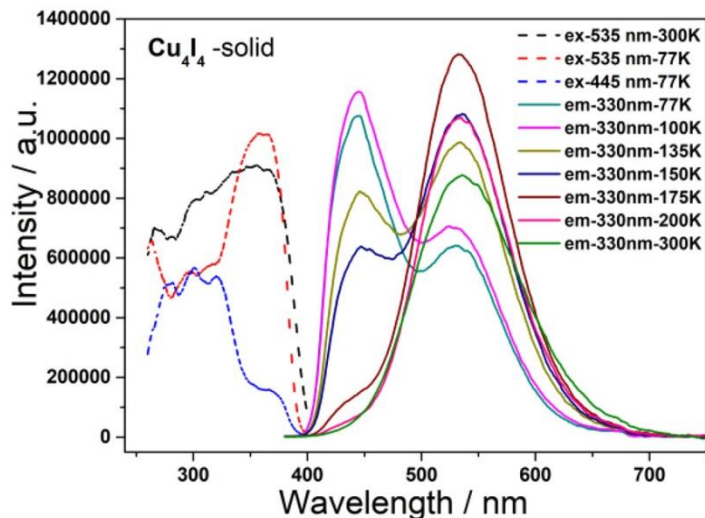


Figure 35. Typical behaviour of solid state emission of Cu_4I_4 cubane displaying a high and a low energy band switching intensity with temperature [155]. Reproduced with permission from *Inorg. Chem.* **2019**, *58*, 10736–10742. <https://doi.org/10.1021/acs.inorgchem.9b00876>. Copyright (2019) American Chemical Society.

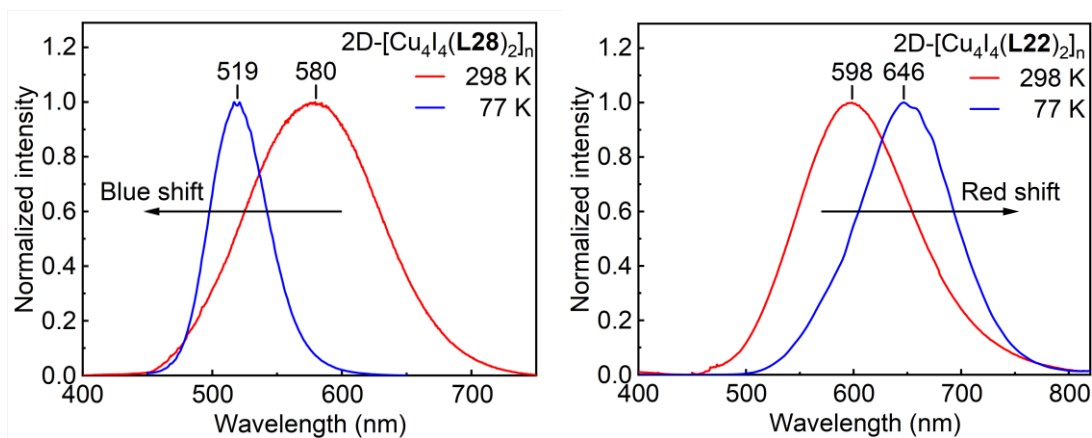


Figure 36. Left, illustration of the blue shift occurring in the solid state for $2\text{D}-[\text{Cu}_4\text{I}_4(\text{L28})_2]_n$ upon cooling to 77K. Right, illustration of the red shift occurring in the solid state for $2\text{D}-[\text{Cu}_4\text{I}_4(\text{L22})_2]_n$ upon cooling to 77K. Modified with permission from *Inorg. Chem.* **59** (2020) 3686–3708 [27]. <https://doi.org/10.1021/acs.inorgchem.9b03275>. Copyright (2019) American Chemical Society.

Table 32. Photophysical parameters of the *globular* $\text{Cu}_x\text{I}_x\text{S}_y$ species (note that examples reporting only λ_{em} with no other photophysical parameters are not included in this list).

SBU	xD-Formula	T (K)	λ_{em} (nm) {FWHM} [Φ_e]	τ_c (μ s) (% contribution)	Ref
Cubane	2D-[Cu ₄ I ₄ (L33) ₂] _n	298	606 {4000} [0.36]	6.3 ± 0.3	[27]
		77	594 {2900}	8.6 ± 0.4	
Cubane	2D-[Cu ₄ I ₄ (L28) ₂] _n	298	580 {4700} [0.61]	8.7 ± 0.4	[27]
		77	517 {2100}	6.3 ± 0.3	
Cubane	2D-[Cu ₄ I ₄ (L25) ₂] _n	298	613 {3600} [0.18]	9.3 ± 0.5	[27]
		77	613 {2200}	8.1 ± 0.4	
Cubane	2D-[Cu ₄ I ₄ (L22) ₂] _n	298	601 {3300} [0.14]	8.9 ± 0.5	[27]
		77	646 {2500}	14.9 ± 0.7	
1D-polycubane	3D-[Cu ₄ I ₄ (L15) _{1.5}] _n	298	504 {3700} [0.15]	1.82 ± 0.09	[27]
		77	505 {2300}	2.13 ± 0.10	
Cubane	2D-[Cu ₄ I ₄ (L13) ₂] _n	298	575	0.85 ± 0.01	[22]
		77	600	3.36 ± 0.01	
Hexagonal prism	3D-[Cu ₆ I ₆ (L18) ₃] _n	298	555	2.62 ± 0.03	[22]
		77	565	3.40 ± 0.06	
Cubane	1D-[Cu ₄ I ₄ (L52) ₃] _n	298	565 {3680}	7.34 ± 0.05	[48,64]
		77	565 {1900}	8.80 ± 0.06	
Cubane	2D-[Cu ₄ I ₄ (L11) ₂] _n	298	575	8.26 ± 0.18	[44]
		77	550	5.96 ± 0.21	
Cubane	2D-[Cu ₄ I ₄ (L12) ₂] _n	298	547	4.69 ± 0.13	[44]
		77	540	3.99 ± 0.56	
Cubane	2D-[Cu ₄ I ₄ (L9) ₂] _n	298	520	1.64 ± 0.01	[28]
		77	525	6.03 ± 0.10	
Cubane	1D-[Cu ₄ I ₄ (L19) ₂] _n	298	560	1.04 ± 0.05	[28]
		77	555	8.04 ± 0.01	
Cubane	?D-[Cu ₄ I ₄ (L14) ₂] _n	298	560	7.00 ± 0.50	[31]
		77	560	7.20 ± 0.01	
Cubane	2D-[Cu ₄ I ₄ (L17) ₂] _n	298	520	1.24 ± 0.06	[29]
		77	520	4.46 ± 0.01	
Cubane	1D-[Cu ₄ I ₄ (L1) ₂] _n	298	515	1.0 ± 0.1	[30]
		77	515	1.2 ± 0.1	
Cubane	1D-[Cu ₄ I ₄ (L2) ₂] _n	298	500	1.4 ± 0.1	[30]
		77	510	1.4 ± 0.1	
Cubane	1D-[Cu ₄ I ₄ (L5) ₂] _n	298	550	10.3 ± 0.1	[30]
		77	546	24.2 ± 0.2	
Cubane	1D-[Cu ₄ I ₄ (L7) ₂] _n	298	537	10.3 ± 0.1	[30]
		77	520	5.9 ± 0.1	
Cubane	1D-[Cu ₄ I ₄ (L3) ₂] _n	298	570	1.1 ± 0.1	[30]
		77	640	9.2 ± 0.1	
Cubane	1D-[Cu ₄ I ₄ (L27) ₂] _n	298	525 {3600}	4.02 ± 0.01	[21]
		77	525 {4230}	4.18 ± 0.01	
Fused dicubane	2D-[Cu ₈ I ₈ (L30) ₃] _n	298	530 {2580}	2.72 ± 0.01	[21]
		77	538 {1820}	5.27 ± 0.01	
Open cubane	2D-[Cu ₄ I ₄ (L48) ₃] _n	298	549	5.04 ± 0.04	[36]
		77	551	15.71 ± 0.23	
Closed cubane	1D-[Cu ₄ I ₄ (L49) ₃] _n	298	550	4.66 ± 0.04	[36]
		77	540	11.55 ± 0.25	
Cubane	1D-[Cu ₄ I ₄ (L50) ₃] _n	298	544	6.74 ± 0.25	[36,41]
		77	535	8.49 ± 0.09	
		298	623	5.17 ± 0.01 (27%)	
Cubane	0D-[Cu ₄ I ₄ (L53) ₄]	77	667	2.57 ± 0.01 (43%)	[36]
				2.08 ± 0.01 (84%)	
				1.93 ± 0.01 (16%)	
Cubane	0D-[Cu ₄ I ₄ (L54) ₄]	77	601	3.57 ± 0.01 (85%)	[36]
				12.75 ± 0.01 (15%)	
				1.02 ± 0.01 (95%)	
Fused dicubane	0D-[Cu ₄ I ₄ (L55) ₄]	77	526	3.51 ± 0.01 (5%)	[36]
				0.45 ± 0.01	
				2.12 ± 0.01 (47%)	
Fused dicubane	0D-[Cu ₈ I ₈ (L55) ₆]	77	503	3.34 ± 0.01 (46%)	[36]
				0.20 ± 0.01	
				0.26 ± 0.01 (49%)	

					2.69 ± 0.01 (51%)	
Cubane	2D-[Cu ₄ I ₄ (L131) ₂] _n	298	515		1.03 ± 0.11	[24]
		77	560		1.32 ± 0.01	
Cubane	1D-[Cu ₄ I ₄ (L29) ₂] _n	298	533 {3726}	[0.21]	2.81 ± 0.10	[34]
		77	532 {2087}		5.88 ± 0.10	
Cubane	1D-[Cu ₄ I ₄ (L29) ₂] _n •EtCN	298	519 {3554}	[0.19]	2.50 ± 0.10	[34]
		77	530 {1992}		4.93 ± 0.10	
Fused dicubane	2D-[Cu ₈ I ₈ (L30) ₃] _n	298	561 {3881}	[0.40]	5.11 ± 0.10	[34]
		77	555 {2470}		5.23 ± 0.10 (50%)	
Fused dicubane	2D-[Cu ₈ I ₈ (L30) ₃] _n •MeCN	298	530 {4230}	[0.56]	8.37 ± 0.10 (50%)	[34]
		77	538 {1820}		2.72 ± 0.10	
Fused dicubane	2D-[Cu ₈ I ₈ (L30) ₃] _n •EtCN	298	539 {3853}	[0.10]	5.27 ± 0.10	[34]
		77	551 {1953}		1.09 ± 0.10	
Cubane	2D-[Cu ₄ I ₄ (L10) ₂] _n	298	585 {3800}	[0.37]	4.88 ± 0.10	[18]
		77	588 {2300}		8.94 ± 0.30	
Fused open dicubane	3D-[Cu ₈ I ₈ (L47) ₄] _n	298	534 {5900}	[0.36]	8.36 ± 0.30	[74]
		77	574 {2900}		2.41	
Cubane	3D-[Cu ₄ I ₄ (L56) ₂] _n	293	519		2.51	[37]
		77	528		12.1	
Cubane + rhomboid	1D-[Cu ₁₀ I ₁₀ (L56) ₇ (MeCN)] _n	293	552		10.4	[37]
		77	575		23.7	
Cubane	0D-[Cu ₄ I ₄ (L56) ₄]	293	590		15.5	[37]
		77	583		19.1	
Cubane	0D-[Cu ₄ I ₄ (L56) ₄]	293	541		15.0	[37]
		77	529		9.97	
Cubane	0D-[Cu ₄ I ₄ (L56) ₄]	293	541		6.60	[37]
		77	576		8.99	
					15.5	

Although much less common than the Cu₄I₄L₄ species (L = N-, P-, S- and Se-donors), closed cubane Cu₄Br₄L₄-containing materials (L = N- and P-donors) are also occasionally found to be luminescent with parameters similar to their iodide congeners [139,146,157–161]. Concerning Cu₄X₄E₄ cubanes (X = Br, Cl; E = S, Se, Te), no examples have been observed so far (see text above).

The second category of chromophores consists of *quasi-planar* Cu_xX_xS_y species (**Table 33**; X = Cl, Br, I; note that no luminescence was reported for Cu_xX_xE_y-containing materials where E = Se, Te). The number of examples for which luminescence is observed for this type of chromophore is significantly less than that of the *globular* clusters because they are often weakly emissive or not at all. In contrast with the *globular* species, which exhibit specific windows of photophysical parameters (*i.e.* 500 < λ_{em} < 670 nm, ~0.2 < τ_e < ~25 μs), the emissive rhomboids and *quasi-planar* species show much larger ranges of λ_{em} (378 < λ_{em} < 640 nm, X = I; 380 < λ_{em} < 560 nm, X = Br; 423 < λ_{em} < 592 nm, X = Cl) and the emission lifetimes may be as short as 30 ps and as long as 0.54 ms, and often their emission decays are multi-exponential. Noteworthy, the number of Br-containing species that have been reported to be emissive surpasses

overwhelmingly those for X = Cl and I. The reason remains unknown. The nature of the emissive excited state of the Cu₂I₂S₄ rhomboids imbedded inside the 1D-chain of [Cu₂I₂(μ-cyclic-S(CH₂)₄S)]_n was addressed by DFT computations and was assigned to an M/XLCT triplet excited state [80]. This conclusion is consistent with that of earlier theoretical calculations on a series of rhomboid-shaped complexes of formula [Ag₂X₂(dmb)₂] (X = I, Br, Cl; dmb = 1,8-diisocyano-p-menthane) [162], suggesting that the outcome is largely structure based, when the halide-containing tetravalent metal has a d¹⁰ electronic configuration and there is no significant M-M interactions. The role of the halide in the filled frontier MOs is well demonstrated by the conclusion drawn by theoretical calculations on the lowest energy excited states of the {[M(dmb)₂](Y)}_n polymers, which has no halide (M = Cu(I), Ag(I); Y = BF₄⁻, PF₆⁻, NO₃⁻, ClO₄⁻, CH₃CO₂⁻; metal-to-ligand charge transfer, MLCT) [163].

The first two entries of **Table 33** provide extreme cases. The long emission lifetimes of ~0.54 ms reflect the lesser heavy atom effect of the chloride ligands compared to bromide and iodide. The particularly short lifetimes (ps-ns) exhibit poly-exponential decays (see starred data). This behaviour arise from triplet-triplet annihilation as demonstrated by the quadratic power dependence of the emission intensity and lifetimes [17,18]. This behavior is associated with efficient excitation energy migration across the lattice where the rhomboids are closely spaced. This is the case for the isostructural 3D-[Cu₂X₂(L)]_n polymers (X = Br, Cl) where the lattice is built upon 2D-layers of Cu₂X₂S₄'s bridged by a S-atom of a EtS(CH₂)₄SEt ligand, which interconnect the layers. The excitation energy migration occurs because of the short separation between the rhomboid clusters. These investigations are interesting as they were reporting, surprisingly for the first time, the presence of an excitation energy migration between coordination entities. Normally such photophysical behaviour occurs for organic chromophores and inorganic solids only. Other CPs also exhibit short-lived emission poly-exponential decays, notably the 1D-[Cu₂Br₂(L)₂]_n CPs (L = ArS(CH₂)_mSAr; Ar = Ph, p-Tol, m = 3,5), but the quadratic dependence of the emission intensity and lifetimes was not verified in these cases [28]. This behavior disappears when the pendent group on the S-atom imposes some steric restrictions as observed for the 1D-[Cu₂X₂(L)₂]_n CPs (X = I, Br; L = CyS(CH₂)₃SCy) [31]. It is noteworthy that no cubane or *globular* species exhibit efficient excitation energy migration. This absence is due to the generally large distances between the clusters. Except of a few exceptions, the other τ_e

data range between 0.4 to 26 μ s, which resemble to that for the $\text{Cu}_4\text{I}_4\text{S}_4$ cubanes and the related globular clusters and is typical of triplet emission of coordination complexes. Similarly, attempts to correlate the photophysical parameters with the structure prove difficult.

Table 33. Photophysical parameters of the $\text{Cu}_2\text{I}_2\text{S}_4$ rhomboids and other *quasi-planar* $\text{Cu}_x\text{I}_x\text{S}_y$ species (note that one *globular* specie ($2\text{D}-[\text{Cu}_5\text{Br}_5(\text{MeSPr})_3]_n$) is included).

SBU	$x\text{D}$ -Formula	T (K)	λ_{em} (nm) {FWHM}	τ_e (μ s)	Ref
Linked rhomboid	$2\text{D}-[\text{Cu}_4\text{Cl}_4(\text{L78})]_n$	298	592 {5650}	532 ± 1	[29]
		77	525 {2380}	544 ± 1	
		298	434 {3600}	0.00003*	
Rhomboid	$3\text{D}-[\text{Cu}_2\text{Cl}_2(\text{L10})]_n$	77	423 {3100}	0.00093*	[17]
				0.00102*	
				0.00352*	
Step staircase + rhomboid	$2\text{D}-[(\text{Cu}_3\text{Br}_3)(\text{L49})_3]_n$	298	442	< 0.1	[36]
		77	440	4.98 ± 0.07	
			510 (sh.)	8.29 ± 0.20	
Open- $[\text{Cu}_4\text{Br}_4]+[\text{Cu}_2\text{Br}_2]$	$1\text{D}-[\text{Cu}_3\text{Br}_3(\text{L50})_3]_n$	298	425	0.89 ± 0.01	[48]
			550	0.78 ± 0.01	
		77	440	2.53 ± 0.05	
Rhomboid	$3\text{D}-[\text{Cu}_2\text{Br}_2(\text{L10})]_n$	298	430 {2900}	0.00345*	[18]
		77	416 {2800}	0.00335*	
		298	385	1.34 ± 0.01	
Square pyramidal cluster	$2\text{D}-[(\text{Cu}_5\text{Br}_5)(\text{L50})_3]_n$	77	400	1.08 ± 0.01	[41]
			525 (sh.)	2.70 ± 0.01	
		298	420	0.64 ± 0.01	
Rhomboid	$2\text{D}-[\text{Cu}_2\text{Br}_2(\text{L16})_2]_n$	77	470	1.32 ± 0.03	[24]
			370	3.43 ± 0.07	
			470	Not measured	
Rhomboid	$0\text{D}-[\text{Cu}_2\text{Br}_2(\text{L131})_2]$	298	448	1.58 ± 0.02	[24]
		77	459	1.85 ± 0.05	
Rhomboid	$?\text{D}-[\text{Cu}_2\text{Br}_2(\text{L75})_2]_n$	298	450	2.98 ± 0.01	[24]
		77	456	4.05 ± 0.08	
Rhomboid	$2\text{D}-[\text{Cu}_2\text{Br}_2(\text{L74})_2]_n$	298	444	1.75 ± 0.20	[24]
		77	463	6.62 ± 0.10	
Rhomboid	$1\text{D}-[\text{Cu}_2\text{Br}_2(\text{L9})]_n$	298	380	10.0 ± 0.1	[28]
			503	12.0 ± 0.1	
		77	410	11.5 ± 0.2	
$[\text{Cu}_2\text{Br}_2]$	$1\text{D}-[\text{Cu}_2\text{Br}_2(\text{L})_2]_n$ BzS(CH ₂) ₃ SBz	298	550	11.3 ± 0.1	[30]
			380	24.2 ± 0.1	
		77	410	26.2 ± 1.3	
Rhomboid	$1\text{D}-[\text{Cu}_2\text{Br}_2(\text{L9})]_n$	298	480	0.00015*	[28]
		77	490	0.00020*	
Rhomboid	$1\text{D}-[\text{Cu}_2\text{Br}_2(\text{L19})]_n$	77	470	0.00002*	[28]
Rhomboid	$1\text{D}-[\text{Cu}_2\text{Br}_2(\text{L20})]_n$	77	470	0.00024*	[28]
Rhomboid	$1\text{D}-[\text{Cu}_2\text{Br}_2(\text{L14})_2]_n$	298	425	4.91 ± 0.08	[31]
		77	425	5.17 ± 0.10	
			480	8.66 ± 0.01	
Rhomboid	$1\text{D}-[\text{Cu}_2\text{I}_2(\text{L14})_2]_n$	298	510	4.13 ± 0.10	[31]
		77	422	5.34 ± 0.02	
			530	9.30 ± 0.10	
Rhomboid	$1\text{D}-[\text{Cu}_2\text{I}_2(\text{L99})_2]_n$	298	378	1.04 ± 0.01	[80]
			535	0.97 ± 0.04	
		77	413	1.43 ± 0.02	
Step staircase	$2\text{D}-[\text{Cu}_4\text{I}_4(\text{L83})_3]_n$		640	1.49 ± 0.04	[23]
		298	481 ($\Phi = 0.17$)	0.43 (47%)	

		77	499	1.52 (53%)
				1.88 (94%)
				12.3 (6%)
Step staircase	$3D-[Cu_4I_4(L123)_5]_n$	298	550	9.13 [110]

*Other components exist and the τ_e 's vary with the laser power due to triplet-triplet annihilation.

Copper Halide-Chalcogenoether and -Chalcogenone

For comparison purposes with 0D CuX complexes and coordination polymers built upon N- and P-containing ligands and to slightly enlarge the scope of this section on the photophysical properties of the copper halide-chalcogenoether networks, several reports on the recent advances on organonitrogen and organophosphorus ligand-containing networks are now described. Indeed, there is an increasing interest in the optical properties of this related systems and their uses in material science [75].

An interesting phenomenon reported for Cu_nX_n (generally $X = I$) SBUs stabilized by organophosphorus and organonitrogen ligands is the possible thermally activated delayed fluorescence (TADF) in the solid state [164] where an emissive singlet excited state is thermally populated by a non-emitting triplet states. This process is called reversed intersystem crossing (rISC) as illustrated in **Figure 37**. The requirement for this process to be possible is that the energy gap between S_1 and T_1 be small enough so that the external thermal energy is sufficient to populate T_1 from S_1 . This process differs from delayed fluorescence: $T_1 + T_1 \rightarrow S_0 + S_1 + \text{heat}$. For example, the 0D- $[Cu(I)(POP)(pz_2BH_2)]$ complex is a blue/white-blue phosphor (POP = bis(2-(diphenylphosphanyl)phenyl)ether, pz_2BH_2 = bis(pyrazol-1-yl)borohydrate; **Figure 38, a**) [165,166]. This complex is described to be a good candidate for singlet harvesting in OLED technologies [164,167,168] as its S_1 state (lifetime = 30 ns) is easily accessible from thermal activation at room temperature. TADF is reported to be the dominant deactivation phenomenon, even though, the lifetime of the 0D-complex's triplet state is reported to be rather long (20 μ s at 300K) rendering its application the OLEDs non ideal.

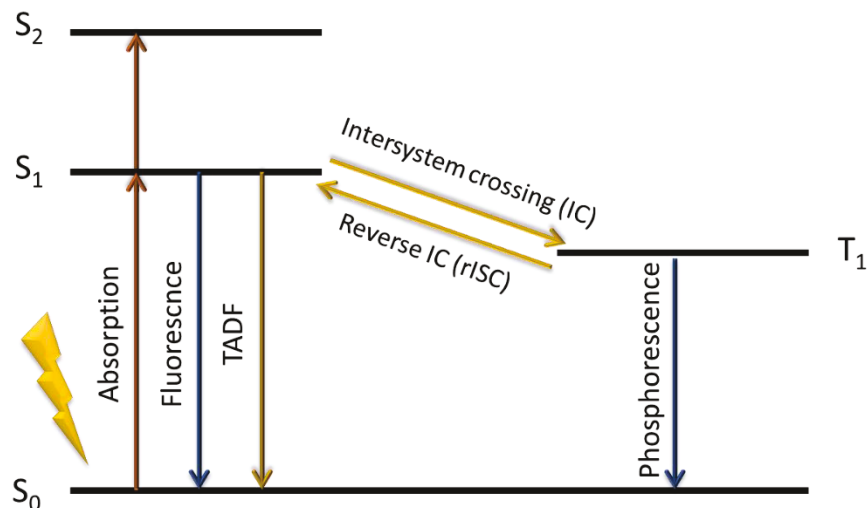


Figure 37. State diagram showing the photophysical events processes for TADF bearing species after absorption of light.

A solvent-free thermal method to access Cu_2I_2 containing discrete complexes that could be easily implemented as thin films for OLEDs applications was also designed for the 0D-complexes $[\text{Cu}_2\text{I}_2(\text{pyrpy})_2(\text{PR}_3)_2]$ (pyrpy = 4-pyrrolidinopyridine; PR_3 = triphenylphosphine (**Figure 38**, b), tri-*m*-tolylphosphine and tri-*p*-tolylphosphine) which display blue TADF centered at 450 nm with respectable emission quantum yields (0.24, 0.31 and 0.51 respectively) [169].

This behaviour was also observed for the coordination polymers 1D- $[\text{Cu}_2\text{I}_2(\text{PPh}_3)_2(3\text{-tpyb})]_n$ (3-tpyb = 1,3,5-tris(3-pyridyl)benzene) [170] and 2D- $[\text{Cu}_2\text{I}_2(4,4'\text{-bpy})_2]_n$ [171] (**Figure 38**, c and d). These two motifs exhibit a rhomboid Cu_2I_2 core with blue-to-yellow and weak red TADF respectively coming from the MLCT* (metal-to-ligand charge-transfer excited state) mixed with XLCT* (halide-to-ligand charge-transfer excited states). After grinding, these materials were found to display mechanochromism properties with an emission band characteristic from phosphorescence arising from a $^3\text{CC}^*$ (triplet cluster centered excited state). This allows for a switch between TADF and phosphorescence upon mechanical stimuli.

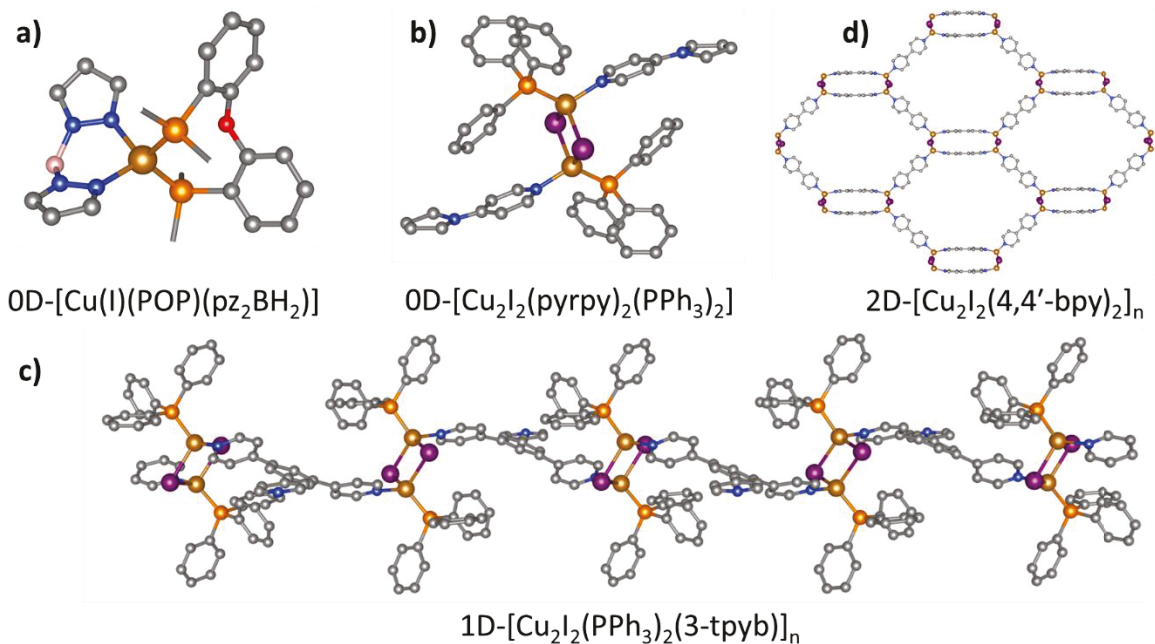


Figure 38. X-ray structures of a) $0D-[Cu(I)(POP)(pz_2BH_2)]$ (C_6H_5 groups on phosphines were omitted for clarity), b) $0D-[Cu_2I_2(pyrpy)_2(PR_3)_2]$, c) $1D-[Cu_2I_2(PPh_3)_2(3-tpyb)]_n$ and c) $2D-[Cu_2I_2(4,4'-bpy)_2]_n$. Color code: Cu, orange ; I, purple ; P, light orange ; C, grey ; N, blue ; O, red ; B, beige ; Hydrogen atoms were omitted for clarity. The images were reproduced using the cif files from the Cambridge Crystallographic Data Centre; CCDC number: a) 851397, b) 1821141 c) 1843261 and d) 1886408.

Other 0D- complexes constructed with mono- and bis-arylphosphine are more prone to the Cu_4I_4 cubane formation with similar spectral properties as the one constructed with chalcogenoethers. For example, Perruchas highlights the different photophysical properties of this complexes with insight on their thermo- and mechanochromic properties [172–174]. The alkoxysilane phosphine $PPh_2(CH_2)_2Si(CH_3)_2(OCH_2CH_3)$ ligand reacts with CuI , and after an hydrolysis-condensation to forming a chelating ligand, a Cu_4I_4 cubane SBU was formed. Two polymorphic crystals of $0D-[Cu_4I_4(PPh_2(CH_2)_2(CH_3)_2SiOSi(CH_3)_2(CH_2)_2PPh_2)_2]$ were obtained displaying green and yellow emissions ($\lambda_{exc} = 312$ nm; **Figure 39**, a). Upon grinding, the “green” polymorph changes its emission color to yellow mimicking the spectral behaviour of the yellow polymorph probably induced by the *harmonisation* of the Cu-Cu distances as suggested by the authors [172]. A series of cubane-containing $0D-[Cu_4I_4(PR_3)_4]$ complexes were prepared by reacting CuI with PAR_3 ($Ar = 4-C_6H_5CF_3, 4-C_6H_5OMe, 4-C_6H_5Me$) [173]. A photophysical study of these complexes revealed

that their optical properties could be tailored by controlling the electron withdrawing ability induced by the substituents. Thermochromism was also detected within the range of 8 to 290K (**Figure 39**, b). More recently, Utrera-Melero et al. [174] reported another discrete complex $0D-[Cu_4I_4[PPh_2(C_6H_4OMe)]_4] \cdot 3THF$ with mechanochromic behaviour (**Figure 39**, c).

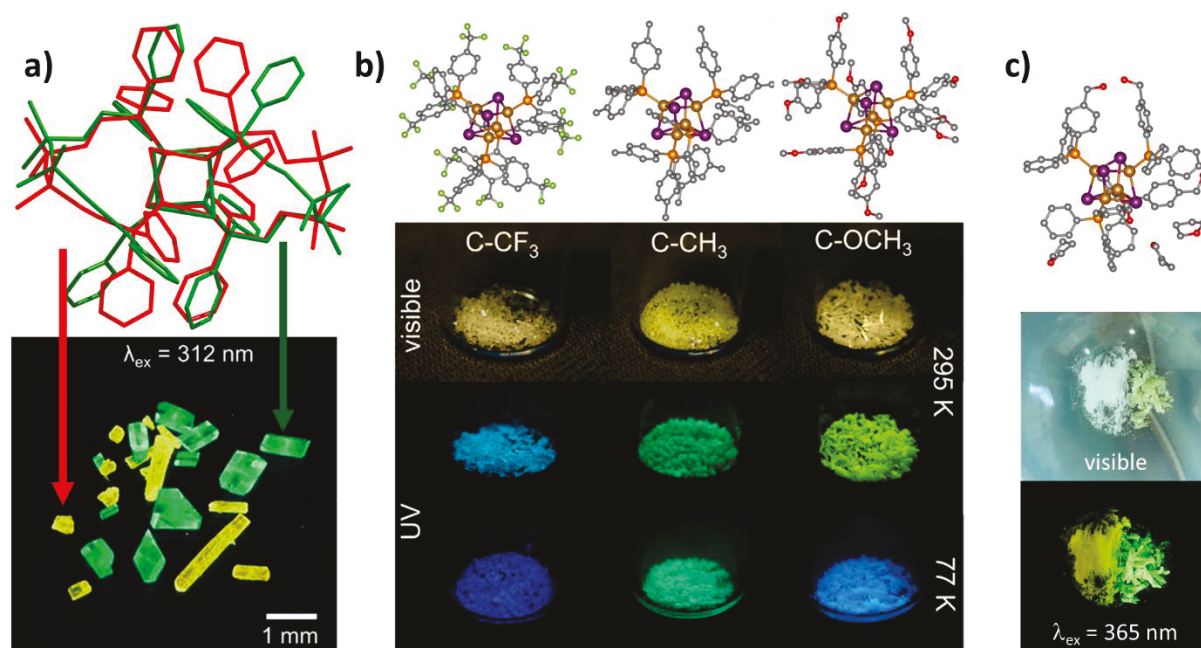


Figure 39. a) Top, comparison of the two polymorphs of $0D-[Cu_4I_4(PPH_2(CH_2)_2(CH_3)_2SiOSi(CH_3)_2(CH_2)_2PPH_2)_2]$. Bottom, emissions under UV-light (green structure = green polymorph and red structure = yellow polymorph). Adapted with permission from *J. Am. Chem. Soc.* 2014, 136, 32, 11311–11320. Copyright 2021 American Chemical Society. b) Top, X-ray structure of $0D-[Cu_4I_4(PR_3)_4]$ (R = PhCF₃, PhOMe, PhMe). Bottom color of the crystals under visible and UV-light at room temperature and 77 K. Reprinted with permission from *Inorg. Chem.* 2018, 57, 8, 4328–4339. Copyright 2021 American Chemical Society. c) Top, X-ray structure of $0D-[Cu_4I_4[PPH_2(C_6H_4OMe)]_4] \cdot 3THF$. Bottom, crushed and crystalline samples of $0D-[Cu_4I_4[PPH_2(C_6H_4OMe)]_4] \cdot 3THF$ under visible and UV-light at room temperature. Adapted with permission from *Inorg. Chem.* 2020, 59, 18, 13607–13620. Copyright 2021 American Chemical Society. Color code: Cu, orange ; I, purple ; P, light orange ; C, grey ; F, green ; O, red ; Hydrogen atoms were omitted for clarity. The images were reproduced using the cif files from the Cambridge Crystallographic Data Centre; CCDC number: a) 980393-980394, b) 1582204-1582206 and c) 2005965.

It is also worth mentioning that the high fluxionality of the coordination sphere of the copper(I) ions and the presence of Cu-Cu interactions are highly connected and impact greatly the structure and the photophysical properties of this class of compounds. For further references, one can consult the work of Lescop [175–177] and Steffen [178,179] as well as the short review by Tsai focussing on the cuprophilic interactions [150].

10. Related topics and comments

The first section of this review focused on the occurrence of *globular* and *quasi-planar* SBUs in the reported 0D-, 1D-, 2D- and 3D-species. In comparison with the seleno- and telluro-analogues, the thioether and thione assembling ligands have been overwhelmingly used. This observation may be related to the high toxicity of the former two elements. Based on the basic research performed in this field, several patents were also deposited. For recent examples, the 3D CP $[\text{Cu}_4\text{I}_4(\text{L166})_4]_n$ (**L166** = 2-mercaptobenzothiazol) was successfully used for selective sensing of *o*-nitrophenol in waste water (*Chair form copper iodine cluster (Cu₄I₄(Etmbt)₄) and its application in selective recognition of o-nitrophenol in wastewater*, CN 110054638 A 20190726) [181], and a series of 1D and 2D CPs of a general formula $[\text{Cu}_m\text{X}_m\text{L}_a]_n$ (X = Br, I; L = ferrocenyl-E-R-E-ferrocenyl; E = Se, Te; R = (CH₂)_x, 1,4- and 1,3-C₆H₄; m and a ≥ 1) were used as homogeneous catalysts for catalytic coupling reaction of carbon-nitrogen (*ferrocene cuprous cluster catalyst for catalytic coupling reaction of carbon-nitrogen, and preparation method thereof*, CN 107803223 A 20180316) [182]. The use of CuCN and AgX salts (X = Cl, Br, I), and design and coordination of metal-containing chalcogenide ligands, are obvious alternatives or extensions to this chemistry. Surprisingly, literature proves that examples are extremely rare (below).

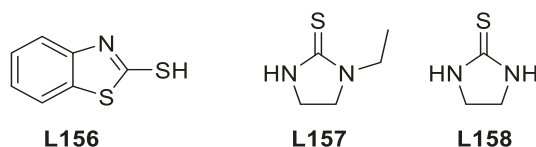


Figure 40. Other selected ligands.

10.1. Silver species

Despite the expected similarity in the chemistry of the silver and copper salts, the literature based on silver halides drastically differs from copper as precursors of chalcogenoether and -chalcogenone materials. Indeed, and to the best of our knowledge, no network or CP have been reported with the silver salts, excluding some ditopic ligands. Moreover, the number of discrete complexes that were isolated and characterized turns out to be extremely limited. In earlier days, two $\text{Ag}_4\text{X}_4\text{L56}_4$ cubanes ($\text{X} = \text{Br}, \text{I}$; **L56** = tetrahydrothiophene, THT), were prepared and characterized by large angle X-ray crystallography [183,184]. The structure is assigned as a stella quadrangular with distances that slightly differ from the copper homologues ($\text{Ag}_4\text{I}_4\text{L56}_4$: Ag-I, 2.799(4); Ag-Ag, 3.072(6), I-I, 4.638(19) Å, $\text{Ag}_4\text{Br}_4\text{L56}_4$: Ag-Br, 2.592(3); Ag-Ag, 2.866(5) and Br-Br, 4.25(4) Å [183]. The sum of the van der Waals radii is 3.74 Å, which suggest that $\text{Ag}\cdots\text{Au}$ interactions are present. The structure of **L156** is in **Figure 40**. Recently, two rhomboid-shaped complexes, $[\text{Ag}_2\text{Cl}_2(\mu\text{-L157})_2(\text{L157})_2]$ and $[\text{Ag}_2(\mu\text{-Br})_2(\text{L158})_4]$ were prepared with the thione ligands **L157** and **L158** and were examined for antimicrobial activity against Gram positive, Gram negative and a yeast (**Figure 41**) [185]. Both complexes show high activities (low minimum inhibitory concentration), somewhat better than that obtained for some the copper(I)-containing species in some cases. There seems to be room for further studies.

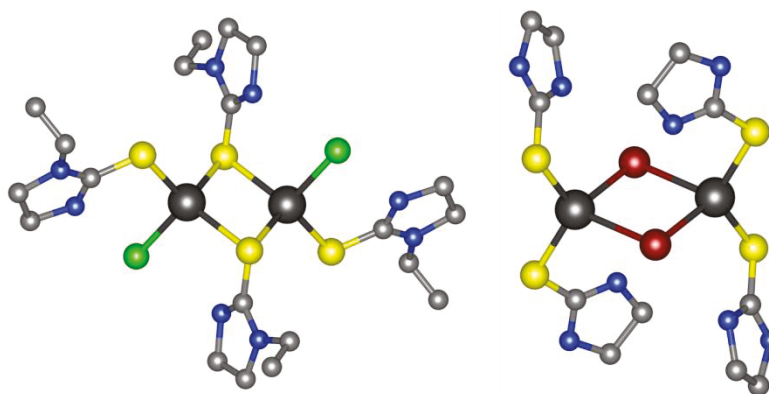


Figure 41. X-ray structure of the two dimeric silver complexes $[\text{Ag}_2\text{Cl}_2(\mu\text{-L157})_2(\text{L157})_2]$ left and $[\text{Ag}_2(\mu\text{-Br})_2(\text{L158})_4]$ right. Ag, dark grey; Cl, green; S, yellow; Br, deep red; N, blue ; C, grey, Hydrogen atoms were omitted for clarity. The images were reproduced using the cif files from the Cambridge Crystallographic Data Centre; CCDC numbers: 1956609 and 1956611.

10.2. The thioether within multitopic ligands

One of the key issues is the relative propensity of Cu-S bonds to be formed relative to other copper-ligand coordination linkages, namely Cu-N and Cu-P. Many examples of multitopic ligands binding CuX salts (X = Cl, Br, I) involving thioether moieties, exist, but just almost systematically no Cu-S bonds is formed. Indeed, multiple examples of phosphine-containing ditopic ligands exists and the Cu-P bond is uniquely formed stressing the well-known stronger ligand properties of the phosphines [186–188]. Similarly, pyridyls and imines are also dominantly favored over the thioethers [189–196] and selenoethers [197] in such ditopic ligands. On some occasions when placed in a chelating geometry, both the pyridyl and thioether moieties combined to link the Cu(I) atom of the SBU to form mixed coordination 0D complexes and 1D-, 2D- and or 3D-CPs [198–200]. Similarly, the (2-pyridyl-Se)₂CH₂ ligand also binds a staircase Cu₄I₄ *via* two Cu-N and two Cu-Se bonds [197]. This mixed-ligand binding scheme is occasionally found with the solvent molecule MeCN as N-donor ligand (several examples were provided in this review). To the best of our knowledge, there are only two reports where the thioether ligand binds the Cu-containing species but not the imine residue (*i.e.* 1D-[Cu₄I₄(L36)₂]_n [33] entry 1, **Table 2** and 2D-[Cu₂I₂(L113)]_n [100] entry 13,

Table 9).

Similarly, several examples of thione-containing multitopic ligands are also provided in this review and again systematically the electron rich thione function binds the copper(I) metal first, even before thioethers [108,121,122,129]. Interestingly, this weaker affinity for the thioether ligands to competitively bind the Cu(I) center of the (CuX)_n SBUs (X = Cl, Br, I) in comparison with some common heteroatomic donors, namely phosphines, imines, pyridyls, and amines, and even thiones, makes the corresponding discrete complexes and CPs (for example 1D-[Cu₄I₄(L36)₂]_n), particularly special. Concurrently, the use of multitopic ligands containing thioether and ether groups systematically leads to the formation of Cu-S coordination bonds demonstrating that the softer Lewis base is favorably interacting with the electron rich and softer Lewis acid copper(I). Moreover, the recently demonstrated selectivity for the thioether group over the ethynyls in (MeS)₂C₆H₄C≡C-9,10-anthracenyl-C≡CC₆H₄(SMe)₂ [201], MeSC₆H₄C≡C-C≡CC₆H₄SMe [23], and *p*-MeC₆H₄SCH₂C≡CCH₂SC₆H₄-*p*-Me [25], two soft ligands with the possibility of back-bonding, for the copper atoms of the CuCN chains, staircase Cu₄I₄ SBU, and Cu₄I₄ cubane unit in their respective 2D networks is interesting. Indeed, an opposite trend was

observed with the organometallic ligands containing the negatively charged ethynyl moiety ($\text{RC}\equiv\text{C}^-$) (see section on the organometallic ligands). A recent example of an organometallic ligand, *trans*- $\text{MeSC}_6\text{H}_4\text{C}\equiv\text{C}\text{Pt}(\text{PMe}_3)_2\text{C}\equiv\text{N}$, where the hierarchy of affinity has been well demonstrated ($\text{Cu-N}\equiv\text{C} > \text{Cu}-(\eta^2\text{-C}\equiv\text{C}) > \text{Cu-S}$) [202].

10.3. $(\text{Cu}_m\text{X}_{m+n})^{n-}$ halogenocuprates

One of the main conclusions of the preliminary structural survey is that the cubane Cu_4I_4 and rhomboid Cu_2X_2 ($\text{X} = \text{Cl}, \text{Br}, \text{I}$) are generally favored as SBUs and that steric reasons could often account for this outcome. This observation indicates that the weaker Cu-X coordination bonds play an adaptive role in the stabilisation of the crystalline state. Regardless the nature of the ligand, the $(\text{Cu}_m\text{X}_{m+n})^{n-}$ halogenocuprates are often generated upon creating a stoichiometric imbalance between the Cu^+ and X^- ions [203–205]. The number of thioether-containing ligands exhibiting Cu-S bonds is very small. One example uses an excess of I^- ions (as NaI salt) and a 2D CP, $[\text{Na}_2\text{Cu}_6\text{I}_8(\mathbf{L91})_2(\text{MeCN})_4]_n$, is obtained in which the SBU is a $\text{Cu}_6\text{I}_8^{2-}$ anion (adopting a pseudo staircase geometry) and the excess of Na^+ cations are captured by the ether-thioether-containing macrocycle (**Figure 42**) [79]. Using this same approach, ligand **L44** and KI react with CuI to form a non-emissive CP $[\text{KCu}_{4.25}\text{I}_{5.25}(\mathbf{L44})(\text{MeCN})_2\cdot(\text{CH}_2\text{Cl}_2)_{0.75}]_n$ where the SBU consists of a 1D distorted ribbon and the K^+ cations are trapped inside the macrocycle (**Figure 43**) [46]. Moreover, the use of 1,7-dithia-18-crown-6, **L93**, with CuI and an excess of KI or CsI also form 1D CPs formulated as $[\text{cation}_2\text{Cu}_6\text{I}_8(\mathbf{L93})]_n$ (cation = K^+ or Cs^+), in which the cations are captured by the macrocycle as well and the $\text{Cu}_6\text{I}_8^{2-}$ cuprates are employed as SBUs (**Figure 44**) [86]. It is worth noting that these $\text{Cu}_6\text{I}_8^{2-}$ SBUs differ structurally from that shown in **Figure 42**. Concurrently, the 2D $[\text{RbCu}_4\text{I}_5(\mathbf{L43})_2]_n$ and 3D $[\text{CsCu}_5\text{I}_6(\mathbf{L43})_2]_n$ CPs are formed when the 1,10-dithia-18-crown-6 ligand, **L43**, is reacted with CuI in the presence of respectively RbI and CsI (**Figure 45**) [206]. **L43** acts as a trapping agent thus creating cuprate SBUs, Cu_4I_5^- . The polyanionic SBU of the former CP is composed of Cu_4I_4 units (like opened cube) bridged by iodides. The latter CP also exhibits the Cu_4I_4 open cubes as SBUs but these are bridged by ICuI units. The use of macrocycle trapping agent appears to be a good way to provoke this imbalance as other examples appeared [76].

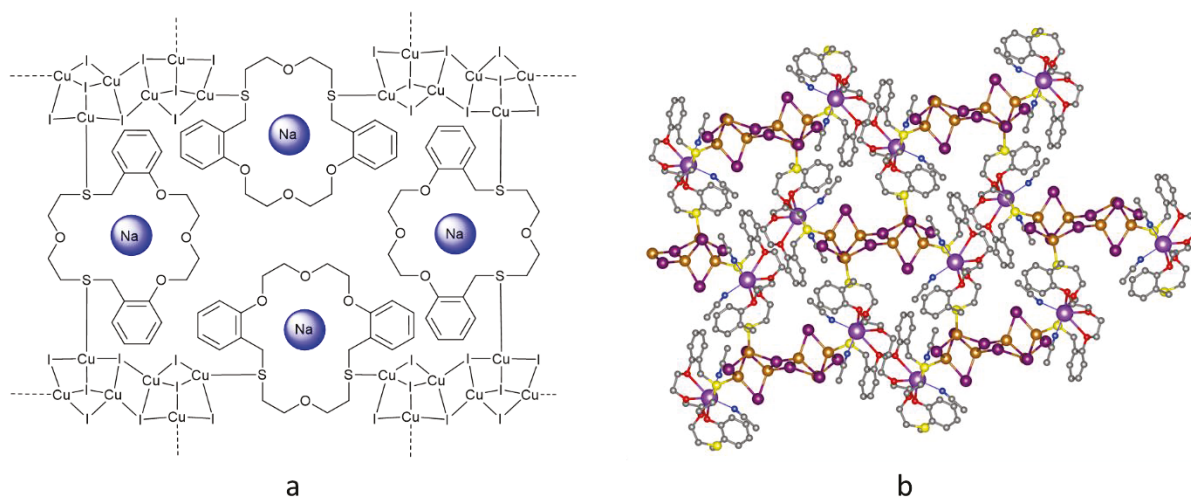


Figure 42. (a) Schematic representation of the $[\text{Na}_2\text{Cu}_6\text{I}_8(\text{L91})_2(\text{MeCN})_4]_n$ CP. MeCN molecules are omitted for clarity (b) X-ray structure of the $[\text{Na}_2\text{Cu}_6\text{I}_8(\text{L91})_2(\text{MeCN})_4]_n$ CP. Na, lavender ; O, red, ; S, yellow; Cu, orange ; I, purple ; N, blue ; C, grey, Hydrogen atoms were omitted for clarity. The image was reproduced using the cif files from the Cambridge Crystallographic Data Centre; CCDC number: 965571.

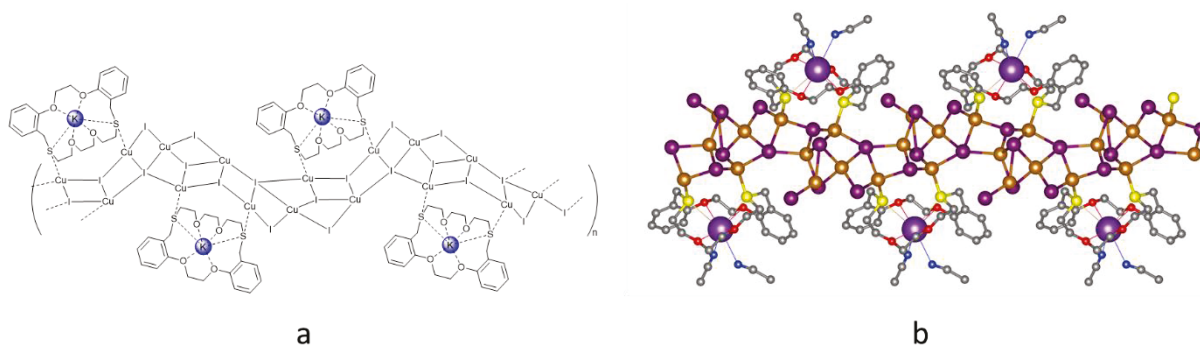


Figure 43. (a) Schematic representation of the $[\text{KCu}_{4.25}\text{I}_{5.25}(\text{L44})(\text{MeCN})_2 \cdot (\text{CH}_2\text{Cl}_2)_{0.75}]_n$ CP. (b) X-ray structure of the 1D- $[\text{KCu}_{4.25}\text{I}_{5.25}(\text{L44})(\text{MeCN})_2 \cdot (\text{CH}_2\text{Cl}_2)_{0.75}]_n$ CP. K, lavender ; O, red, ; S, yellow; Cu, orange ; I, purple ; N, blue ; C, grey, Hydrogen atoms and CH_2Cl_2 molecules were omitted for clarity. The image was reproduced using the cif files from the Cambridge Crystallographic Data Centre; CCDC number: 787696.

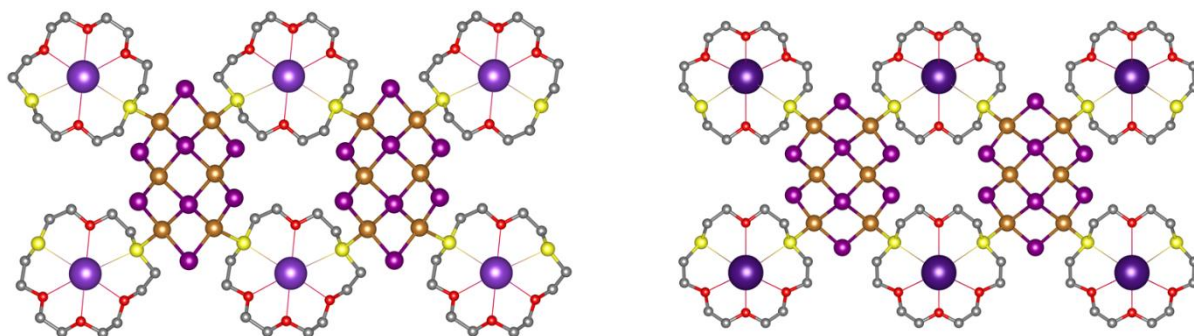


Figure 44. X-ray structures of the 1D CP $[\text{cation}_2\text{Cu}_6\text{I}_8(\text{L93})]_n$ (cation = K^+ , left; or Cs^+ , right). K, lavender ; Cs, dark lavender ; O, red ; S, yellow; Cu, orange ; I, purple ; C, grey, Hydrogen atoms were omitted for clarity. The images were reproduced using the cif files from the Cambridge Crystallographic Data Centre; CCDC number: 207826 and 207827.

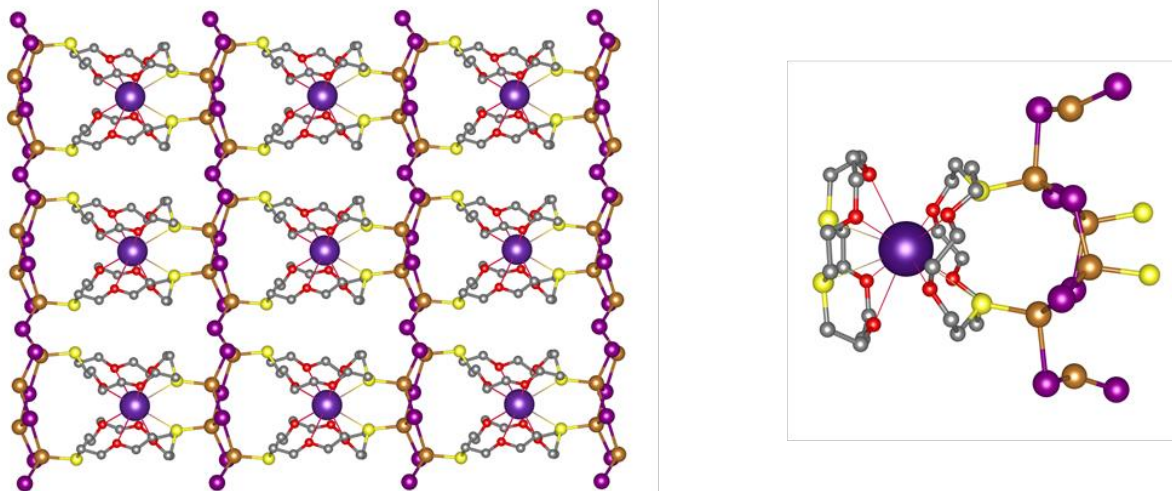


Figure 45. X-ray structure of the 2D $[\text{RbCu}_4\text{I}_5(\text{L43})_2]_n$ (left) and fragment of the 3D $[\text{CsCu}_5\text{I}_6(\text{L43})_2]_n$ CPs (right). Rb and Cs, dark lavender; O, red ; S, yellow; Cu, orange ; I, purple ; C, grey, Hydrogen atoms were omitted for clarity. The images were reproduced using the cif files from the Cambridge Crystallographic Data Centre; CCDC number: 177278 and 177279.

The doping with elemental iodine can also be performed in the presence of CuI and a thioether to form CPs containing halogenocuprates such as the CP $[\text{Cu}_3\text{I}_4(\text{dodecylMeS})_3]^- (\text{dodecylMe}_2\text{S})^+$ [62]. The Cu_3I_4^- SBU appears as a cubane missing a Cu atom. The general observations are as follows. First, the number of discrete complexes and CPs built upon halogenocuprates as SBUs is rather very limited compared to the neutral species. Second, these examples appear to be

solely found for the CuI salt. Third, the structures of the $(\text{Cu}_m\text{X}_{m+n})^{n-}$ SBU is highly variable in stoichiometry ($m = 3-6$) and structure (for an identical m). And fourth, neither an emission nor other property or applications was reported in most cases.

10.4. Relevant particularities

The adaptability of the $(\text{CuX})_n$ SBUs ($X = \text{Cl}, \text{Br}, \text{I}$) is remarkable, not only in metal/ligand stoichiometry (n) and geometry (Cu_4I_4 cubane, open cubane, opened cube, step staircase for example), but also in bidentate connectivity. This latter feature can have a direct consequence on the dimensionality of the resulting CP. An example for such a case concerns the 14-membered ring dithioether ligand **L90** (**Figure 46**) [82]. In this example, the $\text{SCH}_2\text{CH}_2\text{S}$ -moiety can form chelates and bridges respectively leading to a 0D-complex and 1D-CP with the same metal/ligand ratio. Another example is the dithioether ligand $\text{XC}_6\text{H}_4\text{S}(\text{CH}_2)_5\text{SC}_6\text{H}_4\text{X}$ ($X = \text{H}, \text{Me}$), which forms 1D CP of general formula $[(\text{Cu}_2\text{Br}_2)(\text{XC}_6\text{H}_4\text{S}(\text{CH}_2)_5\text{SC}_6\text{H}_4\text{X})_2]_n$ with the particularity that the two bridging ligands coordinating the next rhomboid unit may come from the same Cu atom or two different copper metals (**Figure 47**) [30].

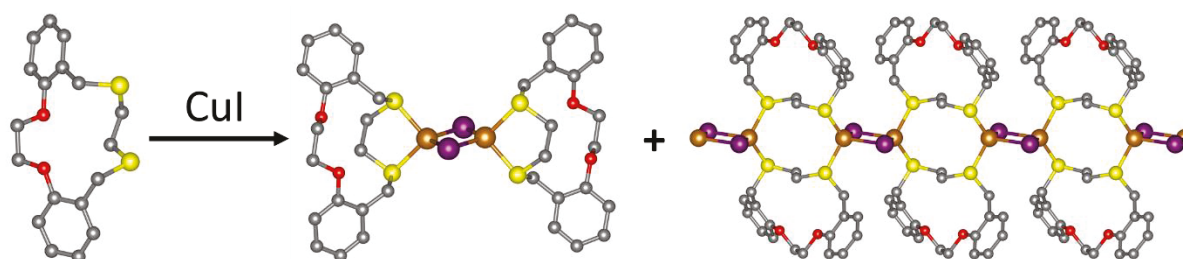


Figure 46. Left: Structure of **L90**. Right: Structures of the two products obtained during the reaction between **L90** and CuI. O, red ; S, yellow; Cu, orange ; I, purple ; C, grey, Hydrogen atoms were omitted for clarity. The images were reproduced using the cif files from the Cambridge Crystallographic Data Centre; CCDC number: 790793 and 790794.

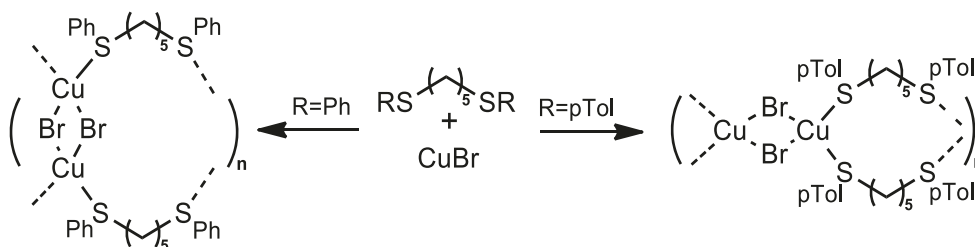


Figure 47. Scheme showing the two different connectivity patterns employed by the Cu_2Br_2 rhomboid SBU to secure the 1D-dimensionality upon changing H for Me in the bridging ligand $\text{XC}_6\text{H}_4\text{S}(\text{CH}_2)_5\text{SC}_6\text{H}_4\text{X}$.

The fact that the sulfur atom bears two lone pairs makes it prone to use one or both during the formation of the CPs. This feature is well illustrated by the rigid ligands **L83** forming 2D- $[\text{Cu}_4\text{I}_4(\text{L83})_3]_n$ [23] and 2,4,6,8-tetrathiaadamantane **L146** forming 1D- $[\text{Cu}_4\text{Cl}_4(\text{L146})_2]_n$ [127] in which both SBUs adopt the step staircase geometry (**Figure 48**). The adamantane structure may promote the chelate connectivity whereas **L83** does not. The consequence is that a single S-atom may use both of its lone pairs (for steric reasons) to bridge two SBUs. The use of both lone pairs is indeed common for monothioethers (see **Table 3**, **Table 4**, **Table 8**, **Table 13**, **Table 14**, **Table 19**, **Table 20**). This point is important since the S-donor differs from the common phosphine, amine, imine and pyridyl ligands, and hence leading to better adaptability of the S-containing ligand towards CuX salts and consequently to a larger scope of corresponding CPs. However, there are a few scarce exception of bridging phosphane ligands coordinated with Cu_nX_n ($\text{X} = \text{Cl}, \text{Br}, \text{I}$) clusters [207–209].

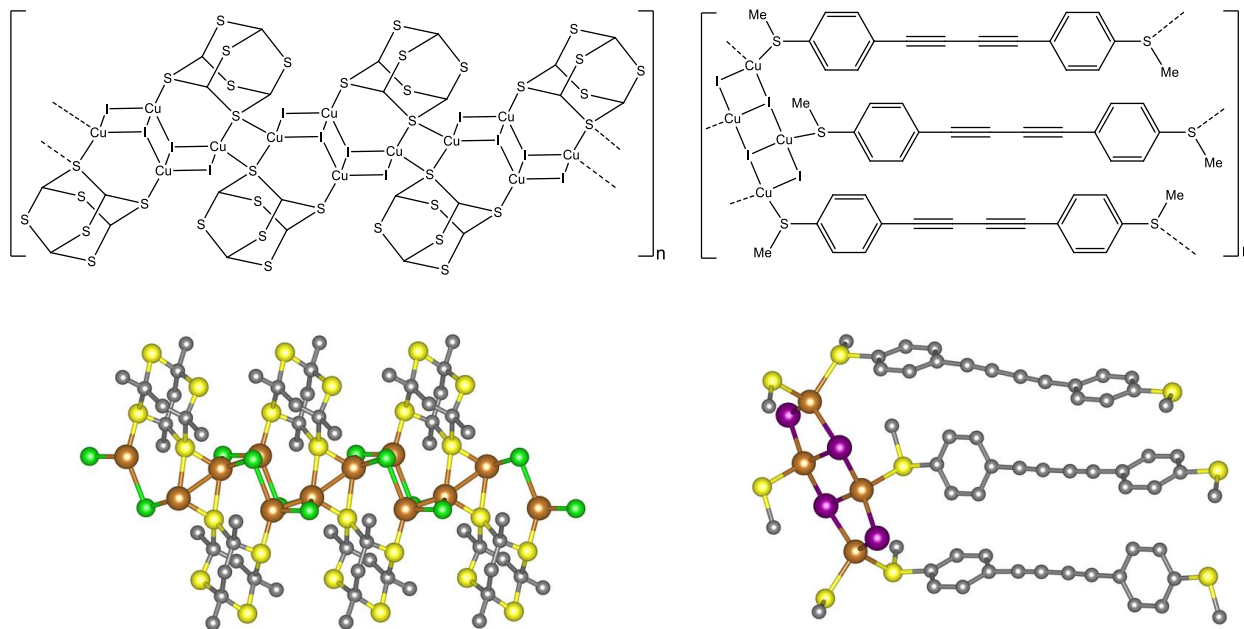


Figure 48. Comparison of the S-connectivity between 2,4,6,8-tetrathiaadamantane **L146** and **L83**. Right, 1D- $[\text{Cu}_4\text{Cl}_4(\text{L146})_2]_n$, left, 2D- $[\text{Cu}_4\text{I}_4(\text{L83})_3]_n$. S, yellow; Cu, orange; I, purple; Cl, green; C, grey, Hydrogen atoms were omitted for clarity. The X-ray images were reproduced

using atomic coordinates from ref [127] and using the cif file provided in supplementary data of ref [23].

During the course of this survey, a few studies showing attempts to vary the metal/ligand ratio in order to monitor its outcome on the SBU geometry and perhaps the dimensionality of the resulting CP, were performed. Among a few studies, one investigation focussed more on this parameter [28]. Interestingly, when the salt is CuI, a 2/1 and 1/1 ratios generally lead to Cu₄I₄ and rhomboid Cu₂I₂ SBUs, respectively, which in turn helps to predict the geometry of the SBU. Concurrently, when the salts are CuBr and CuCl, there is no or very little effect of this ratio on the resulting geometry of the SBU, where the rhomboid geometry is largely observed. This trend certainly helps predict the nature of the anticipated SBU, but literature proves that this trend is not absolute. Indeed, about 80% of the reported structures of the Cu_xBr_xS_y motifs are rhomboids (Table 28), and concurrently about 67% of the reported Cu_xCl_xS_y motifs were also rhomboid (Table 30). These ratios mean that about 20% and 33% are other *quasi-planar* motifs, respectively.

One of the parallel features is that many 0D complexes and 1D-, 2D- and 3D-CPs containing chalcogenoethers or chalcogenothiones also bear coordinated monodentate MeCN ligand (just a few examples were listed in this review). Beside the solubility issue meaning that such species are reaction intermediates, the main obvious reason is the easier crystallisation process with this geometrically small and stronger ligand. The understated advantage is that new CPs bearing their own specificity, properties, and applications become accessible, but the disadvantage is that higher dimensionality CP is not possible since this monodentate ligand is simply not prone to act as a bridging ligand.

The quasi-absence of MOFs or highly porous CPs is chronic, but not totally absent, with this family of materials. Indeed, a very large number of rigid ligands were investigated, and yet, the quest proved difficult, but not illusive. The main reason is again the large adaptability of the (CuX)_n SBUs to adapt to ring stresses and solid-state packing.

One of the notable missing neutral SBU in this review is the Cu_nI_n where n = 7. It has previously been observed for a P-donor ligand (0D-[Cu₇I₇(P(C₆H₄CF₃)₃)₆(MeCN)]) [210], a tridentate N-donor ligand (2D-[Cu₇I₇((3-Py-NH)₃(P=S))]_n) [211], and a ditopic N,S-ligand (0D-[Cu₇I₇(2-Py-

CH₂CH₂S*t*Bu₃)) [212]. In these three cases, the structure consists of layers exhibiting the 1 Cu / 3 L / 3 Cu / 3 L / 3 Cu / 1 L geometry where the tetravalent metals exhibit more or less Cu•••Cu interactions of Cu-Cu bonding. The tetrahedral geometry of the ligands (P(C₆H₄CF₃)₃) and (3-Py-NH)₃(P=S) must definitely play a role in the outcome of the Cu₇I₇ stoichiometry. One may also suspect that the 0D-[Cu₇I₇(2-Py-CH₂CH₂S*t*Bu₃)₃] complex, which exhibit no strong Cu•••Cu interactions, was obtained serendipitously by changing the reaction stoichiometry M/L from 7:3 to 1:1, which lead to the rhomboid species 0D-[Cu₂I₂(2-Py-CH₂CH₂S*t*Bu₂)₂].

11. Conclusion

The networks built upon chalcogenothioether and chalcogenone ligands and copper salts are a research topic of growing interests (**Figure 1**). The large survey and analysis conducted in this review indicated that structurally predetermined rigid, free of potential steric issues, and preferably multidentate ligands (> 2 thioethers or thiones), whether they are strictly bridging or very prone to chelation, along with an appropriate L/M stoichiometry, can lead to a quasi-predictable outcome of both the SBU and CP dimensionality, and thus often of the resulting properties and potential applications as well. Indeed, multiple investigations indicated that the 1:1 and 2:1 L/M ratio respectively led to the formations of *globular*, generally significantly emissive, and *quasi-planar* SBUs, which are generally modestly emissive or simply silent. The copper iodide salt exhibits a strong tendency to generate the closed cubane Cu₄I₄S₄ cluster with an occurrence of 83% among the *globular* motif, and the Cu₂I₂S₄ rhomboid with a probability of 80% among the *quasi-planar* motifs. This larger propensity for this particular structure, therefore higher stability, appears to be related to the presence of multiple Cu-I bonds and of multiple weak cuprophyllic interactions. By examining the nature of the ligands, the formation of other structures and geometries different from closed cubane and rhomboid stems from the sometime obvious ring stress and the presence of steric hindrance. This observation leads to the important conclusion that the SBU adapts its size and structure consequently. Further evidence for this large flexibility and adaptability of the SBUs arises from the comparison of the Cu•••Cu distances in the closed Cu₄I₄S₄ cubanes and Cu₂X₂S₄ rhomboids (the two most encountered motifs). Indeed, the span is very large between the smallest and largest reported Cu•••Cu distances ($d = 0.325, 0.785, 0.508$ and 0.635 Å for Cu₄I₄S₄ and Cu₂X₂S₄; X = I, Br, Cl,

respectively). It is noteworthy that there is no relationship between the Cu^{•••}Cu distances and the resulting dimensionality of the CP, thus indicating that the structural property must be directed by the nature of the ligand. However, the largest piece of evidence for this conclusion on the adaptability of the SBU (structure and Cu^{•••}Cu distance) is that of seleno- and telluroether ligands, excluding the CPs containing coordinated acetonitrile, only the closed cubane and rhomboid motifs have been observed as SBUs (**Table 23**). Conversely, the copper bromide and copper chloride salts do not form closed cubane Cu₄X₄E₄ clusters at all (X = Cl, Br; E = S, Se, Te) and are not prone to generate *globular* SBUs (respectively 2.4 and 8.6% of occurrence when E = S, and 0% when E = Se, Te). This observation comes as a surprise since many closed cubane Cu₄X₄L₄ clusters where X = Cl, Br and L = N- and P-donors are known. Moreover, the quasi-absence of *globular* species characterized by X-ray crystallography for the Se- and Te-containing materials seems to suggest that the longer Se-C and Te-C bonds provide the room necessary for the CP to form without causing too much stress on the most stable SBUs (closed cubane and rhomboid). In addition, the multitopic ligands bearing two types of heteroatoms show that the very large tendency where a given heteroatom or function will bind the Cu(I) center but not the thioether. This observed trend is Cu-P > Cu-N > Cu-S and consistent with the relative ligand strength. Very rare examples (*i.e.* 2) where the thioether bonded the Cu(I) metal, but not the N-donor. These two cases may reveal that more favorable crystal packing is obtained when Cu(I) binds the thioether. Similarly, the neutral acetynyl function, R-C≡C-R, is considered to be a stronger ligand than the thioether and yet all examples in this review (**L17, L18, L78, L83**) show that the thioether fragment binds the metal and not the acetynyl group. This observation also applies for the cis- and trans-ethylene (**L16, L74, L75** and **L130**).

In general, the most encountered dimensionalities of the resulting CPs are 1D- and 2D-CPs. However, the most astonishing observation is the evolution of this trend of forming 1D- and 2D-CPs in comparison with that of 0D-complexes and 3D-CPs for an identical geometry of SBU (rhomboid Cu₂X₂S₄). Indeed, the survey indicates that the probability of forming 1D- and 2D-CPs increases going from I → Br → Cl and inversely for the 0D-species and 3D-CPs. This counter intuitive observation remains unexplained. For the selenoether, telluroether and selone ligands, the sampling is too small for any reliable trends, but the 1D-CP case occurs most often (**Table 23**).

Declaration of Competing Interest

The authors declare no competing financial interest.

Acknowledgements

This work was supported by the Natural Sciences and Engineering Research Council of Canada, the Fonds de Recherche du Québec-Nature et Technologies and the Centre Québécois sur les Matériaux Fonctionnels.

Author Contributions

Conceptualization, A.S and P.D.H.; methodology, A.S.; software, A.S.; validation, A.S., and P.D.H.; formal analysis, A.S., and P.D.H.; investigation, A.S., and P.D.H.; resources, P.D.H.; data curation, A.S.; writing—original draft preparation, A.S., and P.D.H.; writing—review and editing, A.S., K.T., and P.D.H.; visualization, A.S.; supervision, P.D.H.; project administration, A.S.; funding acquisition, P.D.H.; All authors have read and agreed to the published version of the manuscript.

Biographies



Adrien Schlachter completed a bachelor's degree in chemistry in 2014 and a master's degree in physical chemistry of interfaces in 2016 at the Université de Bourgogne Franche-Comté, France. He is currently completing a PhD degree in the field of functional polymeric coordination compounds based on copper(I) in Prof. Harvey's group at the Université de Sherbrooke. He won best oral presentation twice at SACIQ (Symposium Annuel de Chimie Inorganique du Québec).



Kevin Tanner is completing a bachelor's degree in chemistry at the Université de Sherbrooke. He joined the Harvey group in 2018 as a summer student and will join the Harvey Group in January 2022. He also received a grant from the FRQNT-Mitacs International Scholarship Globalink Program.



Prof. P.D. Harvey obtained his MSc at the U. de Montréal (1982) and his PhD at McGill U. (1986). He was a NSERC postdoctoral fellow at CalTech (1986-

88) and MIT (1988) under the supervisions of Profs H.B. Gray and M.S. Wrighton, respectively. He was appointed assistant professor (1989) and promoted to full professor (1998) at the U. de Sherbrooke (Canada). He awarded a Chaire d'Excellence de Recherche from the ANR (France) held at the U. de Bourgogne, Dijon (2008-10). He serves on the Editorial Boards of the *Journal of Cluster Science* and *Journal of Inorganic and Organometallic Polymers*. He published over 320 research papers and 8 book chapters, and he was awarded the Rio Tinto Alcan Award from the Canadian Society for Chemistry (2013), among many other prizes.

References

- [1] P.D. Harvey, M. Knorr, Luminescent coordination polymers built upon Cu_4X_4 ($\text{X}=\text{Br}, \text{I}$) clusters and mono- and dithioethers, *Macromol. Rapid Commun.* 31 (2010) 808–826. <https://doi.org/10.1002/marc.200900893>.
- [2] P.D. Harvey, M. Knorr, Stabilization of $(\text{CuX})_n$ Clusters ($\text{X} = \text{Cl}, \text{Br}, \text{I}; n = 2, 4, 5, 6, 8$) in Mono- and Dithioether-Containing Layered Coordination Polymers, *J. Clust. Sci.* 26 (2015) 411–459. <https://doi.org/10.1007/s10876-014-0831-0>.
- [3] P.D. Harvey, M. Knorr, Designs of 3-Dimensional Networks and MOFs Using Mono- and Polymetallic Copper(I) Secondary Building Units and Mono- and Polythioethers: Materials Based on the Cu–S Coordination Bond, *J. Inorg. Organomet. Polym. Mater.* 26 (2016) 1174–1197. <https://doi.org/10.1007/s10904-016-0378-7>.
- [4] A. Schlachter, P.D. Harvey, Properties and applications of copper halide-chalcogenoether and -chalcogenone networks and functional materials, *J. Mater. Chem. C.* 9 (2021) 6648–6685. <https://doi.org/10.1039/d1tc00585e>.
- [5] S.M. Roodan, A. Ghaderi, Copper-catalyzed demethylative esterification of arylmethylketones: a new route for the synthesis of benzocaine, *J. Iran. Chem. Soc.* 16 (2019) 2327–2332. <https://doi.org/10.1007/s13738-019-01698-z>.
- [6] S. Saha, K. Biswas, P. Ghosh, B. Basu, New 1,2-dithioether based 2D copper(I) coordination polymer: from synthesis to catalytic application in A_3 -coupling reaction, *J. Coord. Chem.* 72 (2019) 1810–1819. <https://doi.org/10.1080/00958972.2019.1627339>.
- [7] S. Saha, K. Biswas, B. Basu, 1-D copper(I) coordination polymer based on bidentate 1,3-dithioether ligand: Novel catalyst for azide-alkyne-cycloaddition (AAC) reaction, *Tetrahedron Lett.* 59 (2018) 2541–2545. <https://doi.org/10.1016/j.tetlet.2018.05.040>.
- [8] V.R. Akhmetova, N.S. Akhmadiev, G.M. Nurtdinova, V.M. Yanybin, A.B. Glazyrin, A.G. Ibragimov, S,S-Complexes of Copper(I) Halides with 1,2-Bis(3,5-dimethyloxazol-4-

- ylmethylsulfanyl)ethane as New Catalysts for Phenylacetylene Aminomethylation, *Russ. J. Gen. Chem.* 88 (2018) 1418–1424. <https://doi.org/10.1134/S1070363218070113>.
- [9] R.Y. Zhao, R.D. Xu, G.N. Liu, Y. Sun, C. Li, Water stable tetranuclear copper(I)iodide cluster for visible-light driven photocatalytic application, *Inorg. Chem. Commun.* 105 (2019) 135–139. <https://doi.org/10.1016/j.inoche.2019.04.045>.
- [10] J. He, J. Huang, Y. He, P. Cao, M. Zeller, A.D. Hunter, Z. Xu, A Boiling-Water-Stable, Tunable White-Emitting Metal-Organic Framework from Soft-Imprint Synthesis, *Chem. Eur. J.* 22 (2016) 1597–1601. <https://doi.org/10.1002/chem.201504941>.
- [11] P.R. Martínez-Alanis, V.M. Ugalde-Saldivar, I. Castillo, Electrochemical and structural characterization of tri- and dithioether copper complexes, *Eur. J. Inorg. Chem.* 2011 (2011) 212–220. <https://doi.org/10.1002/ejic.201000960>.
- [12] S.Q. Bai, I.H.K. Wong, N. Zhang, K. Lin Ke, M. Lin, D.J. Young, T.S.A. Hor, A new 3-D coordination polymer as a precursor for CuI-based thermoelectric composites, *Dalton Trans.* 47 (2018) 16292–16298. <https://doi.org/10.1039/c8dt03219j>.
- [13] M. Jayapal, A. Haque, I.J. Al-Busaidi, N. Al-Rasbi, M.K. Al-Suti, M.S. Khan, R. Al-Balushi, S.M. Islam, C. Xin, W. Wu, W.Y. Wong, F. Marken, P.R. Raithby, Dicopper(I) Complexes Incorporating Acetylide-Functionalized Pyridinyl-Based Ligands: Synthesis, Structural, and Photovoltaic Studies, *Inorg. Chem.* 57 (2018) 12113–12124. <https://doi.org/10.1021/acs.inorgchem.8b01684>.
- [14] S.Q. Liu, H. Konaka, T. Kuroda-Sowa, Y. Suenaga, H. Ito, G.L. Ning, M. Munakata, Porous copper(I) complexes of 2,11-dithia[3.3]paracyclophane: Desorption and adsorption of guest molecules, *Inorganica Chim. Acta.* 357 (2004) 3621–3631. <https://doi.org/10.1016/j.ica.2004.03.057>.
- [15] M. Munakata, L.P. Wu, T. Kuroda-Sowa, M. Maekawa, One-, two- And three-dimensional copper(I) and silver(I) complexes of 2,11-dithia [3.3] paracyclophane, *J. Chem. Soc. - Dalt. Trans.* (1996) 1525–1530. <https://doi.org/10.1039/dt9960001525>.
- [16] J. Ramos, V.M. Yartsev, S. Golhen, L. Ouahab, P. Delhaès, Synthesis and characterization of an extended tetrathiafulvalene derivative coordinated to copper iodide and its charge-transfer and radical ion salts, *J. Mater. Chem.* 7 (1997) 1313–1319. <https://doi.org/10.1039/a608575j>.
- [17] A. Schlachter, A. Bonnot, D. Fortin, P.L. Karsenti, M. Knorr, P.D. Harvey, Unusual triplet-triplet annihilation in a 3D copper(i) chloride coordination polymer, *Phys. Chem. Chem. Phys.* 21 (2019) 16538–16548. <https://doi.org/10.1039/c9cp02891a>.
- [18] A. Bonnot, P.L. Karsenti, F. Juvenal, C. Golz, C. Strohmam, D. Fortin, M. Knorr, P.D. Harvey, The 3D [(Cu₂Br₂)_n{μ-EtS(CH₂)₄SEt}]_n material: A rare example of a coordination polymer

- exhibiting triplet-triplet annihilation, *Phys. Chem. Chem. Phys.* 18 (2016) 24845–24849. <https://doi.org/10.1039/c6cp04728a>.
- [19] H. Hernández-Toledo, H. Torrens, M. Flores-Álamo, L. De Cola, G. Moreno-Alcántar, Self-Assembly and Aggregation-Induced Emission in Aqueous Media of Responsive Luminescent Copper(I) Coordination Polymer Nanoparticles, *Chem. – A Eur. J.* (2021) chem.202100865. <https://doi.org/10.1002/chem.202100865>.
- [20] A. Raghuvanshi, C. Strohmann, J.B. Tissot, S. Clément, A. Mehdi, S. Richeter, L. Viau, M. Knorr, Assembly of Coordination Polymers Using Thioether-Functionalized Octasilsesquioxanes: Occurrence of (CuX)_n Clusters (X=Br and I) within 3D-POSS Networks, *Chem. Eur. J.* 23 (2017) 16479–16483. <https://doi.org/10.1002/chem.201704911>.
- [21] P.D. Harvey, A. Bonnot, A. Lapprand, C. Strohmann, M. Knorr, Coordination RC6H4S(CH₂)₈SC6H4R/(CuI)_n polymers (R (n) = H (4); Me (8)): An innocent methyl group that makes the difference, *Macromol. Rapid Commun.* 36 (2015) 654–659. <https://doi.org/10.1002/marc.201400659>.
- [22] M. Knorr, F. Guyon, A. Khatyr, C. Däschlein, C. Strohmann, S.M. Aly, A.S. Abd-El-Aziz, D. Fortin, P.D. Harvey, Rigidity effect of the dithioether spacer on the size of the luminescent cluster (Cu₂I₂)_n (n = 2, 3) in their coordination polymers, *Dalton Trans.* 0 (2009) 948–955. <https://doi.org/10.1039/b816987j>.
- [23] A. Bonnot, F. Juvenal, A. Schlachter, D. Fortin, P.D. Harvey, Completely Unexpected Coordination Selectivity of Copper Iodide for Thioether Over Ethynyl, *Chem. Africa.* 1 (2018) 67–77. <https://doi.org/10.1007/s42250-018-0004-x>.
- [24] A. Bonnot, M. Knorr, F. Guyon, M.M. Kubicki, Y. Rousselin, C. Strohmann, D. Fortin, P.D. Harvey, 1,4-Bis(arylthio)but-2-enes as Assembling Ligands for (Cu₂X₂)_n (X = I, Br; N = 1, 2) Coordination Polymers: Aryl Substitution, Olefin Configuration, and Halide Effects on the Dimensionality, Cluster Size, and Luminescence Properties, *Cryst. Growth Des.* 16 (2016) 774–788. <https://doi.org/10.1021/acs.cgd.5b01360>.
- [25] S.M. Aly, A. Pam, A. Khatyr, M. Knorr, Y. Rousselin, M.M. Kubicki, J.O. Bauer, C. Strohmann, P.D. Harvey, Cluster-Containing Coordination Polymers Built Upon (Cu₂I₂S₂)_m Units (m = 2, 3) and ArSCH₂C≡CCH₂SAr Ligands: Is the Cluster Size Dependent Upon Steric Hindrance or Ligand Rigidity?, *J. Inorg. Organomet. Polym. Mater.* 24 (2014) 190–200. <https://doi.org/10.1007/s10904-013-9984-9>.
- [26] M. Knorr, F. Guyon, Luminescent Oligomeric and Polymeric Copper Coordination Compounds Assembled by Thioether Ligands, in: A.S. Abd-El Aziz, C.E. Carraher, P.D. Harvey, C.U. Pittman, M. Zeldin (Eds.), *Macromol. Contain. Met. Met. Elem.*, John Wiley & Sons, Inc.,

- Hoboken, NJ, USA, 2010: pp. 89–158. <https://doi.org/10.1002/9780470604090.ch3>.
- [27] A. Schlachter, A. Lapprand, D. Fortin, C. Strohmann, P.D. Harvey, M. Knorr, From Short-Bite Ligand Assembled Ribbons to Nanosized Networks in Cu(I) Coordination Polymers Built Upon Bis(benzylthio)alkanes (BzS(CH₂)_nSBz; n = 1–9), *Inorg. Chem.* 59 (2020) 3686–3708. <https://doi.org/10.1021/acs.inorgchem.9b03275>.
- [28] M. Knorr, F. Guyon, A. Khatyr, C. Strohmann, M. Allain, S.M. Aly, A. Lapprand, D. Fortin, P.D. Harvey, Construction of (CuX)_{2n} cluster-containing (X = Br, I; N = 1, 2) coordination polymers assembled by dithioethers ArS(CH₂)_mSAr (Ar = Ph, p-Tol; M = 3, 5): Effect of the spacer length, aryl group, and metal-to-ligand ratio on the dimensionality, cluster, *Inorg. Chem.* 51 (2012) 9917–9934. <https://doi.org/10.1021/ic301385u>.
- [29] A. Bonnot, M. Knorr, C. Strohmann, C. Golz, D. Fortin, P.D. Harvey, CuX (X = Cl, Br, I) Containing Coordination Polymers Built Upon Isomeric RSCH₂C≡CCH₂SR (R = p-Tolyl, Benzyl) Dithioether Ligands: First Example of a Luminescent (CuCl)_n/Dithioether Network, *J. Inorg. Organomet. Polym. Mater.* 25 (2015) 480–494. <https://doi.org/10.1007/s10904-015-0204-7>.
- [30] M. Knorr, A. Khatyr, A. Dini Aleo, A. El Yaagoubi, C. Strohmann, M.M. Kubicki, Y. Rousselin, S.M. Aly, D. Fortin, A. Lapprand, P.D. Harvey, Copper(I) halides (X = Br, I) coordinated to bis(arylothio)methane ligands: Aryl substitution and halide effects on the dimensionality, cluster size, and luminescence properties of the coordination polymers, *Cryst. Growth Des.* 14 (2014) 5373–5387. <https://doi.org/10.1021/cg500905z>.
- [31] A. Bonnot, C. Strohmann, M. Knorr, P.D. Harvey, Metal-to-Ligand Ratio Effect on the Size of Copper Iodide and Copper Bromide Clusters in 1,4-Bis(cyclohexylthio)butane-Spanned Coordination Polymers, *J. Clust. Sci.* 25 (2014) 261–275. <https://doi.org/10.1007/s10876-013-0637-5>.
- [32] M. Chaabéne, A. Khatyr, M. Knorr, M. Askri, Y. Rousselin, M.M. Kubicki, Bis{(4-methylthio)phenylthio}methane as assembling ligand for the construction of Cu(I) and Hg(II) coordination polymers. Crystal structures and topological (AIM) analysis of the bonding, *Inorganica Chim. Acta.* 451 (2016) 177–186. <https://doi.org/10.1016/j.ica.2016.07.023>.
- [33] E. Lee, S.G. Lee, I.H. Park, S. Kim, H. Ju, J.H. Jung, M. Ikeda, Y. Habata, S.S. Lee, Endo- and Exocyclic Coordination of a 20-Membered N₂O₂S₂-Macrocyclic and Cascade Complexation of a 40-Membered N₄O₄S₄-Macrocyclic, *Inorg. Chem.* 57 (2018) 6289–6299. <https://doi.org/10.1021/acs.inorgchem.8b00154>.
- [34] A. Bonnot, F. Juvenal, A. Lapprand, D. Fortin, M. Knorr, P.D. Harvey, Can a highly flexible copper(i) cluster-containing 1D and 2D coordination polymers exhibit MOF-like properties?, *Dalton Trans.* 45 (2016) 11413–11421. <https://doi.org/10.1039/c6dt01375a>.

- [35] S. Kim, A.D. Siewe, E. Lee, H. Ju, I.H. Park, K.M. Park, M. Ikeda, Y. Habata, S.S. Lee, Ligand-Induced Formation of Copper(I) Iodide Clusters: Exocyclic Coordination Polymers with Bis-dithiamacrocycle Isomers, *Inorg. Chem.* 55 (2016) 2018–2022. <https://doi.org/10.1021/acs.inorgchem.5b02314>.
- [36] M. Knorr, A. Bonnot, A. Lapprand, A. Khatyr, C. Strohmann, M.M. Kubicki, Y. Rousselin, P.D. Harvey, Reactivity of CuI and CuBr toward dialkyl sulfides RSR: From discrete molecular Cu₄I₄S₄ and Cu₈I₈S₆ clusters to luminescent copper(I) coordination polymers, *Inorg. Chem.* 54 (2015) 4076–4093. <https://doi.org/10.1021/acs.inorgchem.5b00327>.
- [37] K.M. Henline, C. Wang, R.D. Pike, J.C. Ahern, B. Sousa, H.H. Patterson, A.T. Kerr, C.L. Cahill, Structure, dynamics, and photophysics in the copper(I) iodide- tetrahydrothiophene system, *Cryst. Growth Des.* 14 (2014) 1449–1458. <https://doi.org/10.1021/cg500005p>.
- [38] H. Chiang, C.J. Moon, E. Kwon, H. Park, H. Im, M.Y. Choi, T.H. Kim, J. Kim, Copper(I) Complexes Based on Pentamethylene Sulfide: Luminescence Thermochromism of Cu₄I₄(C₅H₁₀S)₄, *Bull. Korean Chem. Soc.* 39 (2018) 1139–1143. <https://doi.org/10.1002/bkcs.11562>.
- [39] H.J. Kim, I.H. Park, J.E. Lee, K.M. Park, S.S. Lee, Supramolecular silver(I), copper(I), and mercury(II) complexes with thiamacrocycles exhibiting different types of endo- or exocoordination modes: From monomer and dimer to one-dimensional and two-dimensional polymers, *Cryst. Growth Des.* 14 (2014) 6269–6281. <https://doi.org/10.1021/cg500966z>.
- [40] S. Kim, E. Lee, K.M. Park, S.S. Lee, Exocyclic coordination chemistry of an O₂S₂- macrocycle with copper(i), mercury(ii) and palladium(ii) ions, *CrystEngComm.* 15 (2013) 8544–8551. <https://doi.org/10.1039/c3ce41573b>.
- [41] A. Lapprand, A. Bonnot, M. Knorr, Y. Rousselin, M.M. Kubicki, D. Fortin, P.D. Harvey, Formation of an unprecedented (CuBr)₅ cluster and a zeolite-type 2D-coordination polymer: A surprising halide effect, *Chem. Commun.* 49 (2013) 8848–8850. <https://doi.org/10.1039/c3cc45284k>.
- [42] I.H. Park, H.J. Kim, S.S. Lee, Anion-dependent coordinative networking of macrocycle with copper(i) halides, *CrystEngComm.* 14 (2012) 4589–4595. <https://doi.org/10.1039/c2ce25111f>.
- [43] I.H. Park, S.S. Lee, Networking of macrocycles: 1D and 2D coordination polymers of dithia-18-crown-6 with copper(ii) and copper(i), *CrystEngComm.* 13 (2011) 6520–6525. <https://doi.org/10.1039/c1ce05587a>.
- [44] M. Knorr, F. Guyon, M.M. Kubicki, Y. Rousselin, S.M. Aly, P.D. Harvey, Effect of t-BuS vs. n-BuS on the topology, Cu···Cu distances and luminescence properties of 2D Cu₄I₄/RS(CH₂)₄SR metal-organic frameworks, *New J. Chem.* 35 (2011) 1184–1188.

- <https://doi.org/10.1039/c0nj00923g>.
- [45] J. Zhang, Y.S. Xue, Y.Z. Li, H. Bin Du, X.Z. You, Cuprous iodide coordination polymers (CuI)_x(L)_y·z(solvent) built on linear thioether linkers, *CrystEngComm*. 13 (2011) 2578–2585. <https://doi.org/10.1039/c0ce00685h>.
- [46] Y. Jin, H.J. Kim, J.Y. Lee, S.Y. Lee, W.J. Shim, S.H. Hong, S.S. Lee, Hard/soft heterometallic network complex of a macrocycle with endo/exocyclic coordination, *Inorg. Chem.* 49 (2010) 10241–10243. <https://doi.org/10.1021/ic101880r>.
- [47] E.J. Kang, S.Y. Lee, H. Lee, S.S. Lee, Sulfur-containing mixed-donor tribenzo-macrocycles and their endo-and exocyclic supramolecular silver(I) and copper(I) complexes, *Inorg. Chem.* 49 (2010) 7510–7520. <https://doi.org/10.1021/ic1007473>.
- [48] M. Knorr, A. Pam, A. Khatyr, C. Strohmann, M.M. Kubicki, Y. Rousselin, S.M. Aly, D. Fortin, P.D. Harvey, Reactivity of CuI and CuBr toward Et₂S: A reinvestigation on the self-assembly of luminescent copper(I) coordination polymers, *Inorg. Chem.* 49 (2010) 5834–5844. <https://doi.org/10.1021/ic901906h>.
- [49] T.H. Kim, H. Yang, G. Park, K.Y. Lee, J. Kim, Γ-CuI Nanocrystals From Self-Assembled Coordination Polymers, *Chem. - An Asian J.* 5 (2010) 252–255. <https://doi.org/10.1002/asia.200900416>.
- [50] C. Xie, L. Zhou, W. Feng, J. Wang, W. Chen, Varying the frameworks of coordination polymers with (CuI)₄ cubane cluster by altering terminal groups of thioether ligands, *J. Mol. Struct.* 921 (2009) 132–136. <https://doi.org/10.1016/j.molstruc.2008.12.043>.
- [51] Y.L. Jai, Y.L. So, W. Sim, K.M. Park, J. Kim, S.L. Shim, Temperature-dependent 3-D CuI coordination polymers of calix[4]-bis- dithiacrown: Crystal-to-crystal transformation and photoluminescence change on coordinated solvent removal, *J. Am. Chem. Soc.* 130 (2008) 6902–6903. <https://doi.org/10.1021/ja8008693>.
- [52] H.K. Tae, G. Park, W.S. Yong, K.M. Park, Y.C. Myong, J. Kim, Self-assembled copper(I) complexes of symmetric dithioether ligands, *Bull. Korean Chem. Soc.* 29 (2008) 499–502. <https://doi.org/10.5012/bkcs.2008.29.2.499>.
- [53] T.H. Kim, Y.W. Shin, J.H. Jung, J.S. Kim, J. Kim, Crystal-to-crystal transformation between three CuI coordination polymers and structural evidence for luminescence thermochromism, *Angew. Chem. Int. Ed.* 47 (2008) 685–688. <https://doi.org/10.1002/anie.200704349>.
- [54] H.N. Peindy, F. Guyon, A. Khatyr, M. Knorr, C. Strohmann, Construction of 1D and 2D copper(I) coordination polymers assembled by PhS(CH₂)_nSPh (n = 1, 2) dithioether ligands: Surprising effect of the spacer length on the dimensionality, cluster nuclearity and the fluorescence properties of the metal-organic frame, *Eur. J. Inorg. Chem.* 2007 (2007) 1823–1828.

- <https://doi.org/10.1002/ejic.200600954>.
- [55] Y.L. Jai, J.K. Hyun, H.J. Jong, W. Sim, S.L. Shim, Networking of calixcrowns: From heteronuclear endo/exocyclic coordination polymers to A photoluminescence switch, *J. Am. Chem. Soc.* 130 (2008) 13838–13839. <https://doi.org/10.1021/ja805337n>.
- [56] Y.L. Jai, Y.L. So, J. Seo, S.P. Chul, N.G. Jung, W. Sim, S.L. Shim, Calix[4]bis(thiacrown): Assembly of an endocyclic disilver(I) complex and exocyclic 3D copper(I) coordination polymers, *Inorg. Chem.* 46 (2007) 6221–6223. <https://doi.org/10.1021/ic7005875>.
- [57] T.H. Kim, Y.W. Shin, S.S. Lee, J. Kim, Supramolecular assembly of one-dimensional channels and two-dimensional brick-wall networks from asymmetric dithioether ligands and copper(I) iodide, *Inorg. Chem. Commun.* 10 (2007) 11–14. <https://doi.org/10.1016/j.inoche.2006.09.001>.
- [58] J. Zhou, G.Q. Bian, J. Dai, Y. Zhang, Q.Y. Zhu, W. Lu, Luminescent 2-D double-layered polymer, [(CuI)₄(CH₃SCH₃)₃]_∞, containing helical chains constructed by flower-basket-shaped Cu₄I₄ clusters, *Inorg. Chem.* 45 (2006) 8486–8488. <https://doi.org/10.1021/ic060972t>.
- [59] M. Heller, A novel huge diamond-like three-fold interpenetrated network of CuI and crown ether, *Zeitschrift Fur Anorg. Und Allg. Chemie.* 632 (2006) 441–444. <https://doi.org/10.1002/zaac.200500394>.
- [60] T.H. Kim, K.Y. Lee, Y.W. Shin, S.T. Moon, K.M. Park, J.S. Kim, Y. Kang, S.S. Lee, J. Kim, New crystalline framework formed from a podal ligand with S₂O₂ donor and CuI: Non-interpenetrating square-grid with cubane-like Cu₄I₄ cluster nodes, *Inorg. Chem. Commun.* 8 (2005) 27–30. <https://doi.org/10.1016/j.inoche.2004.10.017>.
- [61] W.S. Sheldrick, Lamellar copper(I) thiocyanate-based coordination polymers containing the alkali cation ligating thiacrown ether 1,10-dithia-18-crown-6, *Zeitschrift Fur Anorg. Und Allg. Chemie.* 627 (2001) 1976–1982. [https://doi.org/10.1002/1521-3749\(200108\)627:8<1976::aid-zaac1976>3.0.co;2-x](https://doi.org/10.1002/1521-3749(200108)627:8<1976::aid-zaac1976>3.0.co;2-x).
- [62] H. Paulsson, M. Berggrund, A. Fischer, L. Kloo, Novel layered structures formed by iodocuprate clusters stabilized by dialkylsulphide ligands, *Zeitschrift Fur Anorg. Und Allg. Chemie.* 630 (2004) 413–416. <https://doi.org/10.1002/zaac.200300379>.
- [63] N.R. Brooks, A.J. Blake, N.R. Champness, P.A. Cooke, P. Hubberstey, D.M. Proserpio, C. Wilson, M. Schröder, Discrete molecular and extended polymeric copper(I) halide complexes of tetradentate thioether macrocycles, *J. Chem. Soc. Dalt. Trans.* (2001) 456–465. <https://doi.org/10.1039/b008202n>.
- [64] J.S. Filippo, L.E. Zyontz, J. Potenza, Synthesis and Characterization of Some Halocopper(I)-Alkyl Sulfide Complexes Including the Crystal Structure of μ-(diethyl Sulfide)-bis(diethyl sulfide)tetra-μ-iodo-tetracopper(I), [(C₂H₅)₂S]₃[CuI]₄, *Inorg. Chem.* 14 (1975) 1667–1671.

- <https://doi.org/10.1021/ic50149a047>.
- [65] B. Lenders, D.M. Grove, W.J.J. Smeets, P. van der Sluis, A.L. Spek, G. van Koten, Use of Dimethyl Sulfide in Organocopper Chemistry: X-ray Crystal Structures of cyclo-Tetrakis(μ -2-methylphenyl)bis(dimethyl sulfide)tetracopper(I) and of the Polymeric Copper Bromide Adduct Bromo(dimethyl sulfide)copper(I), *Organometallics*. 10 (1991) 786–791. <https://doi.org/10.1021/om00049a046>.
- [66] H. Maelger, F. Olbrich, J. Kopf, D. Abein, E. Weiss, Synthese und Struktur der Basenaddukte von Kupfer(I)-Halogeniden mit Dimethylsulfid und Tetrahydrothiophen, *Zeitschrift Fur Naturforsch. - Sect. B J. Chem. Sci.* 47 (1992) 1276–1280. <https://doi.org/10.1515/znb-1992-0911>.
- [67] M. Jo, J. Seo, L.F. Lindoy, S. Sung Lee, Supramolecular copper(I) halide complexes of O₂S₂X (X = S, O and NH) macrocycles exhibiting dinuclear, 1D- and 2D-coordination polymeric structures, *J. Chem. Soc. Dalton Trans.* (2009) 6096–6098. <https://doi.org/10.1039/b906474e>.
- [68] P.R. Ashton, A.L. Burns, C.G. Claessens, G.K.H. Shimizu, K. Small, J. Fraser Stoddart, A.J.P. White, D.J. Williams, Thiamacrocyclic chemistry: Synthesis of a novel oxadithiacrown and its copper iodide complex, *J. Chem. Soc. - Dalton Trans.* (1997) 1493–1496. <https://doi.org/10.1039/a608218a>.
- [69] T.H. Kim, S. Lee, Y. Jeon, Y.W. Shin, J. Kim, Reversible photoluminescence switch: A stair-step Cu₄I₄ 4 coordination polymer based on a dithioether ligand, *Inorg. Chem. Commun.* 33 (2013) 114–117. <https://doi.org/10.1016/j.inoche.2013.04.018>.
- [70] W. Ji, J. Qu, S. Jing, D. Zhu, W. Huang, Copper(i) halide clusters based upon ferrocenylchalcogenoether ligands: Donors, halides and semi-rigidity effects on the geometry and catalytic activity, *Dalton Trans.* 45 (2016) 1016–1024. <https://doi.org/10.1039/c5dt03993b>.
- [71] Y.Q. Liu, W. Ji, H.Y. Zhou, Y. Li, S. Jing, D.R. Zhu, J. Zhang, Anthracene-based ferrocenylselenoethers: Syntheses, crystal structures, Cu(i) complexes and sensing property, *RSC Adv.* 5 (2015) 42689–42697. <https://doi.org/10.1039/c5ra06591g>.
- [72] R.D. Adams, K.T. McBride, R.D. Rogers, A new route to polyselenoether macrocycles. Catalytic macrocyclization of 3,3-dimethylselenetane by Re₂(CO)₉SeCH₂CMe₂CH₂, *Organometallics*. 16 (1997) 3896–3901. <https://doi.org/10.1021/om970406t>.
- [73] S. Gahlot, E. Jeanneau, F. Dappozze, C. Guillard, S. Mishra, Precursor-mediated synthesis of Cu₂-xSe nanoparticles and their composites with TiO₂ for improved photocatalysis, *Dalton Trans.* 47 (2018) 8897–8905. <https://doi.org/10.1039/c8dt01625a>.
- [74] A. Schlachter, L. Viau, D. Fortin, L. Knauer, C. Strohmman, M. Knorr, P.D. Harvey, Control of Structures and Emission Properties of (CuI)_n 2-Methyldithiane Coordination Polymers, *Inorg. Chem.* 57 (2018) 13564–13576. <https://doi.org/10.1021/acs.inorgchem.8b02168>.

- [75] J. Troyano, F. Zamora, S. Delgado, Copper(I)-iodide cluster structures as functional and processable platform materials, *Chem. Soc. Rev.* 50 (2021) 4606–4628. <https://doi.org/10.1039/D0CS01470B>.
- [76] T. Röttgers, W.S. Sheldrick, Alkali cation ligating iodocuprate(I)-based coordination networks with the thiacyclic ether 1,10-dithia-18-crown-6, *J. Solid State Chem.* 152 (2000) 271–279. <https://doi.org/10.1006/jssc.2000.8692>.
- [77] A. Raghuvanshi, M. Knorr, L. Knauer, C. Strohmann, S. Boullanger, V. Moutarlier, L. Viau, 1,3-Dithianes as Assembling Ligands for the Construction of Copper(I) Coordination Polymers. Investigation of the Impact of the RC(H)S₂C₃H₆ Substituent and Reaction Conditions on the Architecture of the 0D-3D Networks, *Inorg. Chem.* 58 (2019) 5753–5775. <https://doi.org/10.1021/acs.inorgchem.9b00114>.
- [78] Y. Kang, I.H. Park, M. Ikeda, Y. Habata, S.S. Lee, A double decker type complex: Copper(I) iodide complexation with mixed donor macrocycles via [1:1] and [2:2] cyclisations, *Dalton Trans.* 45 (2016) 4528–4533. <https://doi.org/10.1039/c5dt03751d>.
- [79] H. Ryu, K.M. Park, M. Ikeda, Y. Habata, S.S. Lee, A ditopic O₄S₂ macrocycle and its hard, soft, and hard/soft metal complexes exhibiting endo-, exo-, or endo/exocyclic coordination: Synthesis, crystal structures, NMR titration, and physical properties, *Inorg. Chem.* 53 (2014) 4029–4038. <https://doi.org/10.1021/ic4030475>.
- [80] M. Knorr, F. Guyon, A. Khatyr, M. Allain, S.M. Aly, A. Lapprand, D. Fortin, P.D. Harvey, Unexpected Formation of a Doubly Bridged Cyclo-1,2-dithian 1D Coordination Cu₂I₂-Containing Luminescent Polymer, *J. Inorg. Organomet. Polym. Mater.* 20 (2010) 534–543. <https://doi.org/10.1007/s10904-010-9389-y>.
- [81] H.N. Peindy, F. Guyon, A. Khatyr, M. Knorr, V.H. Gessner, C. Strohmann, Formation of extended 1D and 2D coordination polymers in tetrathioether complexes of mercury(II) and copper(I): crystal structures of $\{ \{ \text{Ge}(\text{CH}_2\text{SPh})_4\text{HgBr}_2 \}_n$ and $[\{ \{ \text{Ge}(\text{CH}_2\text{SPh})_4 \} \text{Cu}_2 \}_n]$, *Zeitschrift Fur Anorg. Und Allg. Chemie.* 635 (2009) 2099–2105. <https://doi.org/10.1002/zaac.200900003>.
- [82] S.Y. Lee, S. Park, S.S. Lee, Copper(I), silver(I), and palladium(II) complexes of a thioxamacrocycle displaying unusual topologies, *Inorg. Chem.* 48 (2009) 11335–11341. <https://doi.org/10.1021/ic901902t>.
- [83] J.K. Hyun, R.S. Mi, Y.L. So, Y.L. Jai, S.L. Shim, Silver(I) and copper(I) coordination polymers based on thioxa-macrocycles, *Eur. J. Inorg. Chem.* 2008 (2008) 3532–3539. <https://doi.org/10.1002/ejic.200800284>.
- [84] Y.C. Yang, S.T. Lin, W.S. Chen, Structural analyses of tetrathiadodecahydro[3.3.3.3]paracyclophane complexes with copper(I) and silver(I), *J. Chem.*

- Res. 2008 (2008) 280–284. <https://doi.org/10.3184/030823408X321042>.
- [85] Y.C. Yang, S.T. Lin, C.C. Cao, Synthesis and structural study of copper(I) or silver(I) complexes of 2,11-dithia-4,5,6,7,8,9-hexahydro[3.3]paracyclophanes, *J. Chinese Chem. Soc.* 54 (2007) 587–594. <https://doi.org/10.1002/jccs.200700085>.
- [86] M. Heller, W.S. Sheldrick, Alkali cation ligating chains and sheets of the macrocycle 1,7-dithia-18-crown-6 with bridging iodo- and thiocyanatocuprate(i) units, *Zeitschrift Fur Anorg. Und Allg. Chemie.* 629 (2003) 1589–1595. <https://doi.org/10.1002/zaac.200300157>.
- [87] H.W. Yim, D. Rabinovich, K.C. Lam, J.A. Golen, A.L. Rheingold, Di- μ -iodo-bis{[methyltris(methylthiomethyl)silane- κ S,S']} copper(I)}, *Acta Crystallogr. Sect. E Struct. Reports Online.* 59 (2003) m556–m558. <https://doi.org/10.1107/S1600536803012947>.
- [88] R.D. Adams, M. Huang, S. Johnson, New compounds with extended structure lattices from the reactions of cuprous iodide with cyclic polydisulfides, *Polyhedron.* 17 (1998) 2775–2780. [https://doi.org/10.1016/S0277-5387\(97\)00318-5](https://doi.org/10.1016/S0277-5387(97)00318-5).
- [89] Y. SUENAGA, M. MAEKAWA, T. KURODA-SOWA, M. MUNAKATA, H. MORIMOTO, N. HIYAMA, S. KITAGAWA, Crystal Structure of Dinuclear Copper(I) Complex with 1,2,4,5-Tetramethylmercaptobenzene, (Cu(tmmb)I)₂., *Anal. Sci.* 13 (1997) 651–652. <https://doi.org/10.2116/analsci.13.651>.
- [90] Y. Suenaga, M. Maekawa, T. Kuroda-Sowa, M. Munakata, H. Morimoto, N. Hiyama, S. Kitagawa, Comparative X-Ray Studies of a Copper(I) Coordination Polymer with 1,2,4,5-Tetramethylmercaptobenzene (tmmb), [(CuX)₂(tmmb)]_n (X=Br, I), *Anal. Sci.* 13 (1997) 1047–1049. <https://doi.org/10.2116/analsci.13.1047>.
- [91] B. Norén, Å. Oskarsson, H.A. Øye, O. Maberg, A. Scheie, D. Louër, Bond Length Variations in Tetrahydrothiophene Solvates of the Coinage Metals. The Crystal Structure of Di- μ -iodo-bis[bis(tetrahydrothiophene)copper(I)]., *Acta Chem. Scand.* 41a (1987) 12–17. <https://doi.org/10.3891/acta.chem.scand.41a-0012>.
- [92] W. Ji, J. Qu, C.A. Li, J.W. Wu, S. Jing, F. Gao, Y.N. Lv, C. Liu, D.R. Zhu, X.M. Ren, W. Huang, In situ surface assembly of core-shell TiO₂-copper(I) cluster nanocomposites for visible-light photocatalytic reduction of Cr(VI), *Appl. Catal. B Environ.* 205 (2017) 368–375. <https://doi.org/10.1016/j.apcatb.2016.12.041>.
- [93] W. Lu, Z.M. Yan, J. Dai, Y. Zhang, Q.Y. Zhu, D.X. Jia, W.J. Guo, Coordination assembly of TTF derivatives through CuI bridges, *Eur. J. Inorg. Chem.* 2005 (2005) 2339–2345. <https://doi.org/10.1002/ejic.200401002>.
- [94] J. Ramos, C.J. Gómez-García, E. Coronado, P. Delhaès, Magnetic transition metal complexes of tetrathiafulvalene (TTF) derivatives, *Synth. Met.* 86 (1997) 1807–1808.

- [https://doi.org/10.1016/s0379-6779\(97\)80913-7](https://doi.org/10.1016/s0379-6779(97)80913-7).
- [95] E.W. Ainscough, A.M. Brodie, K.C. Palmer, Sulphur ligand metal complexes. Part 6. Copper complexes of 2,5-dithiahexane and 3,6-dithiaoctane, *J. Chem. Soc. Dalt. Trans.* (1976) 2375–2381. <https://doi.org/10.1039/DT9760002375>.
- [96] M. Heller, W.S. Sheldrick, Copper(I) coordination polymers with alkanedithiol and -dinitrile bridging ligands, *Zeitschrift Fur Anorg. Und Allg. Chemie.* 630 (2004) 1869–1874. <https://doi.org/10.1002/zaac.200400165>.
- [97] A. Raghuvanshi, N.J. Dargallay, M. Knorr, L. Viau, L. Knauer, C. Strohmam, 1,3-Dithiolane and 1,3-Ferrocenyl-dithiolane as Assembling Ligands for the Construction of Cu(I) Clusters and Coordination Polymers, *J. Inorg. Organomet. Polym. Mater.* 27 (2017) 1501–1513. <https://doi.org/10.1007/s10904-017-0610-0>.
- [98] T.H. Kim, Y.W. Shin, S.S. Lee, J. Kim, Two-dimensional coordination polymer of 3-(methylthio)-1-thiomorpholinopropan-1-one propagated by rhomboid Cu-I2-Cu linker, *Anal. Sci. X-Ray Struct. Anal. Online.* 22 (2006) x287–x288. <https://doi.org/10.2116/analsci.22.x287>.
- [99] P.M. Boorman, K.A. Kerr, R.A. Kydd, K.J. Moynihan, K.A. Valentine, Synthetic, structural, and spectroscopic studies of the ligating properties of organic disulphides: X-ray structure of copper(I) iodide-diethyl disulphide (2/1), *J. Chem. Soc. Dalt. Trans.* (1982) 1401–1405. <https://doi.org/10.1039/DT9820001401>.
- [100] T. Assoumatine, H. Stoeckli-Evans, Poly[[μ 4 -3,4,8,10,11,13-hexahydro-1 H ,6 H -bis([1,4]dithiocino)[6,7- b :6',7'- e]pyrazine]di- μ -iodido-dicopper(I)]: a two-dimensional copper(I) coordination polymer , *IUCrData.* 5 (2020) x200467. <https://doi.org/10.1107/s2414314620004678>.
- [101] J. Troyano, E. Zapata, J. Perles, P. Amo-Ochoa, V. Fernández-Moreira, J.I. Martínez, F. Zamora, S. Delgado, Multifunctional Copper(I) Coordination Polymers with Aromatic Mono- and Ditopic Thioamides, *Inorg. Chem.* 58 (2019) 3290–3301. <https://doi.org/10.1021/acs.inorgchem.8b03364>.
- [102] T.S. Lobana, R. Sultana, R.J. Butcher, A. Castineiras, T. Akitsu, F.J. Fernandez, M.C. Vega, Chemistry of heterocyclic 2-thiones: In situ generation of 3-(2-thiazolin-2-yl)thiazolidine-2-thione and 1,1'-dimethyl-2,2'- diimidazolyl sulfide and their coordination to CuI and Cu II, *Eur. J. Inorg. Chem.* 2013 (2013) 5161–5170. <https://doi.org/10.1002/ejic.201300676>.
- [103] D. Mentzafos, A. Terzis, P. Karagiannidis, P. Aslanidis, Structure of bis(μ -pyridine-2-thione- μ -S)-bis[iodo(pyridine-2-thione-S)copper(I)], *Acta Crystallogr. Sect. C Cryst. Struct. Commun.* 45 (1989) 54–56. <https://doi.org/10.1107/s0108270188010546>.
- [104] L.I. Victoriano, M.T. Garland, A. Vega, Reaction of Bis(N,N-dimethylthiocarbamoyl) Sulfide with Copper(II) Halides and the Crystal and Molecular Structures of Halogeno(bis(N,N-dimethylthiocarbamoyl) sulfido)copper(I) Complexes, *Inorg. Chem.* 36 (1997) 688–693.

- <https://doi.org/10.1021/ic960625r>.
- [105] L. Han, X. Pan, H.P. Li, Y. Yang, Synthesis and characterization of copper(I) halide complexes with thiourea and heterocyclic thione, *Jiegou Huaxue*. 34 (2015) 1571–1578. <https://doi.org/10.14102/j.cnki.0254-5861.2011-0629>.
- [106] L.I. Victoriano, M.T. Garland, A. Vega, C. Lopez, Syntheses, properties, crystal and molecular structure of a novel neutral pentanuclear copper(I) iodide species. Copper(I) complexes with tetraethylthiuram monosulfide, *J. Chem. Soc. - Dalt. Trans.* (1998) 1127–1131. <https://doi.org/10.1039/a709210e>.
- [107] L.I. Victoriano, M.T. Garland, A. Vega, C. Lopez, Crystal and Molecular Structures of a Neutral Pentanuclear Copper(I)-Iodide Complex, *Inorg. Chem.* 37 (1998) 2060–2062. <https://doi.org/10.1021/ic970114k>.
- [108] J. Dai, M. Munakata, L.P. Wu, T. Kuroda-Sowa, Y. Suenaga, An S ... S contact assembled tetranuclear copper(I) complex with sulfur-rich ligand, 4,5-ethylenedithio-1,3-dithiole-2-thione, *Inorganica Chim. Acta*. 258 (1997) 65–69. [https://doi.org/10.1016/S0020-1693\(96\)05513-2](https://doi.org/10.1016/S0020-1693(96)05513-2).
- [109] D. Wang, S.Y. Wu, H.P. Li, Y. Yang, H.W. Roesky, Synthesis and Characterization of Copper Complexes with the N-(2,6-Diisopropylphenyl)-N'-acylthiourea Ligands, *Eur. J. Inorg. Chem.* 2017 (2017) 1406–1413. <https://doi.org/10.1002/ejic.201601451>.
- [110] G.N. Liu, R.Y. Zhao, R.D. Xu, X. Zhang, X.N. Tang, Q.J. Dan, Y.W. Wei, Y.Y. Tu, Q.B. Bo, C. Li, A Novel Tetranuclear Copper(I) Iodide Metal-Organic Cluster [Cu₄I₄(Ligand)₅] with Highly Selective Luminescence Detection of Antibiotic, *Cryst. Growth Des.* 18 (2018) 5441–5448. <https://doi.org/10.1021/acs.cgd.8b00819>.
- [111] L.I. Kursheva, O.N. Kataeva, D.B. Krivolapov, E.S. Batyeva, O.G. Sinyashin, Transformation of copper(I) thiophosphite complexes into copper(I) clusters bridged by diisopropyl disulfides and diethyl disulfides, *Heteroat. Chem.* 17 (2006) 542–546. <https://doi.org/10.1002/hc.20274>.
- [112] L. Chen, L.K. Thompson, J.N. Bridson, Coordination chemistry of thioether–pyridazine macrocycles II. Synthesis, structural and spectroscopic studies of dinuclear copper(II) and polynuclear copper(I) and silver(I) complexes of a tetrathiapyridazinophane macrocyclic ligand, *Can. J. Chem.* 70 (1992) 2709–2716. <https://doi.org/10.1139/v92-343>.
- [113] S. Toyota, Y. Matsuda, S. Nagaoka, M. Oki, H. Akashi, Reaction of 2-(Alkylthiomethyl)phenyllithium with Copper(I) Halides and Structure and Properties of One of the Products - Copper(I) Complexes of 2,2'-Bis(alkylthiomethyl)biphenyl, *Bull. Chem. Soc. Jpn.* 69 (1996) 3115–3121. <https://doi.org/10.1246/bcsj.69.3115>.
- [114] S. Toyota, Y. Matsuda, M. Oki, H. Akashi, Catenation of 2,2'-Bis(ethylthiomethyl)biphenyl with Copper(I) Bromide, *Chem. Lett.* 24 (1995) 31–32. <https://doi.org/10.1246/cl.1995.31>.

- [115] C.R. Lucas, W. Liang, D.O. Miller, J.N. Bridson, Metal Complexes of 1-Oxa-4,7-dithiacyclononane, *Inorg. Chem.* 36 (1997) 4508–4513. <https://doi.org/10.1021/ic961536h>.
- [116] V. Olijnyk, B. Dziuk, Spectral and structural insights of copper reduction pathways in the system of $\text{CuX}_2\text{-R}_2\text{S}$ ($\text{X}=\text{Cl}, \text{Br}$; $\text{R}=\text{allyl}, \text{n-propyl}$), *J. Mol. Struct.* 1225 (2021) 129113. <https://doi.org/10.1016/j.molstruc.2020.129113>.
- [117] T. Kokoli, S. Olsson, P.M. Björemark, S. Persson, M. Håkansson, Toward absolute asymmetric synthesis of coordination polymers with bidentate sulfide ligands, *J. Organomet. Chem.* 724 (2013) 17–22. <https://doi.org/10.1016/j.jorganchem.2012.10.035>.
- [118] C.R. Lucas, S. Liu, Thiophenophane metal complexes. IV. Effects from ligand changes outside the coordination sphere, *Can. J. Chem.* 74 (1996) 2340–2348. <https://doi.org/10.1139/v96-261>.
- [119] H.W. Yim, L.M. Tran, E.E. Pullen, D. Rabinovich, L.M. Liable-Sands, T.E. Concolino, A.L. Rheingold, One-dimensional copper(I) coordination polymers based on a tridentate thioether ligand, *Inorg. Chem.* 38 (1999) 6234–6239. <https://doi.org/10.1021/ic990642r>.
- [120] M.A. Tsiaggali, E.G. Andreadou, A.G. Hatzidimitriou, A.A. Pantazaki, P. Aslanidis, Copper(I) halide complexes of N-methylbenzothiazole-2-thione: Synthesis, structure, luminescence, antibacterial activity and interaction with DNA, *J. Inorg. Biochem.* 121 (2013) 121–128. <https://doi.org/10.1016/j.jinorgbio.2013.01.001>.
- [121] A. Hameau, F. Guyon, A. Khatyr, M. Knorr, C. Strohmann, 4,5-Bis(methylthio)-1,3-dithiole-2-thione, a versatile sulphur-rich building block for the self-assembly of Cu(I) and Ag(I) coordination polymers: Dithioether versus thiocarbonyl bonding, *Inorganica Chim. Acta.* 388 (2012) 60–70. <https://doi.org/10.1016/j.ica.2012.02.032>.
- [122] C. Bellitto, F. Bigoli, P. Deplano, M.L. Mercuri, M.A. Pellinghelli, G. Staulo, E.F. Trogu, Reactions of Copper(II) Halides (Chloride, Bromide) with the Sulfur-Rich Donor 1,3-Dithiacyclohexane-2-thione (ptc). Synthesis, Crystal Structures, and Characterization of Three Different Copper Compounds: Trinuclear Mixed-Valence $[\text{Cu}_2\text{CuII}(\text{ptc})_4\text{Cl}_4]$, *Pol. Inorg. Chem.* 33 (1994) 3005–3009. <https://doi.org/10.1021/ic00091a047>.
- [123] I. Romero, G. Sánchez-Castelló, F. Teixidor, C.R. Whitaker, J. Rius, C. Miravittles, T. Flor, L. Escriche, J. Casabó, Silver(I), mercury(II) and copper(I) complexes of acyclic and macrocyclic dithioether, metaxylyl based ligands, *Polyhedron.* 15 (1996) 2057–2065. [https://doi.org/10.1016/0277-5387\(95\)00445-9](https://doi.org/10.1016/0277-5387(95)00445-9).
- [124] F. Teixidor, J. Rius, C. Miravittles, C. Viñas, L. Escriche, E. Sanchez, J. Casabó, Reactivity of the anion 7,8-(ethane-1',2'-dithiolato-SS')-nido-undecaborate. Molecular structure of [7,8-(ethane-1',2'-dithiolato-SS')-dicarba-nido-undecaborate]bis(triphenylphosphine)rhodium(I), *Inorganica Chim. Acta.* 176 (1990) 61–65. [https://doi.org/10.1016/S0020-1693\(00\)85092-6](https://doi.org/10.1016/S0020-1693(00)85092-6).

- [125] E. Solari, S. De Angelis, M. Latronico, C. Floriani, A. Chiesi-Villa, C. Rizzoli, A structural variability of copper(I) chloride-tetrahydrothiophene adducts crystallizing in polymeric forms and exhibiting polymorphism: The role of the solvent, *J. Clust. Sci.* 7 (1996) 553–566. <https://doi.org/10.1007/BF01165801>.
- [126] L. Chen, L.K. Thompson, S.S. Tandon, J.N. Bridson, Synthetic, Structural, and Spectroscopic Studies on Copper (II), Copper(I), and Silver(I) Complexes of a Series of Pyridazinophane and Phthalazinophane Macrocycles. Unusual Extended Metallo-cyclic Structures, *Inorg. Chem.* 32 (1993) 4063–4068. <https://doi.org/10.1021/ic00071a016>.
- [127] Z. Hong-Hui, W. Ding-Ming, H. Jian-Quan, H. Jin-Ling, Synthesis and Crystal Structure of $[\text{Cu}_4\text{Cl}_4(\text{TFTA})_2]$, *Acta Physico-Chimica Sin.* 12 (1996) 761–765. <https://doi.org/10.3866/pku.whxb19960818>.
- [128] Y. Bi, W. Liao, X. Wang, R. Deng, H. Zhang, Self-assembly from two-dimensional layered networks to tetranuclear structures: Syntheses, structures, and properties of Four copper-thiacalix[4] arene compounds, *Eur. J. Inorg. Chem.* 2009 (2009) 4989–4994. <https://doi.org/10.1002/ejic.200900699>.
- [129] F. Bigoli, M. Angela Pellinghelli, P. Deplano, M. Laura Mercuri, E.F. Trogu, Synthetic, structural and spectroscopic studies of the donating properties of sulfur-rich molecules: X-ray structure of [copper(I)chloride-(1,3-dithiolane-2-thione)(2/1)]_n, *Inorganica Chim. Acta.* 204 (1993) 9–13. [https://doi.org/10.1016/S0020-1693\(00\)88107-4](https://doi.org/10.1016/S0020-1693(00)88107-4).
- [130] M.M. Kimani, C.A. Bayse, J.L. Brumaghim, Synthesis, characterization, and DFT studies of thione and selone Cu(i) complexes with variable coordination geometries, *Dalton Trans.* 40 (2011) 3711–3723. <https://doi.org/10.1039/c1dt10104h>.
- [131] W. Ji, H. Wang, C.A. Li, F. Gao, Z.F. An, L. Huang, H. Wang, Y. Pan, D.R. Zhu, J.Q. Wang, C. Guo, J.A. Mayoral, S. Jing, Cuprous cluster as effective single-molecule metallaphotocatalyst in white light-driven C–H arylation, *J. Catal.* 378 (2019) 270–276. <https://doi.org/10.1016/j.jcat.2019.08.017>.
- [132] C.A. Li, W. Ji, J. Qu, S. Jing, F. Gao, D.R. Zhu, A PEG/copper(i) halide cluster as an eco-friendly catalytic system for C–N bond formation, *Dalton Trans.* 47 (2018) 7463–7470. <https://doi.org/10.1039/c8dt01310a>.
- [133] M.J. Poropudas, J.M. Rautiainen, R. Oilunkaniemi, R.S. Laitinen, Synthesis, characterization, and ligand behaviour of a new ditelluroether (C₁₀H₇)Te(CH₂)₄Te(C₁₀H₇) and the concurrently formed ionic [(C₁₀H₇)Te(CH₂)₄]Br, *Dalton Trans.* 45 (2016) 17206–17215. <https://doi.org/10.1039/c6dt02599d>.
- [134] W.F. Liaw, C.H. Lai, S.J. Chiou, Y.C. Horng, C.C. Chou, M.C. Liaw, G.H. Lee, S.M. Peng,

- Synthesis and Characterization of Polymeric Ag(I)-Telluroether and Cu(I)-Diorganyl Ditelluride Complexes: Crystal Structures of $[\text{Ag}(\text{MeTe}(\text{CH}_2)_3\text{TeMe})_2]_n[\text{BF}_4]_n$, $[(\mu_2\text{-MeTeTeMe})\text{Cu}(\mu\text{-Cl})]_n$, and $[\text{Ag}_2(\text{NCCCH}_3)_4(\mu_2\text{-}(p\text{-C}_6\text{H}_4\text{F})\text{TeTe}(p\text{-C}_6\text{H}_4\text{F}))_2][\text{BF}_4]_2$, *Inorg. Chem.* 34 (1995) 3755–3759. <https://doi.org/10.1021/ic00118a024>.
- [135] O.N. Kataeva, D.B. Krivolapov, A.T. Gubaidullin, I.A. Litvinov, L.I. Kursheva, S.A. Katsyuba, Conformations and coordination properties of trialkyltrithiophosphites in copper(I) complexes, *J. Mol. Struct.* 554 (2000) 127–140. [https://doi.org/10.1016/S0022-2860\(00\)00665-7](https://doi.org/10.1016/S0022-2860(00)00665-7).
- [136] L.I. Kursheva, O.N. Kataeva, S. V. Perova, E.S. Batyeva, O.G. Sinyashin, R. Freilich, Synthesis and structure of copper(II) phosphonodithioite complexes, *Russ. J. Gen. Chem.* 75 (2005) 851–855. <https://doi.org/10.1007/s11176-005-0332-9>.
- [137] W.H. Fang, J.F. Wang, L. Zhang, J. Zhang, Titanium-Oxo Cluster Based Precise Assembly for Multidimensional Materials, *Chem. Mater.* 29 (2017) 2681–2684. <https://doi.org/10.1021/acs.chemmater.7b00324>.
- [138] A. Koutsari, F. Karasmani, E. Kapetanaki, D.I. Zainuddin, A.G. Hatzidimitriou, P. Angaridis, P. Aslanidis, Luminescent thione/phosphane mixed-ligand copper(I) complexes: The effect of thione on structural properties, *Inorganica Chim. Acta.* 458 (2017) 138–145. <https://doi.org/10.1016/j.ica.2017.01.007>.
- [139] P. Roesch, J. Nitsch, M. Lutz, J. Wiecko, A. Steffen, C. Müller, Synthesis and photoluminescence properties of an unprecedented phosphinine- Cu_4Br_4 cluster, *Inorg. Chem.* 53 (2014) 9855–9859. <https://doi.org/10.1021/ic5014472>.
- [140] A. Vega, J.Y. Saillard, Bonding in tetrahedral $\text{Cu}_4(\mu_3\text{-X})_4\text{L}_4$ Copper(I) clusters: A DFT investigation, *Inorg. Chem.* 43 (2004) 4012–4018. <https://doi.org/10.1021/ic035262r>.
- [141] W. Zhang, R.G. Xiong, S.D. Huang, 3D framework containing Cu_4Br_4 cubane as connecting node with strong ferroelectricity, *J. Am. Chem. Soc.* 130 (2008) 10468–10469. <https://doi.org/10.1021/ja803021v>.
- [142] G. Glatz, T. Irrgang, R. Kempe, Crystal structure of tetra- μ_3 -bromo-tetrakis(tert-butyl-(4-methylpyridin-2-yl)-amine)-tetracopper(I), $\text{Cu}_4\text{Br}_4(\text{C}_{10}\text{H}_{16}\text{N}_2)_4$, *Zeitschrift Fur Krist. - New Cryst. Struct.* 222 (2007) 261–262. <https://doi.org/10.1524/ncrs.2007.0110>.
- [143] P. Ai, C. Gourlaouen, A.A. Danopoulos, P. Braunstein, Novel Di- and Trinuclear Palladium Complexes Supported by N,N'-Diphosphanil NHC Ligands and N,N'-Diphosphanylimidazolium Palladium, Gold, and Mixed-Metal Copper-Gold Complexes, *Inorg. Chem.* 55 (2016) 1219–1229. <https://doi.org/10.1021/acs.inorgchem.5b02382>.
- [144] E. Vega, E. De Julián, G. Borrajo, J. Díez, E. Lastra, M.P. Gamasa, Copper(I) and silver(I) complexes containing the enantiopure N,N-bidentate 1,3-bis[4'-(S)-isopropylloxazolin-2'-

- yl]benzene ((S,S)-iPr-pheboxH) ligand, *Polyhedron*. 94 (2015) 59–66. <https://doi.org/10.1016/j.poly.2015.04.014>.
- [145] G. Otero-Irurueta, I. Hernández-Rodríguez, J.I. Martínez, R. Palacios-Rivera, F.J. Palomares, M.F. López, A.I. Gallego, S. Delgado, F. Zamora, J. Méndez, J.A. Martín-Gago, On-surface self-organization of a robust metal-organic cluster based on copper(i) with chloride and organosulphur ligands, *Chem. Commun.* 51 (2015) 3243–3246. <https://doi.org/10.1039/c4cc08471c>.
- [146] Z.J. Lv, P.N. Jin, Y.H. Wang, X.B. Wei, G. Yang, Synthesis, Structures and Luminescent Properties of 3D Copper(I) 1,2,4-Triazolates Containing Cubic Cu₄X₄ Clusters (X = Cl, Br), *J. Clust. Sci.* 26 (2015) 1389–1401. <https://doi.org/10.1007/s10876-014-0821-2>.
- [147] S. Becker, U. Behrens, S. Schindler, Synthesis, structure and reactivity of the compound [Cu(C₇H₇NH₂)Cl]₄ derived from CuCl and benzylamine (C₇H₇NH₂), *Zeitschrift Fur Anorg. Und Allg. Chemie.* 641 (2015) 430–435. <https://doi.org/10.1002/zaac.201400395>.
- [148] F. De Angelis, S. Fantacci, A. Sgamellotti, E. Cariati, R. Ugo, P.C. Ford, Electronic transitions involved in the absorption spectrum and dual luminescence of tetranuclear cubane [Cu₄I₄(pyridine)₄] cluster: A density functional theory/time-dependent density functional theory investigation, *Inorg. Chem.* 45 (2006) 10576–10584. <https://doi.org/10.1021/ic061147f>.
- [149] F. Claveria-Cadiz, R. Arratia-Perez, R. Guajardo-Maturana, A. Muñoz-Castro, Survey of short and long cuprophilic d10-d10 contacts for tetranuclear copper clusters. Understanding of bonding and ligand role from a planar superatom perspective, *New J. Chem.* 42 (2018) 8874–8881. <https://doi.org/10.1039/c8nj00698a>.
- [150] N.V.S. Harisomayajula, S. Makovetskyi, Y.C. Tsai, Cuprophilic Interactions in and between Molecular Entities, *Chem. Eur. J.* 25 (2019) 8936–8954. <https://doi.org/10.1002/chem.201900332>.
- [151] M. Vitale, W.E. Palke, P.C. Ford, Origins of the double emission of the tetranuclear copper(I) cluster Cu₄I₄(pyridine)₄: An ab initio study, *J. Phys. Chem.* 96 (1992) 8329–8336. <https://doi.org/10.1021/j100200a023>.
- [152] K.R. Kyle, W.E. Palke, P.C. Ford, The photoluminescence properties of the copper(I) clusters Cu₄I₄A₄ (A = aromatic amine) in solution, *Coord. Chem. Rev.* 97 (1990) 35–46. [https://doi.org/10.1016/0010-8545\(90\)80078-8](https://doi.org/10.1016/0010-8545(90)80078-8).
- [153] P.C. Ford, E. Cariati, J. Bourassa, Photoluminescence Properties of Multinuclear Copper(I) Compounds, *Chem. Rev.* 99 (1999) 3625–3647. <https://doi.org/10.1021/cr960109i>.
- [154] A. Kobayashi, M. Kato, Stimuli-responsive luminescent copper(I) complexes for intelligent emissive devices, *Chem. Lett.* 46 (2017) 154–162. <https://doi.org/10.1246/cl.160794>.
- [155] S.-Y. Yin, Z. Wang, Z.-M. Liu, H.-J. Yu, J.-H. Zhang, Y. Wang, R. Mao, M. Pan, C.-Y. Su, Multiresponsive UV-One-Photon Absorption, Near-Infrared-Two-Photon Absorption, and X/γ-

- Photoelectric Absorption Luminescence in One [Cu₄I₄] Compound, *Inorg. Chem.* 58 (2019) 10736–10742. <https://doi.org/10.1021/acs.inorgchem.9b00876>.
- [156] P.D. Harvey, Z. Murtaza, Properties of PdI-PdI Bonds. Theoretical and Spectroscopic Study of Pd₂(dmb)₂X₂ Complexes (dmb = 1,8-Diisocyano-p-menthane; X = Cl, Br), *Inorg. Chem.* 32 (1993) 4721–4729. <https://doi.org/10.1021/ic00074a013>.
- [157] E.G. Percástegui, C. Reyes-Mata, M. Flores-Alamo, B. Quiroz-García, E. Rivera, I. Castillo, Transformations in Chemically Responsive Copper-Calixarene Architectures, *Chem. - An Asian J.* 13 (2018) 520–527. <https://doi.org/10.1002/asia.201701741>.
- [158] A. Gallego, O. Castillo, C.J. Gómez-García, F. Zamora, S. Delgado, Reversible solvent-exchange-driven transformations in multifunctional coordination polymers based on copper-containing organosulfur ligands, *Eur. J. Inorg. Chem.* 2014 (2014) 3879–3887. <https://doi.org/10.1002/ejic.201400085>.
- [159] J.P. Safko, J.E. Kuperstock, S.M. McCullough, A.M. Noviello, X. Li, J.P. Killarney, C. Murphy, H.H. Patterson, C.A. Bayse, R.D. Pike, Network formation and photoluminescence in copper(i) halide complexes with substituted piperazine ligands, *Dalton Trans.* 41 (2012) 11663–11674. <https://doi.org/10.1039/c2dt31241g>.
- [160] C.K. Ryu, M. Vitale, P.C. Ford, Photoluminescence Properties of the Structurally Analogous Tetranuclear Copper(I) Clusters Cu₄X₄(dpmp)₄ (X = I, Br, Cl; dpmp = 2-(Diphenylmethyl)pyridine), *Inorg. Chem.* 32 (1993) 869–874. <https://doi.org/10.1021/ic00058a020>.
- [161] L.P. Xue, J.J. Tao, A Luminescent Three-Dimensional Coordination Polymer Based on Cu(I) Halide Clusters Showing Dia Topology with 8-Fold Interpenetration, *J. Clust. Sci.* 27 (2016) 1729–1736. <https://doi.org/10.1007/s10876-016-1036-5>.
- [162] D. Piché, P.D. Harvey, The lowest energy excited states of the binuclear silver(I) halide complexes, Ag₂(dmb)₂X₂. Metal-centered or charge transfer states?, *Can. J. Chem.* 72 (1994) 705–713. <https://doi.org/10.1139/v94-095>.
- [163] D. Fortin, M. Drouin, M. Turcotte, P.D. Harvey, Quasi-unidimensional {[M(dmb)₂]Y}(n) organometallic polymers (M = Cu(I), Ag(I); dmb = 1,8-Diisocyano-p-menthane; Y = BF₄⁻, PF₆⁻, NO₃⁻, ClO₄⁻, CH₃CO₂⁻). Structural, calorimetric, and luminescence properties, *J. Am. Chem. Soc.* 119 (1997) 531–541. <https://doi.org/10.1021/ja9600845>.
- [164] H. Yersin, Highly efficient OLEDs: Materials based on thermally activated delayed fluorescence, *Highly Effic. OLEDs Mater. Based Therm. Act. Delayed Fluoresc.* (2018) 1–588. <https://doi.org/10.1002/9783527691722>.
- [165] R. Czerwieniec, J. Yu, H. Yersin, Blue-light emission of Cu(I) complexes and singlet harvesting,

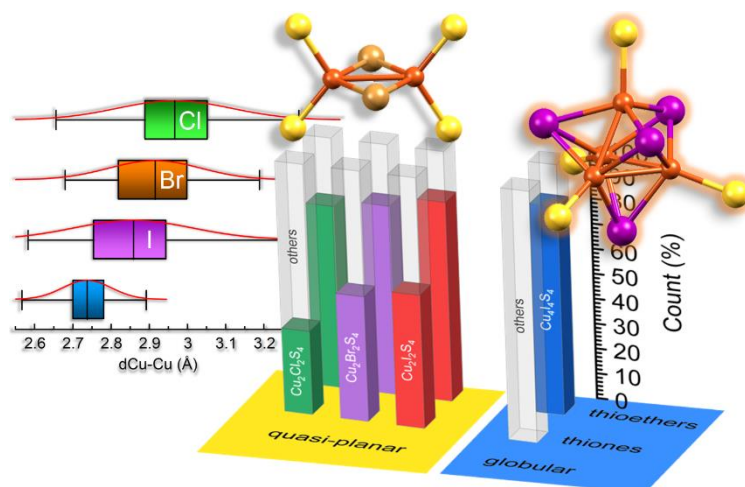
- Inorg. Chem. 50 (2011) 8293–8301. <https://doi.org/10.1021/ic200811a>.
- [166] H. Yersin, A.F. Rausch, R. Czerwieniec, T. Hofbeck, T. Fischer, The triplet state of organo-transition metal compounds. Triplet harvesting and singlet harvesting for efficient OLEDs, *Coord. Chem. Rev.* 255 (2011) 2622–2652. <https://doi.org/10.1016/j.ccr.2011.01.042>.
- [167] W. Liu, Y. Fang, J. Li, Copper Iodide Based Hybrid Phosphors for Energy-Efficient General Lighting Technologies, *Adv. Funct. Mater.* 28 (2018) 1705593. <https://doi.org/10.1002/adfm.201705593>.
- [168] A. Schlachter, K. Tanner, P.D. Harvey, Copper Halide-Chalcogenoether and -Chalcogenone Networks: Chain and Cluster Motifs, Polymer Dimensionality and Photophysical Properties, *Coord. Chem. Rev.* (2021).
- [169] P. Liang, A. Kobayashi, W.M.C. Sameera, M. Yoshida, M. Kato, Solvent-Free Thermal Synthesis of Luminescent Dinuclear Cu(I) Complexes with Triarylphosphines, *Inorg. Chem.* 57 (2018) 5929–5938. <https://doi.org/10.1021/acs.inorgchem.8b00439>.
- [170] A. Kobayashi, Y. Yoshida, M. Yoshida, M. Kato, Mechanochromic Switching between Delayed Fluorescence and Phosphorescence of Luminescent Coordination Polymers Composed of Dinuclear Copper(I) Iodide Rhombic Cores, *Chem. Eur. J.* 24 (2018) 14750–14759. <https://doi.org/10.1002/chem.201802532>.
- [171] A. Kobayashi, M. Fujii, Y. Shigeta, M. Yoshida, M. Kato, Quantitative Solvent-Free Thermal Synthesis of Luminescent Cu(I) Coordination Polymers, *Inorg. Chem.* 58 (2019) 4456–4464. <https://doi.org/10.1021/acs.inorgchem.8b03641>.
- [172] Q. Benito, X.F. Le Goff, S. Maron, A. Fargues, A. Garcia, C. Martineau, F. Taulelle, S. Kahlal, T. Gacoin, J.-P. Boilot, S. Perruchas, Polymorphic Copper Iodide Clusters: Insights into the Mechanochromic Luminescence Properties, *J. Am. Chem. Soc.* 136 (2014) 11311–11320. <https://doi.org/10.1021/ja500247b>.
- [173] B. Huitorel, H. El Moll, R. Utrera-Melero, M. Cordier, A. Fargues, A. Garcia, F. Massuyeau, C. Martineau-Corcus, F. Fayon, A. Rakhmatullin, S. Kahlal, J.Y. Saillard, T. Gacoin, S. Perruchas, Evaluation of Ligands Effect on the Photophysical Properties of Copper Iodide Clusters, *Inorg. Chem.* 57 (2018) 4328–4339. <https://doi.org/10.1021/acs.inorgchem.7b03160>.
- [174] R. Utrera-Melero, B. Huitorel, M. Cordier, J.Y. Mevellec, F. Massuyeau, C. Latouche, C. Martineau-Corcus, S. Perruchas, Combining Theory and Experiment to Get Insight into the Amorphous Phase of Luminescent Mechanochromic Copper Iodide Clusters, *Inorg. Chem.* 59 (2020) 13607–13620. <https://doi.org/10.1021/acs.inorgchem.0c01967>.
- [175] C. Lescop, Coordination-Driven Syntheses of Compact Supramolecular Metallacycles toward Extended Metallo-organic Stacked Supramolecular Assemblies, *Acc. Chem. Res.* 50 (2017) 885–

894. <https://doi.org/10.1021/acs.accounts.6b00624>.
- [176] C. Lescop, Coordination-Driven Supramolecular Synthesis Based on Bimetallic Cu(I) Precursors: Adaptive Behavior and Luminescence, *Chem. Rec.* 21 (2021) 544–557. <https://doi.org/10.1002/tcr.202000144>.
- [177] S. Evariste, A.M. Khalil, M.E. Moussa, A.K.W. Chan, E.Y.H. Hong, H.L. Wong, B. Le Guennic, G. Calvez, K. Costuas, V.W.W. Yam, C. Lescop, Adaptive Coordination-Driven Supramolecular Syntheses toward New Polymetallic Cu(I) Luminescent Assemblies, *J. Am. Chem. Soc.* 140 (2018) 12521–12526. <https://doi.org/10.1021/jacs.8b06901>.
- [178] J. Nitsch, F. Lacemon, A. Lorbach, A. Eichhorn, F. Cisnetti, A. Steffen, Cuprophilic interactions in highly luminescent dicopper(i)-NHC-picolyyl complexes-fast phosphorescence or TADF?, *Chem. Commun.* 52 (2016) 2932–2935. <https://doi.org/10.1039/c5cc09659f>.
- [179] B. Hupp, J. Nitsch, T. Schmitt, R. Bertermann, K. Edkins, F. Hirsch, I. Fischer, M. Auth, A. Sperlich, A. Steffen, Stimulus-Triggered Formation of an Anion–Cation Exciplex in Copper(I) Complexes as a Mechanism for Mechanochromic Phosphorescence, *Angew. Chem. Int. Ed.* 57 (2018) 13671–13675. <https://doi.org/10.1002/anie.201807768>.
- [180] E. Cariati, E. Lucenti, C. Botta, U. Giovanella, D. Marinotto, S. Righetto, Cu(I) hybrid inorganic-organic materials with intriguing stimuli responsive and optoelectronic properties, *Coord. Chem. Rev.* 306 (2016) 566–614. <https://doi.org/10.1016/j.ccr.2015.03.004>.
- [181] R. Xu, G. Liu, R. Zhao, X. Zhang, F. Zheng, C. Li, Chair form copper iodine cluster (Cu₄I₄(Etm₄)₄) and its application in selective recognition of o-nitrophenol in wastewater., 2019.
- [182] S. Jing, C. Li, W. Ji, Ferrocene cuprous cluster catalyst for catalytic coupling reaction of carbon-nitrogen, and preparation method thereof., 2018.
- [183] M. Johnsson, I. Persson, The structure of silver(I) iodide and bromide, and the silver(I) solvate in tetrahydrothiophene solution: An X-ray scattering and raman spectroscopic study, *Inorganica Chim. Acta.* 130 (1987) 215–220. [https://doi.org/10.1016/S0020-1693\(00\)90439-0](https://doi.org/10.1016/S0020-1693(00)90439-0).
- [184] B. Norén, Å. Oskarsson, A. Pajunen, M. Tammenmaa, H. V. Volden, On the Cubane versus the Stella Quadrangula Structure. The Crystal Structure of Tetrakis[iodo(tetrahydrothiophene)silver(I)]., *Acta Chem. Scand.* 39a (1985) 701–709. <https://doi.org/10.3891/acta.chem.scand.39a-0701>.
- [185] J.K. Aulakh, T.S. Lobana, H. Sood, D.S. Arora, I. Garcia-Santos, M. Kaur, J.P. Jasinski, Synthesis, structures, and novel antimicrobial activity of silver(I) halide complexes of imidazolidine-2-thiones, *Polyhedron.* 175 (2020) 114235. <https://doi.org/10.1016/j.poly.2019.114235>.
- [186] X. Li, J. Zhang, Z. Zhao, X. Yu, P. Li, Y. Yao, Z. Liu, Q. Jin, Z. Bian, Z. Lu, C. Huang, Bluish-

- Green Cu(I) Dimers Chelated with Thiophene Ring-Introduced Diphosphine Ligands for Both Singlet and Triplet Harvesting in OLEDs, *ACS Appl. Mater. Interfaces*. 11 (2019) 3262–3270. <https://doi.org/10.1021/acsami.8b15897>.
- [187] Q. Wei, H.T. Chen, L. Liu, X.X. Zhong, L. Wang, F.B. Li, H.J. Cong, W.Y. Wong, K.A. Alamry, H.M. Qin, Syntheses and photoluminescence of copper(i) halide complexes containing dimethylthiophene bidentate phosphine ligands, *New J. Chem.* 43 (2019) 13408–13417. <https://doi.org/10.1039/c9nj01417a>.
- [188] M. Granitzka, P. Stollberg, D. Stalke, Bis-2-thienyldiethylaminophosphane as a ligand in late transition metal complexes and its transformation to bis-2-thienylphosphane, *Zeitschrift Fur Naturforsch. - Sect. B J. Chem. Sci.* 69 (2014) 1429–1440. <https://doi.org/10.5560/ZNB.2014-4138>.
- [189] R. Horikoshi, T. Tominaga, T. Mochida, Mixed-Metal Coordination Polymers and Molecular Squares Based on a Ferrocene-Containing Multidentate Ligand 1,2-Di(4-pyridylthio)ferrocene, *Cryst. Growth Des.* 18 (2018) 5089–5098. <https://doi.org/10.1021/acs.cgd.8b00538>.
- [190] Y.Y. Niu, Z.Y. Li, S.M. Li, F.R. Wang, Five novel copper halide/thiocyanate coordination compounds directed by 4-pyridyl dithioether ligands: syntheses, structures, and photocatalytic properties, *J. Mol. Struct.* 1173 (2018) 763–769. <https://doi.org/10.1016/j.molstruc.2018.07.047>.
- [191] S. Meghdadi, M. Amirnasr, E. Yavari, K. Mereiter, M. Bagheri, Synthesis, characterization, and X-ray crystal structures of copper(I) halide and pseudohalide complexes with 2-(2-quinolyl)benzothiazole. Diverse coordination geometries and electrochemical properties, *Comptes Rendus Chim.* 20 (2017) 730–737. <https://doi.org/10.1016/j.crci.2017.02.005>.
- [192] W. Lu, J.J. Ma, W.Z. Luo, B. Li, T. Zhang, Effect of anions on structure and luminescence property of Cu(I)-4,6-di(3-pyridylethynyl)dibenzothiophene complexes, *Inorganica Chim. Acta.* 442 (2016) 97–104. <https://doi.org/10.1016/j.ica.2015.12.002>.
- [193] H. Bin Zhu, L. Liang, Assembly of 1,3,5-tris(2-alkylthiol-pyrimidin-4-yl)benzene (alkyl = Me, n-Pr) with copper(I) iodide: Effect of alkyl side chain, *J. Coord. Chem.* 68 (2015) 1306–1316. <https://doi.org/10.1080/00958972.2015.1011147>.
- [194] J. Wang, S.L. Zheng, S. Hu, Y.H. Zhang, M.L. Tong, New in situ cleavage of both S-S and S-C(sp²) bonds and rearrangement reactions toward the construction of copper(I) cluster-based coordination networks, *Inorg. Chem.* 46 (2007) 795–800. <https://doi.org/10.1021/ic0616028>.
- [195] S. Demir, B. Eren, M. Hołyńska, (1-Methyl-2-(thiophen-2-yl)-1H-benzo[d]imidazole) and its three copper complexes: Synthesis, characterization and fluorescence properties, *J. Mol. Struct.* 1081 (2015) 304–310. <https://doi.org/10.1016/j.molstruc.2014.10.043>.
- [196] K. Xue, W.X. Chai, Y.W. Wu, C. Ling, L. Song, Syntheses, Structures and Properties of Two

- Coordination Polymers Built Upon CopperI, II Halide Clusters and a New Thiodiazole Ligand, *J. Clust. Sci.* 25 (2014) 1005–1017. <https://doi.org/10.1007/s10876-013-0684-y>.
- [197] R. Cargnelutti, F.D. Da Silva, U. Abram, E.S. Lang, Metal complexes with bis(2-pyridyl)diselenoethers: Structural chemistry and catalysis, *New J. Chem.* 39 (2015) 7948–7953. <https://doi.org/10.1039/c5nj01400j>.
- [198] S. Cho, Y. Jeon, S. Lee, J. Kim, T.H. Kim, Reversible transformation between cubane and stairstep Cu₄I₄ clusters using heat or solvent vapor, *Chem. Eur. J.* 21 (2015) 1439–1443. <https://doi.org/10.1002/chem.201405800>.
- [199] X.J. Yang, H.X. Li, Z.L. Xu, H.Y. Li, Z.G. Ren, J.P. Lang, Spacer length-controlled assembly of [Cu_nI_n]-based coordination polymers from CuI and bis(4-phenylpyrimidine-2-thio)alkane ligands, *CrystEngComm*. 14 (2012) 1641–1652. <https://doi.org/10.1039/c2ce06312c>.
- [200] M. Pan, W.X. Zhou, W.Y. Ma, J. Niu, J. Li, Three copper complexes containing the sulfur-bridged bis-pyridine ligands, 2,2'-dithiodipyridine and di-2-pyridyl sulfide, *J. Coord. Chem.* 67 (2014) 3176–3187. <https://doi.org/10.1080/00958972.2014.960860>.
- [201] Y.Q. Sun, C.K. Tsang, Z. Xu, G. Huang, J. He, X.P. Zhou, M. Zeller, A.D. Hunter, CuCN pillars induce face-to-face π -overlap of anthracene-based thioether molecules within a hybrid coordination network, *Cryst. Growth Des.* 8 (2008) 1468–1470. <https://doi.org/10.1021/cg800033v>.
- [202] F. Juvenal, D. Fortin, P.D. Harvey, A “flexible” Rigid Rod, trans-Pt(PMe₃)₂(C-CC₆H₄CN)₂ (L1), to Form 2D [$\{Cu_2(\mu_2-X)_2\}_2(\mu_4-L1)_n$] Polymers (X = Br, I) Exhibiting the Largest Bathochromic Emissions, *Inorg. Chem.* 57 (2018) 7208–7221. <https://doi.org/10.1021/acs.inorgchem.8b00899>.
- [203] J. Pan, D. Zhang, S. De Han, J.X. Hu, Z.Z. Xue, G.M. Wang, White-Light Emission and Magnetism Behaviors Endowed by Inorganic Lanthanide Templates in Iodocuprates, *Cryst. Growth Des.* 19 (2019) 1825–1831. <https://doi.org/10.1021/acs.cgd.8b01792>.
- [204] C. Wang, J. Niu, J. Li, X. Ma, Synthesis, structures and properties of three copper complexes with dibutylldithiocarbamate ligand, *J. Mol. Struct.* 1135 (2017) 75–81. <https://doi.org/10.1016/j.molstruc.2017.01.021>.
- [205] S. Mishra, E. Jeanneau, G. Ledoux, S. Daniele, Novel barium-organic incorporated iodometalates: Do they have template properties for constructing rare heterotrimetallic hybrids?, *Inorg. Chem.* 53 (2014) 11721–11731. <https://doi.org/10.1021/ic501963y>.
- [206] T. Rttgers, W.S. Sheldrick, One- to three-dimensional CuI and CuCN based coordination polymers containing the alkali cation ligating thiocrown ether 1,10-dithia-18-crown-6, *Zeitschrift Fur Anorg. Und Allg. Chemie.* 628 (2002) 1305–1310. [https://doi.org/10.1002/1521-3749\(200206\)628:6<1305::AID-ZAAC1305>3.0.CO;2-H](https://doi.org/10.1002/1521-3749(200206)628:6<1305::AID-ZAAC1305>3.0.CO;2-H).

- [207] B. Nohra, E. Rodriguez-Sanz, C. Lescop, R. Réau, Chemistry of bridging phosphanes: Cui dimers bearing 2,5-bis(2-pyridyl)phosphole ligands, *Chem. Eur. J.* 14 (2008) 3391–3403. <https://doi.org/10.1002/chem.200701423>.
- [208] E. Rodriguez-Sanz, C. Lescop, R. Réau, A Cu(I) cluster bearing a bridging phosphane ligand, *Comptes Rendus Chim.* 13 (2010) 980–984. <https://doi.org/10.1016/j.crci.2010.06.008>.
- [209] A.Y. Baranov, E.A. Pritchina, A.S. Berezin, D.G. Samsonenko, V.P. Fedin, N.A. Belogorlova, N.P. Gritsan, A. V. Artem'ev, Beyond Classical Coordination Chemistry: The First Case of a Triply Bridging Phosphine Ligand, *Angew. Chemie.* 133 (2021) 12685–12692. <https://doi.org/10.1002/ange.202103037>.
- [210] H. El Moll, M. Cordier, G. Nocton, F. Massuyeau, C. Latouche, C. Martineau-Corcus, S. Perruchas, A Heptanuclear Copper Iodide Nanocluster, *Inorg. Chem.* 57 (2018) 11961–11969. <https://doi.org/10.1021/acs.inorgchem.8b01516>.
- [211] M. Yu, C. Liu, S. Li, Y. Zhao, J. Lv, Z. Zhuo, F. Jiang, L. Chen, Y. Yu, M. Hong, Constructing multi-cluster copper(i) halides using conformationally flexible ligands, *Chem. Commun.* 56 (2020) 7233–7236. <https://doi.org/10.1039/d0cc02472d>.
- [212] S. Cheon, T.H. Kim, Y. Jeon, J. Kim, K.M. Park, Novel heptanuclear copper(i) iodide cluster with a pinwheel shape, *CrystEngComm.* 15 (2013) 451–454. <https://doi.org/10.1039/c2ce26664d>.



Graphic Art